

**Free Lipid Radicals and Nitroxide Radicals  
in Dispersed Systems Studied by  
EPR Spectroscopy**

Dissertation  
zur Erlangung des Doktorgrades  
der Mathematisch-Naturwissenschaftlichen Fakultät  
der Christian-Albrechts-Universität zu Kiel

vorgelegt von

**Dipl. Lebensmittelchemikerin  
Heimke Krudopp**

Kiel, 2014



---

Erste Gutachterin:

Jun. Prof. Dr. Anja Steffen-Heins

Zweiter Gutachter:

Prof. Dr. Felix Tuczek

Tag der mündlichen Prüfung:

15.12.2014

Zum Druck genehmigt:

30.11.2015

gez. Prof. Dr. Wolfgang J. Duschl, Dekan



*dedicated to Lieselotte and Henriette*



## Acknowledgement

I am sincerely grateful to my supervisor, Jun. Prof. Dr. Steffen-Heins, for her guidance, support and generous help throughout the practical work and during the preparation of this thesis.

Special thanks to Prof. Dr. Karin Schwarz for giving me the opportunity to use all the laboratory facilities in, as well as providing a social affiliation with, the department of food technology.

I would like to thank Prof. Dr. Frank Sönnichsen for sharing his expertise in response to numerous questions about NMR diffusion measurements.

I would like to thank the (former) members of the working group of Prof. Dr. Tuzcek for their guidance during my first EPR steps: Prof. Dr. Philipp Kurz, Hans-Martin Berends and Anne Westphal.

I wish to thank AO Prof. Dr. Klaus Stolze for his hospitality, support and the provision of endless lipophilic spin traps.

I would also like to thank Dr. Kalpana Palani for her guidance throughout the synthesis of C17-DMPO.

A special thank you to my colleagues and fellow graduate students: Monika, Tobias, Beate, Johanna, Sonja, Julia, Katinka, Birgit, Anneleen, Kalpana, Kerstin, Sandra and Jonas.

Many thanks to Gitta Noll for proofreading my thesis.

I dearly thank my parents Sybille and Hans-Heinrich, especially for being such great grandparents, and my family and friends who encouraged me during the last years: Anne Süster, Marlies, Arne, Lina, Ole, Anna, Christiane, Tine and Mareike.

Finally, I want to thank Lars not only for formatting my thesis, but for everything he has done for me and enabled for our future. It was a great and exciting family journey.





## Summary

The interfacial structure of multi-phased systems, as found in foods, is well known as the main reaction site of lipid autoxidation. To elucidate this site-directed oxidation process in foods the partitioning behavior as well as the location and reaction kinetic of free lipid radicals and antioxidants were investigated. Various EPR and NMR experiments were carried out to determine the behavior of free lipid radicals in micellar solutions and emulsions of SDS, CTAB, Brij58 and Tween20. Due to the short half-lives of free lipid radicals they are not directly detectable, but with the application of a spin scavenger these radicals could be successfully monitored.

The addition reaction of a free radical to a spin trap leads to a stable radical adduct that can be identified by its fingerprint hyperfine splitting. To localize the generation and partitioning of radicals in dispersed systems, different combinations of hydrophilic and lipophilic radical generators and spin traps were used in the presence and absence of oxidizable linoleic acid. Regardless of the radical initiator, spin trap and emulsifier, the generation of hydroxyl radicals was predominantly due to the oxidation of water molecules from the continuous phase and only in systems containing Tween20 and Brij58 alkyl radical adducts were detected. The non-ionic headgroups promoted the reaction participants in contrast to ionic emulsifiers. A stearic acid DMPO derivate was synthesized as it was supposed to be located in the membrane in close proximity to lipid radicals, but in dispersed systems no stable adducts could be detected. For this reason further work was focused on spin probes.

The partitioning of three nitroxides with increasing lipophilicity (TEMPOL < TEMPO < TB) was determined by ultrafiltration (UF), PFG-NMR and EPR deconvolution. The NMR measurements indicated a highly dynamic system as shown by high diffusion constants. The resulting proportions solubilized in the interfaces were lower compared with UF and EPR data. With increasing lipophilicity, the proportion of interfacial solubilized nitroxides increased in micellar solution with a further increase for TEMPO in emulsions due to an extended interfacial area.

The distinct spin probe location is essential to determine their reaction kinetics towards lipid radicals and antioxidants, which was achieved by NMR  $T_1$  relaxation times and EPR deconvolution. The  $T_1$  relaxation times indicated a solubilization of nitroxides in the palisade layer adjacent to the headgroup regardless of the nitroxide lipophilicity and the type of emulsifier. EPR line shape analysis revealed three spectral domains for the nitroxides adopted by an isotropic free tumbling population and a clustered hindered tumbling population in the aqueous phase and one population in an anisotropic environment such as the interface.

The non-invasive EPR deconvolution technique turned out to be the preferred method to determine the partitioning behavior of paramagnetic molecules in dispersed systems as it enables distinguishing between several populations at their individual solubilization sites. The determination of partitioning of nitroxides using NMR methods is restricted as PFG-

NMR requires diamagnetic substances and therefore reduced nitroxides with theoretically lower lipophilicities were used. Equilibrium between two populations, whose high dynamic was demonstrated by PFG-NMR, is presupposed where the solubilized nitroxide population can be indirectly measured but not quantified by emulsifier proton signals with  $T_1$  relaxation times. UF is an invasive method that also differentiates between two populations whereas the dynamic and location of nitroxides cannot be analyzed.

The reaction of nitroxides towards antioxidants and lipid radicals is given by the interconversion between nitroxide, hydroxylamine and oxoammonium ion. In dispersed systems, the reaction kinetics are known to be accelerated if the reaction participants are in close spatial proximity to one another. The antioxidants propyl gallate, Trolox and  $\alpha$ -tocopherol are well characterized in dispersed systems and reduced nitroxides to TEMPOL < TB < TEMPO with high reaction kinetics compared to buffer solution. Defined lipid radicals were generated by autoxidation of emulsions (alkyl radicals) and heat-induced decomposition of methyl linoleate hydroperoxides (alkoxyl radicals). In all emulsions the spin scavenging ability towards alkyl radicals increased to TEMPOL < TB < TEMPO, while alkoxyl radicals were hardly detectable due to instability of the products and a slower rate constant of nitroxides towards oxygen-centered radicals than carbon-centered radicals.

Regardless of the solubilized proportions of nitroxides in the interface, the emulsifier governed the solubilization site of antioxidants, stable and free radicals resulting in the fastest reaction kinetic for SDS solutions. Compared with the more hydrophilic TEMPOL and the more lipophilic TB all reactions of TEMPO towards alkyl radicals and antioxidants were accelerated. Data thus obtained might support the suggestion of a different orientation of the NO moiety of TEMPO in the interface. The orientation towards the antioxidant or radical implies a direct proximity of the reactants and therefore an accelerated reduction. The reaction between TEMPO and lipid alkyl radicals indicates the suitability of the EPR spin probing technique to monitor lipid oxidation in food matrices. With further investigations, this approach benefits from short induction times, easier quantification of lipid radicals compared with the spin trap method and the possibility to reflect the initial state of autoxidation.

## Zusammenfassung

Lipidoxidation findet in mehrphasigen Systemen, wie zum Beispiel in Lebensmitteln, hauptsächlich an der Grenzflächenstruktur statt. Zur Aufklärung dieses spezifisch lokalisierten Oxidationsprozesses wurden das Verteilungsverhalten, die Lokalisierung und die Reaktionskinetik von freien Lipidradikalen, stabilen Radikalen und Antioxidantien untersucht. Verschiedene ESR- und NMR-Techniken wurden angewandt, um das Verhalten der Radikale in mizellaren Lösungen und Emulsionen mit SDS, CTAB, Brij58 und Tween20 zu untersuchen. Auf Grund ihrer kurzen Halbwertszeit sind Lipidradikale nicht direkt erfassbar, können jedoch durch den Einsatz eines Radikal-Fängers detektiert werden.

Durch die Reaktion von freien Radikalen mit Spinfallen werden stabile Radikal-Addukte gebildet, die durch die Hyperfeinaufspaltung des Spektrums identifiziert werden können. Um den Ort der Entstehung und die Verteilung von Radikalen in dispersen Systemen zu lokalisieren, wurden verschiedene Kombinationen von hydrophilen und lipophilen Radikalbildnern und Spinfallen in An- und Abwesenheit von oxidierbarer Linolsäure verwendet. Unabhängig des eingesetzten Radikalbildners, der genutzten Spinfaller oder des verwendeten Emulgators wurden überwiegend Hydroxylradikal-Addukte detektiert, die auf Grund der Oxidation von Wassermolekülen aus der kontinuierlichen Phase entstehen. Nur in Systemen mit Tween20 und Brij58 wurden Alkylradikal-Addukte detektiert. Dies kann auf die nicht-ionischen Kopfgruppen der Emulgatoren zurückgeführt werden, welche eine direkte Nähe der Reaktionsteilnehmer fördern. Weiterhin wurde ein Stearinsäure-DMPO-Derivat synthetisiert, welches sich auf Grund der lipophilen Struktur in der Nähe der Lipidradikale in der Membran lokalisiert. Es konnten jedoch keine Lipidradikal-Addukte in dispersen Systemen detektiert werden, sodass für die weitere Arbeit Spinsonden eingesetzt wurden.

Das Verteilungsverhalten der drei Nitroxid-Spinsonden mit ansteigender Lipophilie TEMPOL < TEMPO < TB wurde mittels Ultrafiltration (UF), PFG-NMR und ESR Dekonvolution bestimmt. Die NMR-Messungen ergaben hohe Diffusionskonstanten, die auf ein sehr dynamisches System schließen ließen. Die daraus ermittelten Konzentrationen an Nitroxiden an der Grenzfläche waren niedriger im Vergleich zu den Ergebnissen von UF und ESR. Mit steigender Lipophilie der Spinsonde erhöhte sich der Anteil an Nitroxiden, die an den Grenzflächen der Mizellen lokalisiert waren, wobei ein weiterer Anstieg von TEMPO auf Grund der vergrößerten Oberfläche in Emulsionen zu verzeichnen war.

Mittels NMR  $T_1$  Relaxationszeiten und ESR-Dekonvolutionen wurde die spezifische Lokalisierung der Nitroxide in der Phasengrenze ermittelt, da diese entscheidend für die Reaktivität gegenüber Lipidradikalen und Antioxidantien ist. Die  $T_1$  Relaxationszeiten zeigten, dass sich die Nitroxide unabhängig von ihrer Lipophilie und der Art des Emulgators in der Palisadenschicht neben den Kopfgruppen anordnen. Damit konnte die in der Grenzfläche gelöste Nitroxid-Population zwar indirekt erfasst, aber nicht quantifiziert werden. Die ESR-Dekonvolutionen zeigten drei verschiedene spektrale Bereiche für die Nitroxide, wobei eine frei bewegliche Population mit einem isotropen Spektrum und eine konzentriert vorliegende Population mit eingeschränkter Beweglichkeit in der wässrigen Phase sowie eine Population

in einer anisotropen Umgebung, wie der Grenzfläche, angenommen wurden.

Um das Verteilungsverhalten von paramagnetischen Molekülen in dispersen Systemen zu bestimmen, erwies sich die nicht-invasive ESR-Dekonvolutionstechnik als die geeignetste Methode, da eine zusätzliche Charakterisierung der Umgebung der unterschiedlichen Population möglich ist. Die Bestimmung des Verteilungsverhaltens von Nitroxiden mittels PFG-NMR ist nur eingeschränkt möglich, da diese Methode für paramagnetische Substanzen ungeeignet ist, sodass reduzierte Nitroxide mit einer theoretisch niedrigeren Lipophilie eingesetzt wurden. Es konnte jedoch gezeigt werden, dass in den dispersen Systemen eine hohe Dynamik vorherrscht, was ein wichtiger Beitrag zur weiteren Charakterisierung der Systeme mit sich bringt. Die UF ist eine invasive Methode, die wie auch die NMR-Spektroskopie zwischen zwei Populationen differenziert, jedoch weder die Dynamik noch die Lokalisierung der Nitroxide erfasst.

Auf Grund der Interkonversion zwischen Nitroxid, Hydroxylamin und Oxoammoniumion reagieren Nitroxide sowohl mit Antioxidantien als auch mit Radikalen. In dispersen Systemen wird die Reaktionskinetik beschleunigt, wenn sich die Reaktionspartner in direkter räumlicher Nähe zu einander befinden. Die Antioxidantien Propylgallat, Trolox und  $\alpha$ -Tocopherol sind in dispersen Systemen gut charakterisiert und reduzierten die Nitroxide zunehmend von TEMPOL < TB < TEMPO mit einer erhöhten Reaktionsgeschwindigkeit im Vergleich zu einer homogenen Lösung. Durch die Autoxidation einer Emulsion bzw. den Hitze-induzierten Zerfall von Methyllinolat-Hydroxyperoxiden wurden definierte Alkyl- bzw. Alkoxyradikale generiert. Die Alkylradikale oxidierten die Nitroxide zunehmend von TEMPOL < TB < TEMPO, wohingegen die Alkoxyradikale auf Grund der instabilen Reaktionsprodukte und der niedrigeren Reaktionsgeschwindigkeit von sauerstoffzentrierten Radikalen im Vergleich zu kohlenstoffzentrierten Radikalen kaum detektierbar waren.

Der Emulgator beeinflusst den Solubilisierungsort der Spinsonden, Antioxidantien und Lipidradikale, was unabhängig von dem jeweiligen Verteilungsverhalten zu erhöhten Reaktionsgeschwindigkeiten in SDS-Lösungen geführt hat. Die beschleunigte Reaktion von TEMPO, sowohl mit Alkylradikalen als auch mit Antioxidantien, im Vergleich zu dem hydrophileren TEMPOL und dem lipophileren TB unterstützen die Hypothese, dass die Orientierung der Nitroxid-Gruppe von TEMPO zur Phasengrenze hin vorliegt. Die Ausrichtung der reaktiven Gruppe zu den Antioxidantien und Radikalen impliziert eine direkte Nähe der Reaktionspartner und führt somit zu einer beschleunigten Reaktion. Die Ergebnisse der Reaktion von TEMPO mit den Alkylradikalen deuten darauf hin, dass die ESR Spinsonden-Technik geeignet ist, um die Lipidoxidation in einer Lebensmittelmatrix zu erfassen. Nach weiteren Untersuchungen könnte die Methode von der kurzen Induktionszeit sowie, im Gegensatz zu den Spinfallen, von der einfachen Quantifizierung der Lipidradikale profitieren und den Einblick in das frühe Stadium der Lipidautoxidation ermöglichen.

# Contents

Summary . . . . .	IX
Zusammenfassung . . . . .	XI
<b>List of Tables</b>	<b>XVI</b>
<b>List of Figures</b>	<b>XVII</b>
<b>List of Abbreviations</b>	<b>XX</b>
<b>1 General Introduction</b>	<b>1</b>
1.1 Preface . . . . .	1
1.2 Objectives . . . . .	2
1.3 Theoretical background . . . . .	4
1.3.1 Dispersed systems . . . . .	4
1.3.1.1 Micellar solutions . . . . .	4
1.3.1.2 Emulsions . . . . .	5
1.3.1.3 Swollen micelles . . . . .	5
1.3.2 Partitioning, solubilisation and dynamics in dispersed systems . . . . .	6
1.3.3 Lipid oxidation . . . . .	7
1.3.3.1 Lipid oxidation in emulsions . . . . .	9
1.3.3.2 Antioxidative reactions in dispersed systems . . . . .	10
1.4 Experimental approach . . . . .	11
1.4.1 Description of model compounds . . . . .	11
1.4.1.1 Emulsifiers . . . . .	11
1.4.1.2 Spin Traps . . . . .	11
1.4.1.3 Spin Probes . . . . .	12
1.4.1.4 Antioxidants . . . . .	14
1.4.2 Basics of EPR and NMR spectroscopy . . . . .	14
1.4.3 EPR spectroscopy . . . . .	16
1.4.4 EPR characteristics of nitroxides . . . . .	17
1.4.5 EPR deconvolution . . . . .	18
1.4.6 NMR diffusion experiments . . . . .	18
1.4.7 Partitioning of paramagnetic substances . . . . .	20
1.4.7.1 Ultrafiltration . . . . .	20
1.4.7.2 EPRSIM-C . . . . .	20

1.4.7.3	NMR diffusion . . . . .	21
1.4.8	Generation of free lipid radicals . . . . .	21
1.4.8.1	Oxidation of corn oil emulsions . . . . .	21
1.4.8.2	Production and decomposition of MeLOOHs . . . . .	22
	References . . . . .	23
<b>2</b>	<b>The use of spintraps to detect azo-generated lipid radicals in dispersed systems</b>	<b>29</b>
2.1	Abstract . . . . .	29
2.2	Introduction . . . . .	30
2.3	Materials and Methods . . . . .	31
2.3.1	Chemicals . . . . .	31
2.3.2	Synthesis of C17-DMPO . . . . .	31
2.3.3	Preparation of dispersed systems . . . . .	32
2.3.4	EPR general setup . . . . .	33
2.4	Results . . . . .	33
2.4.1	Detection of DMPO- and PBN-adducts . . . . .	33
2.4.2	Detection of DBPMPO- and OMPO-adducts . . . . .	35
2.4.3	C17-DMPO . . . . .	36
2.5	Discussion . . . . .	37
2.5.1	The preferred detection of hydroxyl radicals . . . . .	37
2.5.2	The distinction between radical types . . . . .	38
2.5.3	Cautionary note on highly reactive free radicals . . . . .	39
2.5.4	Cautionary note on azo-initiator generated radicals . . . . .	39
2.5.5	Further investigations to trap alkyl radicals . . . . .	40
2.5.6	Synthesis of spin traps . . . . .	41
2.6	Outlook . . . . .	42
	References . . . . .	43
<b>3</b>	<b>Partitioning of nitroxides in dispersed systems investigated by ultrafiltration, EPR and NMR spectroscopy</b>	<b>47</b>
3.1	Abstract . . . . .	47
3.2	Introduction . . . . .	48
3.3	Materials and Methods . . . . .	50
3.3.1	Chemicals . . . . .	50
3.3.2	Preparation of micellar solutions . . . . .	50
3.3.3	Preparation of emulsions . . . . .	50
3.3.4	Preparation of NMR samples . . . . .	51
3.3.5	Determination of critical micellar concentration . . . . .	51
3.3.6	EPR based partitioning behavior . . . . .	51
3.3.6.1	Ultrafiltration probes . . . . .	51

---

3.3.6.2	Deconvolution of superimposed spectra with EPRSIM-C	52
3.3.7	NMR based partitioning behavior	52
3.4	Results and discussion	53
3.4.1	Diffusion rates of hydroxylamines	53
3.4.2	Different microenvironments of spin probes	56
3.4.3	Partitioning behavior of nitroxides into the micellar and emulsion interface determined by different methods	58
3.5	Conclusion	62
	References	63
<b>4</b>	<b>EPR study on the solubilization side of nitroxide in multiphase systems and its relevance to the reduction capacity of antioxidants</b>	<b>67</b>
4.1	Abstract	67
4.2	Introduction	68
4.3	Materials and Methods	70
4.3.1	Chemicals	70
4.3.2	Sample preparation	70
4.3.3	Partitioning behavior	70
4.3.4	EPR analysis	71
4.3.4.1	Calculation of the rotational correlation time ( $\tau_c$ ) of superimposed spectra	71
4.3.4.2	Calculation of the antioxidative capacity	71
4.3.5	NMR analysis: $T_1$ relaxation time	72
4.3.5.1	Antioxidants	72
4.3.5.2	Nitroxides	72
4.4	Results and Discussion	73
4.4.1	Solubilization site of antioxidants and nitroxides	73
4.4.2	Micro environmental properties of nitroxides in multiphase systems	77
4.4.3	Antioxidant capacity to reduce micellar nitroxides	80
4.5	Conclusion	84
	References	85
<b>5</b>	<b>Generation of alkyl and alkoxy lipid radicals in dispersed systems followed by their reaction with nitroxides</b>	<b>89</b>
5.1	Abstract	89
5.2	Introduction	90
5.3	Materials and Methods	92
5.3.1	Chemicals	92
5.3.2	Preparation of MeLOOH	92
5.3.3	Preparation of emulsions	92
5.3.4	Preparation of swollen micelles	93

5.3.5	Reduction of nitroxides by lipid radicals . . . . .	93
5.3.5.1	Decay products of MeLOOH . . . . .	93
5.3.5.2	Lipid oxidation products . . . . .	93
5.3.6	Photometric measurement of hydroperoxides . . . . .	94
5.3.7	EPR measurements . . . . .	94
5.4	Results and discussion . . . . .	94
5.4.1	Influence of nitroxide concentration and heat stability . . . . .	94
5.4.2	Reactions of nitroxides with lipid radicals from decomposition of MeLOOH . . . . .	96
5.4.3	Reaction of nitroxides with lipid radicals from autoxidation of corn oil	99
5.5	Conclusion . . . . .	102
	References . . . . .	103
<b>6</b>	<b>General discussion</b>	<b>107</b>
6.1	Spin Scavenging . . . . .	107
6.2	Generation of free lipid radicals . . . . .	108
6.3	Solubilisation properties of nitroxide spin probes . . . . .	110
6.4	Reactivity of spin probes towards antioxidants and free lipid radicals . . . .	112
6.4.1	Alkyl radicals but not alkoxy radicals are able to reduce nitroxides .	113
6.4.2	The alignment of the nitroxides NO moiety . . . . .	113
6.4.3	The SDS interface accelerated the nitroxides reactions . . . . .	114
6.5	Concluding remarks and Outlook . . . . .	115
	References . . . . .	117



# List of Tables

2.1	Peak heights (H) of the alkyl (a) and hydroxyl (h) adducts and their ratio ( $P_{H_a/H_h}$ ) depending on the spin trap concentration. . . . .	34
3.1	Critical micellar concentration (cmc) and self-diffusion coefficients ( $D_N$ ) of hydroxylamines TEMPOL-H, TEMPO-H and TB-H in micelles of SDS, CTAB and Brij58 emulsifier monomers ( $D_{mono}$ ) and unloaded micelles ( $D_{mic}$ ). . .	54
3.2	EPRSIM-C deconvolution of rotational correlation time ( $\tau_c$ ), hyperfine coupling ( $a_N$ ) and proportion of populations 1-3 of the nitroxides TEMPOL, TEMPO and TB in micellar solutions of SDS, CTAB and Brij58. . . . .	57
3.3	EPRSIM-C deconvolution of rotational correlation time ( $\tau_c$ ), hyperfine coupling ( $a_N$ ) and proportion of populations 1-3 of the nitroxides TEMPOL, TEMPO and TB in emulsions of SDS, CTAB and Brij58. . . . .	58
3.4	Solubilized proportion ( $d_{sol}$ ) of the nitroxides TEMPOL, TEMPO and TEMPOL-benzoate in SDS, CTAB and Brij58 micellar solutions determined by ultrafiltration technique (UF), NMR and deconvolution of EPR spectra (EPR). .	59
3.5	Solubilized proportion ( $d_{sol}$ ) of TEMPOL, TEMPO and TEMPOL-benzoate in SDS, CTAB and Brij58 emulsions determined by ultrafiltration technique (UF) and deconvolution of EPR spectra (EPR). . . . .	60
4.1	Partitioning of nitroxides ( $P_N$ ) and antioxidants ( $P_{AO}$ ) into the micellar phases of different micellar solutions . . . . .	73
4.2	$^1H$ -NMR parameter for localization of the antioxidants propyl gallate (PG), Trolox and $\alpha$ -tocopherol in the micellar phase of CTAB, SDS and Brij58 micellar solutions . . . . .	74
4.3	$T_1$ -relaxation ratio of individual emulsifier proton signals of CTAB, SDS and Brij58 in the presence of micellar TEMPOL, TEMPO and TEMPOL-benzoate	76
4.4	Hyperfine splitting constants of nitroxides in buffer and micellar solutions ( $n=3$ ) . . . . .	78
4.5	Rotational correlation times of nitroxides in the absence and presents of different antioxidants . . . . .	79
4.6	Antioxidative capacity of PG, Trolox and $\alpha$ -Tocopherol to reduce nitroxides in different micellar solutions. . . . .	83

# List of Figures

1.1	Simplified schemes of interfacial and micellar structures formed by ionic (left) and non-ionic (right) emulsifiers: hydrophobic core (1), palisade layer (2), stern layer with rigid layer (3) and diffuse layer (4), headgroup region (5). . .	5
1.2	Schematic structures of an emulsion with coexisting micellar phases and oil droplets with enlarged interfaces. Solubilisation sites are in the aqueous phase (a), hydrophobic core (b) and in the interface (palisade layer (c) and Stern layer (d)). . . . .	6
1.3	Chemical structures of CTAB (a), SDS (b) and Brij58 (c) . . . . .	11
1.4	Structure of spin traps PBN (a) and DMPO derivates (b). . . . .	12
1.5	Chemical structures of TEMPOL (a), TEMPO (b) and TEMPOL-benzoate (c) . . . . .	13
1.6	Inter-conversion of TEMPO, TEMPOH and oxoammonium salt . . . . .	13
1.7	Chemical structures of $\alpha$ -Tocopherol (a), Trolox (b) and propyl gallate (c). . . . .	14
1.8	Pulse field gradient spin echo sequence. The echo appears after $2\tau$ . After the $90^\circ$ and $180^\circ$ pulse are two pulse magnetic field gradients of length $\delta$ and strength $g$ . . . . .	20
2.1	Synthesis scheme of DMPO-C17. . . . .	32
2.2	Structure of spin traps PBN (a) and DMPO derivates (b). . . . .	33
2.3	Spectra of DMPO-adducts in CTAB (a) and Tween20 (b) with Fenton reaction mix. Black lines show the samples in the presence of LA and dotted lines show the control in the absence of LA. Simulated spectra of DMPO-adducts with alkyl radicals (c), hydroxyl radicals (d) and alkoxy radicals (e). *alkylradicals . . . . .	34
2.4	Spectra of DBPMPO (a, b) and OMPO (c, d) adducts in Tween20. Oxidation was initiated by Fenton reaction mix. LA is present in samples b and d. . .	36
2.5	Spectra of C17-DMPO in chloroform (grey) and Tween20 (black) with AIBN and dimethylsulfoxide in chloroform as radical source. . . . .	37
3.1	Paramagnetic nitroxides TEMPOL (a), TEMPO (b) and TB (c). . . . .	49
3.2	Measured and simulated spectra of TEMPO in SDS emulsion. Best fit simulation of superimposed spectra ended up with three individual TEMPO populations with different solubilization sites. . . . .	56

4.1	Chemical structure of the antioxidants $\alpha$ -tocopherol (a), Trolox (b), propyl gallate (c), of the nitroxides TEMPOL (d), TEMPO (e) and TB (f), and of emulsifiers SDS (g), CTAB (h) and Brij58 (i). Nomenclature of emulsifier proton signals are given for NMR measurements (hg: head group, ac: acyl chain, $\alpha, \beta, \gamma$ : $\alpha$ -CH <sub>2</sub> , $\beta$ -CH <sub>2</sub> , $\gamma$ -CH <sub>2</sub> and $\omega$ : $\omega$ -CH <sub>3</sub> ) . . . . .	68
4.2	<sup>1</sup> H-NMR spectra of SDS in the absence and the presence of TEMPOL, TEMPO and TB. In $T_1$ -relaxation times of individual emulsifier proton signals are included. . . . .	75
4.3	Electron distribution of the NO moiety . . . . .	77
4.4	Exponential decay of different nitroxides by antioxidants in micellar solutions. Comparison of the decay of different nitroxides in buffer and SDS solution by propyl gallate (a), of TEMPO by propyl gallate in SDS, CTAB and Brij58 solution (b), and of TEMPO in SDS micellar solution by propyl gallate, Trolox and $\alpha$ -tocopherol (c). . . . .	81
5.1	Paramagnetic nitroxides TEMPO (a), TEMPOL (b), TB (c) (left) and Inter-conversion of TEMPO (nitroxide), TEMPO-H (hydroxylamine) and oxoammonium ion (right). . . . .	91
5.2	Degradation of TEMPO in emulsions with 10 wt% corn-oil in 1 wt% SDS at 60 °C for 4 h with concentrations of 0.1 mmol, 0.25 mmol, 0.5 mmol, 0.75 mmol, 1.0 mmol and 2 mmol TEMPO. . . . .	95
5.3	Stability of nitroxides during heat exposure: a) TEMPO in emulsions with 10 wt% corn oil and 1 wt% emulsifier (CTAB, Brij58, SDS) at 60 °C for 240 min, b) TEMPOL, TEMPO, TB in micelles of SDS (1 wt%) at 100 °C for 240 min. . . . .	95
5.4	Decomposition of 1 mmol MeLOOH in swollen micelles of 1 % SDS (a), Brij58 (b) and CTAB (c) at 100 °C for 240 min in the presence of TEMPOL, TEMPO and TB and in the absence of nitroxides (control) measured by photometry. . . . .	97
5.5	Reaction of TEMPOL (light), TEMPO (dotted) and TB (dark) with radicals from the decomposition of 1 mmol MeLOOH in swollen micelles of 1 wt% CTAB, Brij58 and SDS after 60 min (a) and 120 min (b) at 100 °C. . . . .	98
5.6	Degradation of nitroxides (1 mmol) in emulsions with 10 wt% corn oil in 1 wt% CTAB, Brij58 and SDS at 60 °C for 240 min, a) TEMPOL, b) TEMPO and c) TB. . . . .	100

# List of Abbreviations

AAPH	2,2'-Azobis(2-amidinopropane) dihydrochloride
AIBN	N,N-Azobisisobutyronitril
$a_N$	hyperfine splitting constant
Brij58	polyoxyethylene-20-cetyl ether
cmc	critical micelle concentration
CTAB	cetyl trimethyl ammonium bromide
D	self-diffusion coefficient
DBPMPO	5-(di-n-Butoxyphosphoryl)-5-methyl-1-pyrroline N-oxide
DEPMPO	5-(Diethoxyphosphoryl)-5-methyl-1-pyrroline N-oxide
DMPO	5,5-Dimethyl-1-pyrroline N-oxide
EPR	electron paramagnetic resonance spectroscopy
ESR	electron spin resonance spectroscopy
FT	Fourier transform
LA	linoleic acid
MCT oil	Middle-chain-triglycerides oil
MeLOOH	methyl linoleate hydroperoxides
MWCO	molecular weight cut-off
NMR	nuclear magnetic resonance
OMPO	5-Octyl-5-methyl-1-pyrroline-N-oxide
o/w emulsion	oil-in-water emulsion
PBN	N-tert-Butyl- $\alpha$ -phenylnitron
PFM-NMR	pulsed-field gradient nuclear magnetic resonance
PRE	paramagnetic relaxation enhancement
PUFAs	polyunsaturated fatty acids
SANS	small angle neutron scattering
SDS	sodium dodecylsulfate
TB	TEMPOL-benzoate, 2,2,6,6-Tetramethyl-4-piperidinol-1-oxyl-benzoate
TB-H	1,4-Dihydroxy-2,2,6,6-tetramethylpiperidine-benzoate
TEMPO	2,2,6,6-Tetramethylpiperidine-1-oxyl
TEMPO-H	1-Hydroxy-2,2,6,6-tetramethylpiperidine
TEMPO-L	2,2,6,6-Tetramethyl-4-piperidinol-1-oxyl
TEMPO-L-H	1,4-Dihydroxy-2,2,6,6-tetramethylpiperidine
TFA	trifluoroacetic acid

TLC	thin layer chromatographic
$\tau_c$	rotational correlation time
UF	ultrafiltration
wt%	weight%



# 1 General Introduction

## 1.1 Preface

A major concern in the food industry is the oxidation of unsaturated lipids. Polyunsaturated fatty acids are a substantial component in the human diet, but they also present a challenge as these fatty acids are highly susceptible to lipid oxidation. This negatively affects not only the shelf life but also causes the loss of nutritional value and off-flavors. During lipid oxidation, free radicals are generated during the well-studied radical chain pathway that is divided into the steps: initiation, propagation and termination (Frankel 2005; Roman et al. 2012). Free radicals do not only spoil food but cause serious damage to biomembranes, proteins and other biomolecules in the human body. It is suspected that certain human diseases are a consequence of the oxidation process (Halliwell 1994). In foods, the addition of antioxidants is necessary to prevent lipid oxidation.

Food matrices are complex emulsion-based systems, where the emulsifier interface surrounds the lipid core in oil-in-water emulsions. This interface has been suggested to be the most relevant region for the occurrence of lipid oxidation and therefore surface-active antioxidants are particularly effective as oxidation inhibitors (Heins et al. 2007a, 2007b; Mosca et al. 2013; McClements und Decker 2000; Waraho et al. 2011). Apart from antioxidants, other reaction participants such as pro-oxidative cations and lipid hydroperoxides accumulate at the interface (McClements und Decker 2000), where the surface charge of the droplets also plays an important role in the lipid oxidation process. The access of antioxidants from the continuous phase to the interface can be limited, and their effectiveness reduced, if their electric charge is the same as the interface (Genot et al. 2003; Boon et al. 2008; Heins et al. 2007a, 2007b; Oehlke et al. 2010, 2011).

The proportion of antioxidants located at the interface is postulated to be more active compared to the populations in the aqueous phase and coexisting pseudo phases (Barclay und Vinqvist 1994). The partitioning of antioxidants was formerly calculated by partitioning coefficients determined in two-phase systems, but recent studies take the influence of a multiphase systems and the partitioning of the emulsifiers into account (Stöckmann et al. 2000; Schwarz et al. 1996; Heins et al. 2007a; Oehlke et al. 2010). Therefore, the antioxidants are well characterized in dispersed systems while information about radicals is rather rare.

However, the detection of free lipid radicals is more complicated as their half-lives are most often too short for a direct detection. Electron paramagnetic resonance (EPR) spectroscopy is considered to be the preferred method to characterize the radicals as the spin scavenging

technique circumvents this problem (Hawkins und Davies 2013). The detection of radicals as an early event in the lipid oxidation process allows mild conditions with a short induction time in contrast to the detection of secondary oxidation products with established methods (Thomsen et al. 2000).

Spin traps are one kind of radical scavenging molecule. They react with radicals and form relatively long-lived radical products that can be studied by EPR (Thomsen et al. 2000; Buettner 1987). Furthermore, stable nitroxide radicals are used in the spin scavenging technique as they react with unstable lipid radicals forming non-radical products (Hawkins und Davies 2013; Soule et al. 2007; Voest et al. 1993; Cimato et al. 2004). The complexity of EPR is a challenge but with further interpretation of spin trap spectra the radical species can be determined and, due to the sensitivity of spin probes towards their microenvironment, the local environment can be investigated (Weil und Bolton 2007; Hawkins und Davies 2013). With a deconvolution technique the experimental spectrum can be analyzed by a biophysical model to evaluate the spectral parameters of individual populations (Štrancar et al. 2005).

The partitioning and distinct location of a spin probe within the dispersed phase is essential for the reactivity and depends on the emulsifier used (Berton-Carabin et al. 2013a, 2013b; Otto et al. 2003; Dupont-Leclercq et al. 2007; Heins et al. 2007b; Stöckmann et al. 2000). Thus, knowledge about the influence of emulsifiers on the partitioning and function of nitroxides is crucial prior to the application of nitroxides as spin probes into foods to characterize lipid radicals. To systematically verify the influence of emulsifier-based interfaces emulsions and micellar solutions consisting of anionic SDS (sodium dodecyl sulphate), cationic CTAB (cetyl trimethyl ammonium bromide) and non-ionic Brij58 (polyoxyethylene-20-cetyl ether) served as model systems.

## 1.2 Objectives

The aim of the present study is to characterize the behavior of free lipid radicals in dispersed systems. A better understanding of the radical solubilization site during the autoxidation process in emulsions is the necessary prerequisite to optimize antioxidant application in order to inhibit autoxidation and to develop a fast and radical-based method for monitoring lipid oxidation. To achieve information about free lipid radicals, electron paramagnetic resonance spectroscopy (EPR) is applied, in which spin traps or stable nitroxide radicals have to be used for suitable detection for free lipid radicals possessing very short half-lives. In dispersed systems, the knowledge of the distinct location of spin probes is essential to determine their reaction kinetic towards lipid radicals and antioxidants. To accomplish the aim of the study, the following objectives shall be proved:



- a) In dispersed systems containing linoleic acid, lipophilic radical initiators and fenton reagent generate lipid radicals that can be detected by the EPR spin trapping technique. Spin traps form stable adducts with free lipid radicals where the spectral shape of the spin-adduct depends on the radical species trapped. As the emulsifier interface represents a barrier between the lipophilic and hydrophilic compartment, lipophilic radical initiators and spin traps are solubilized in the micelle core where free lipid radicals are generated, directly trapped and measured by EPR.
- b) The EPR deconvolution technique is the preferred method to determine the partitioning behavior of paramagnetic molecules in dispersed systems. The partitioning behavior of nitroxides between the phases in dispersed systems is investigated to interpret radical and antioxidant reaction with nitroxides relative to the nitroxide content in distinct phases. EPR line shape deconvolution of different spectral populations is used to calculate the partitioning of paramagnetic substances in comparison with the common methods such as ultrafiltration technique and PFG-NMR.
- c) The solubilization site of nitroxides in dispersed systems can be determined by NMR and EPR. The distinct location of the stable nitroxide radical population within the interface is determined by NMR  $T_1$  relaxation times and EPR deconvolution as it influences reactions toward radicals and antioxidants. In dispersed systems, nitroxide populations with differing molecular tumbling and micro-environmental polarity can be investigated by EPR deconvolution.
- d) An accelerated reduction of nitroxides can be measured when their radical-centered atoms are in close proximity to the free radical or antioxidant within the interface. The reaction kinetic of nitroxides towards lipid radicals and antioxidants depends on their proximity to one another and the orientation of the radical-centered atom which is governed by the nitroxide structure and the type of emulsifier.
- e) The EPR spin probing technique is an alternative and promising method to monitor lipid oxidation. Common approaches to measuring lipid oxidation require a time-consuming induction period to detect primary and secondary oxidation products. The detection of radicals is a fast method that reflects the initial state of autoxidation. Alkyl and alkoxy radicals that are generated by modified Schaal-oven test and heat induced decomposition of methyl linoleate hydroperoxides are used as defined radicals present in the autoxidation process and monitored by EPR spin probing technique.

## 1.3 Theoretical background

### 1.3.1 Dispersed systems

Emulsifiers are surface-active molecules with an amphiphilic nature which is characterized by a non-polar (lipophilic) and a polar (hydrophilic) region. At low concentrations the dissolved emulsifiers are present as monomers. Due to hydrophobic effects, formation of micelles occur at first in the form of premicelles and, above the critical micelle concentration (cmc), as micelles. The cmc is characteristic for the emulsifier and depends on e.g. temperature, pH value, and electrolyte concentration of the system [Cui et al. 2008; Cid et al. 2013; Dörfler 2002]. The micelles formed by emulsifiers in a homogeneous aqueous phase are referred to as micellar pseudophases [Lisi and Milioto 1995; Dörfler 1994]. The spherical micellar structure can shift to rod-like or other forms with increasing emulsifier concentration, addition of co-surfactants or additives [Heins et al. 2006; Sangwai and Sureshkumar 2011; Dunaway et al. 1995; Bernat et al. 2010]. In inhomogeneous solutions with two immiscible components the emulsifiers form an interface between the continuous phase and the dispersed phase resulting in an emulsion.

#### 1.3.1.1 Micellar solutions

Emulsifiers form thermodynamic stable micelles in aqueous solutions. The aggregation of the micelles occurs spontaneously and is reversible. Monomers and micelles are in equilibrium above the cmc by continuous formation and decomposition of micelles while the concentration of monomers is constant [Patist et al. 2001]. The self-assembly of the monomers proceeds in several stages. First the monomers form oligomers which are disordered and unstable but constantly grow to larger aggregates. Collisions and further growth of these premicelles lead to an average aggregate size which is depending on the emulsifier and energy input until equilibrium is reached [Cui et al. 2008; Jorge 2008]. The stability of micelles occurs due to the hydrophobic effect of alkyl chains and the hydrophilic behavior of the headgroups. Therefore, spherical micelles can be described by a core-shell-model (figure 1.1). The hydrophobic core is formed by the alkyl chains which is, according to the Langmuir's principle, free of water and polar headgroups. The alkyl chains show a fluid and disordered character. The shell is referred to as the palisade layer. The headgroup is surrounded by a hydration shell and counter ions concerning ionic emulsifiers [Bruce et al. 2002; Lange 1999; Jönsson et al. 1995].

Ionic emulsifiers usually have small headgroups that are of cationic or anionic nature. The electric repulsion determines their packing as the charge of the headgroup requires a layer of water and counter ions. The polar headgroups of non-ionic emulsifiers are long organic chains in the form of a helical structure. The molecular weight is increased compared to ionic emulsifiers, which results in a larger size of micelles. The packing of the micelles is mainly determined by the steric limit of the emulsifiers, which are governed by the size of the headgroup and the length of the alkyl chain [Dörfler 1994].

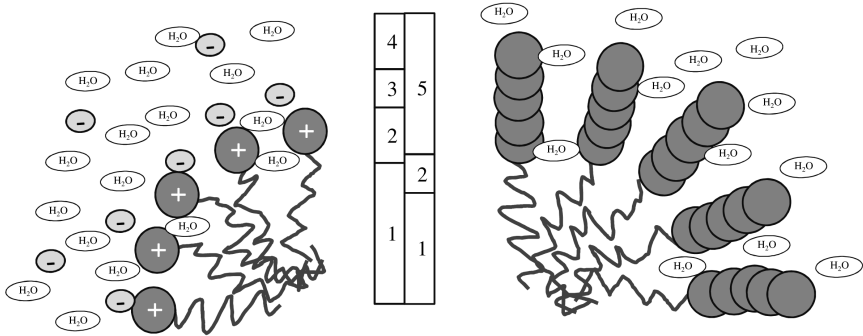


Figure 1.1: Simplified schemes of interfacial and micellar structures formed by ionic (left) and non-ionic (right) emulsifiers: hydrophobic core (1), palisade layer (2), stern layer with rigid layer (3) and diffuse layer (4), headgroup region (5).

### 1.3.1.2 Emulsions

The most important type of dispersed systems on the food product market is the oil-in-water (o/w) emulsion where the aqueous continuous phase surrounds the dispersed phase oil droplets. The emulsifier molecules accumulate at the surface of the oil droplets forming the interface. Pseudophases of unloaded micelles can also present in emulsions as monomeric emulsifiers (figure 1.2). The emulsifiers kinetically stabilize the droplets and prevent coalescence by reducing the interfacial tension between the two phases. The lower the interfacial tension, the lower is the tendency of the two phases to form the smallest possible contact surface. The ability of a surfactant to reduce the interfacial tension is given by the Gibbs' equation [Fox and McSweeney 1998]:

$$d\gamma = -R \cdot T \cdot \Gamma \cdot d\ln\alpha \quad (1.1)$$

Where  $\gamma$  is the interfacial tension,  $\Gamma$  is the excess concentration of the solute at the interface above that in the continuous phase,  $\alpha$  is the activity of the solute in the continuous phase,  $R$  is the universal gas constant and  $T$  is the absolute temperature. The processing of food emulsions is done in colloid mills or high pressure homogenizers where shear forces tear the oil phase into small droplets. The formation of small droplets is limited by the emulsifier concentration [McClements 2010; Dalgleish 2004]. For a laboratory scale an ultrasonic homogenizer can be used to produce small volumes.

### 1.3.1.3 Swollen micelles

The term 'swollen micelle' is used in this thesis for o/w emulsions containing only a very small amount of lipid. The term is not clearly defined and often accompanied or mixed up

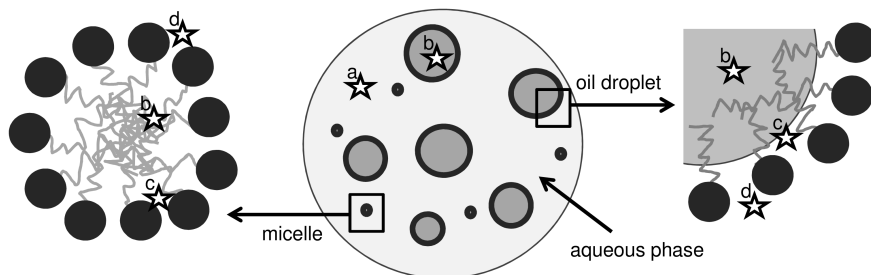


Figure 1.2: Schematic structures of an emulsion with coexisting micellar phases and oil droplets with enlarged interfaces. Solubilisation sites are in the aqueous phase (a), hydrophobic core (b) and in the interface (palisade layer (c) and Stern layer (d)).

with micro- or nano-emulsions. Most authors define the micelles as swollen when a defined ratio between emulsifier wt% and oil wt% is used [Anton and Vandamme 2011; Swafford et al. 1991; Menge et al. 1999].

### 1.3.2 Partitioning, solubilisation and dynamics in dispersed systems

The solubility of lipophilic molecules can be increased by dispersed systems. Therefore, micellar structures are often used in pharmaceuticals, cosmetics and foods [Cid et al. 2013; Coupland and McClements 1996; Romsted and Zhang 2002; McClements 2010; Jores et al. 2003; Kempe et al. 2010]. The logarithm of octanol-water partitioning coefficient ( $\log P$ ) is often used to determine the hydrophobicity of compound is assumed to represent a general tendency of the molecule to partition between an aqueous and an organic phase. Even though the  $\log P$  only gives a vague estimation about the solubilisation site of a solute in dispersed systems it is commonly accepted to quote the fraction of molecules adsorbed into the membrane [Fabris et al. 2008]. The partitioning in dispersed systems depends on many factors such as temperature, pH value, structural properties of the different environments and the concentration of emulsifier and solute [Schwarz et al. 1996]. It has to be noticed that coexisting micellar phases play an important role in the solubilisation properties of emulsions [Stöckmann et al. 2000]. Different methods to determine the partitioning are described in 1.4.7 and in chapter 3. Briefly, there are invasive and non-invasive methods. The invasive methods such as ultrafiltration (UF) require a careful experimental setup as separation techniques often influence the equilibrium [Oehlke et al. 2008; Stöckmann et al. 2000]. Spectroscopic methods such as nuclear magnetic resonance (NMR), electron paramagnetic resonance (EPR) and small angle neutron scattering (SANS) are non-invasive methods [Heins et al. 2007a, 2007b; Dupont-Leclercq et al. 2007; Oehlke et al. 2008]. Other

kinds of non-invasive methods are kinetic models [Romsted and Zhang 2002] and line shape analysis for paramagnetic molecules [Štrancar et al. 2005].

The locations within the dispersed systems depend on the lipophilicity and structure the incorporated molecules apart from the emulsifier properties. Hydrophobic effects occur at solubilisation sites in the core region and interactions between emulsifier and solute predominate in the headgroup region. The increased surface area is the important property of dispersed solutions as it provides space for solutes and either accelerate or reduce molecular reactions. The solutes can also compete with the emulsifier monomers for available position at the interface. The presence of ascorbic acid, e.g., at an air-water interface increases the minimum surface area per molecule of SDS threefold. This significantly alters the structure of the hydration sphere for each emulsifier molecule, and raising the temperature under these conditions significantly increases packing of the surfactant molecules [Cid et al. 2013]. The lipophilic  $\alpha$ -tocopherol is located in the interfacial region to 73 % in a Brij30 stabilized octane-in-water emulsions [Gunaseelan et al. 2006]. Aromatic molecules are solubilized in the Stern layer of anionic micelles, in the palisade layer of cationic micelles and in the headgroup region of non-ionic micelles [Heins et al. 2007b]. Different solubilisation sites are possible for a solute in dispersed systems (figure 1.2) as the solutes are in equilibrium between the different phases.

The dynamics in dispersed systems is another advantage of these systems and can be determined by NMR [Crans et al. 2006] or simulation studies [Faeder and Ladanyi 2000]. Self-diffusion of emulsifier monomers, micelles and solutes affect the system as the molecules move constantly and the formation and degradation of micelles are predominant. Surfactant micelles dissolve solubilized lipid hydroperoxides out of emulsion droplets, which could decrease free radicals in the lipid droplets due to hydroperoxide decomposition. In addition, surfactant micelles can solubilize iron and remove it from emulsion droplets, a factor that could also inhibit lipid oxidation [Cho et al. 2002; Nuchi et al. 2002].

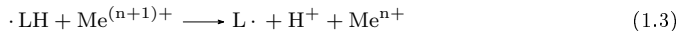
### 1.3.3 Lipid oxidation

The stability and stabilization of polyunsaturated fatty acids (PUFAs) in foods are a challenge because these fatty acids are highly susceptible to lipid oxidation. The oxidation of the PUFAs leads to a decrease in their nutritional value and off-flavor compounds. The oxidative stability of the lipids determines the shelf lives. Lipid oxidation is promoted by some factors concerning the raw material and the conditions during product processing and storage. The main attributes are metal ions, like iron and copper, which are widely present in foods, or a pre-contamination with hydroperoxides. The product processing is usually accompanied by factors that accelerate lipid oxidation such as the presence of oxygen, heating or storage temperature and light exposure [Frankel 1993; Thomsen et al. 2000].

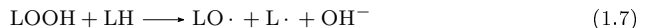
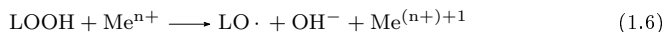
The basic condition for the initiation of autoxidation is the presence of small amounts of free radicals. Radicals are atoms or molecules with an unpaired electron. They can abstract a hydrogen atom from a methylene group situated between two double bonds or as part

of an allyl group. Thereby a free radical is generated on the fatty acid molecule. With an increasing degree of unsaturation the abstraction energy lowers as the radical is stabilized by electron delocalization. Therefore, the lipid oxidation is a free radical chain pathway that is divided into steps: initiation, propagation and termination [Roman et al. 2012; Frankel 2005]. During the initiation step, primary lipid radicals in the form of alkyl radicals ( $L\cdot$ ) are formed from autoxidative processes that are often accelerated due to food processing and storage time. The process starts with the hemolytic fission of the lipid alkyl chain (1.2) or as a consequence from the attack of reactive oxygen species, which are able to abstract hydrogen ( $H\cdot$ ) from the alkyl chain ( $LH$ ). These chemical processes require energy, which can be supplied by heat, electromagnetic radiation, redox reactions, etc. As lipid samples are inevitably contaminated by traces of hydroperoxides the secondary initiation is the most likely initiating event (1.4). The preexistent hydroperoxides lead to the formation of hydroxyl ( $\cdot OH$ ) and alkoxy radicals ( $LO\cdot$ ). Traces of metal ions contribute to both initiation steps (1.3, 1.5 and 1.6). In the propagation step the free alkyl radicals further react with oxygen (1.8) to create peroxy radicals ( $LOO\cdot$ ), which can again abstract a hydrogen atom from a methylene group, leading to a hydroperoxide ( $LOOH$ ) in addition to another alkyl radical (1.9). The alkoxy radicals formed during hydroperoxide decomposition react with acyl chains (1.10) producing acyl radicals and alcohol ( $LOH$ ). The radical chain reaction terminates when two radicals react (1.11-1.14) [Abuja and Albertini 2001; Frankel 2005; Cimato et al. 2004; Roman et al. 2012].

Primary initiation:



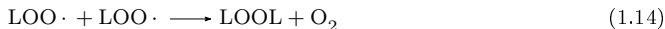
Secondary initiation:



Propagation:



Termination:



In further decomposition reactions, volatile secondary oxidation products such as aldehydes, ketones, alcohols and hydrocarbons are formed [Frankel 2005].

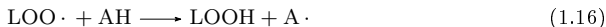
### 1.3.3.1 Lipid oxidation in emulsions

In emulsions the unsaturated fatty acids are mostly located within the oil droplets. A few molecules can also be present in the interface. Lipid hydroperoxides are more polar than the non-oxidized lipid molecules and therefore a higher concentration can be found at the interface than in the more hydrophobic core of the oil droplet [McClements and Decker 2000; Nuchi et al. 2002]. The interface has been suggested to be the most relevant region for occurrence of lipid oxidation and surface active antioxidants are particularly effective oxidation inhibitors [Mosca et al. 2013; Waraho et al. 2011; Heins et al. 2007a, 2007a]. In general, the autoxidation mechanisms in emulsions are thought to be the same as in bulk oils [Genot et al. 2003]. As described above, metal ions and free radicals play an important role in the autoxidation process. The source of metal ions in emulsions is broad. They occur in water, oil, buffer substances and emulsifiers [Boon et al. 2009]. The latter is also discussed to contain traces of peroxides [Mancuso et al. 1999]. The pH value of the emulsion influences the oxidative stability that increases with decreasing pH [Haahr and Jacobsen 2008]. The surface charge of the droplets also plays an important role in the lipid oxidation process. Pro-oxidative cations are electrostatically repelled into the continuous phase by a positive surface charge, away from the interface where lipid hydroperoxides are prone to metal-induced decomposition. In contrast, emulsions stabilized with anionic surfactants oxidize very quickly due to the electrostatic attraction of cationic transition metals to the droplet surface where they promote lipid oxidation [Boon et al. 2008; Genot et al. 2003]. The presence of sodium chloride, that does not affect the oxidation, is supposed to compete with pro-oxidative ions for negatively charged binding sites on the surface and thus decreases the lipid oxidation [Mei et al. 1998].

It is important to predict the oxidative stability of food by rapid and reliable methods in order to determine shelf life and to evaluate the effect of protective antioxidants. Ambient storage conditions are often too time consuming for practical use, but methods with high temperature or addition of prooxidants such as the Schaal oven test, the Rancimat method, and the active oxygen method are often criticized for giving wrong predictions [Frankel 1993]. Therefore, radical detection methods were experimented as the initial oxidation step can be monitored [Thomsen et al. 2000; Hawkins and Davies 2013].

### 1.3.3.2 Antioxidative reactions in dispersed systems

Antioxidants can either prevent initiation or intercept lipid peroxy radicals involved in the propagation phase [Abuja and Albertini 2001]. Primary antioxidants are also called chain-breaking antioxidants. They are reducing agents and inhibit the lipid oxidation process by scavenging free radicals. The antioxidant donates a hydrogen atom to the free radical-bearing molecule such as lipid radicals, hydroxyl radicals, alkoxy radicals or peroxy radicals (1.15, 1.16, 1.17). The free radical is thereby transferred to the antioxidant molecule, on which it is resonance stabilized and less reactive [Roman et al. 2012; Yanishlieva-Maslarova et al. 2001; Genot et al. 2003].



Antioxidant activity can be divided into the hydrogen atom transfer reaction and the single electron transfer reaction [Huang et al. 2005]. Phenoles, like gallate derivatives, have a high antioxidant activity by transferring a hydrogen atom from their hydroxyl group to the oxygen-centered radical. This mechanism most likely involves a concerted transfer of the hydrogen as a proton and of one electron between the two oxygen atoms (proton-coupled electron transfer mechanism). Due to the weak hydrogen bond in the hydroxyl groups they donor a hydrogen atom. The remaining electron is delocalized within the  $\pi$ -electron system of the aromatic ring structure. Solvents accepting hydrogen-bonds, such as alcohols, reduce the antioxidant capabilities of phenols because the hydrogen bond is not available [Foti 2007; Brigati et al. 2002]. Radical scavenging can also be achieved by single electron transfer. This mechanism is influenced by either electron donating or electron withdrawing substituents. The reaction enthalpies of electron donating groups is increased in hydrated environments such as water [Najafi et al. 2011].

Secondary antioxidants can prevent lipids from oxidation by stabilizing unstable intermediate products such as hydroperoxides or they can act as a chelator by building a complex with metal ions. Even continuous phase chelators like EDTA can remove iron ions from the droplet interface, and therefore the lipid core, towards the bulk phase [Cho et al. 2003]. Proteins have also been reported to have chelating properties. The location of chelators is a relevant factor for achieving an effective chelation process.

The location of antioxidants in dispersed systems is determined by their partitioning which often leads to local concentration effects especially at the interface [Oehlke et al. 2010, 2011; Heins et al. 2007a, 2007b]. The access of antioxidants from the continuous phase to the interface can be limited, and their effectiveness reduced, if their electric charge is the same as the interface. The partially negativ charged galloyl derivatives do not associate with SDS stabilized emulsions [Mei et al. 1999]. In anionic SDS micelles antioxidative



spin probes have a protective effect against ascorbate ions, but a spin probe incorporation into cationic DTAB micelles accelerated the spin probe-ascorbate ions interactions [Berton-Carabin et al. 2012]. A high interfacial antioxidant concentration is assumed to be beneficial towards the inhibition of lipid oxidation [Berton-Carabin et al. 2012; Pryor et al. 1993; Barclay and Vinqvist 1994]. In addition, the distinct location within the interface accelerates the reaction as demonstrated for stable free radicals and gallate esters with increasing chain length [Heins et al. 2007a]. The overall effectiveness of free radical scavenging depends on the polarity, location and oxidation stability of the antioxidants and the type and concentration of free radicals in the different phases. The different kinds of antioxidants can inhibit lipid oxidation by complexation of metal ions that initiate the oxidation, scavenge radicals before hydroperoxides are formed or prevent the decomposition of hydroperoxides to secondary oxidation products [Frankel 2005].

## 1.4 Experimental approach

### 1.4.1 Description of model compounds

#### 1.4.1.1 Emulsifiers

The cationic CTAB, anionic SDS and non-ionic Brij58 are used to form differently charged dispersed systems. Comprehensive data are available in literature [Sabatino et al. 2010; Heins et al. 2006, 2007a, 2007b; Sowmiya et al. 2010; Oehlke et al. 2008, 2011; Stöckmann et al. 2000; Berton-Carabin et al. 2012; Barclay et al. 1997; Cid et al. 2013]. Their structures are shown in figure 1.3.

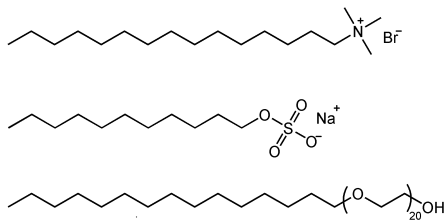


Figure 1.3: Chemical structures of CTAB (a), SDS (b) and Brij58 (c)

#### 1.4.1.2 Spin Traps

The additional reaction of a free radical to a diamagnetic spin trap is a prerequisite for spin trapping experiments. The spin trap-radical adduct is a relatively long-lived free radical product that can be studied by EPR. Therefore, EPR spin trapping provides a sensitive

method for evaluating the oxidative stability of food lipids. Detection of radicals in the lipid as an early event in oxidation allows mild conditions to be used [Thomsen et al. 2000]. The advantage of spin traps is the possibility to identify the radical species. The spectral structure gives information as to whether the radical is carbon-centered, oxygen-centered or nitrogen-centered.

There are two kinds of spin traps, the nitron and nitroso compounds. The nitroso compounds form relatively unstable adducts with oxygen-centered radicals, but with nitrones some information is lost because the trapped radical adds to a carbon adjacent to the nitrogen [Hawkins and Davies 2013]. The hydrophilic DMPO (5,5-dimethyl-1-pyrroline N-oxide) and the more lipophilic PBN (N-tert-butyl- $\alpha$ -phenylnitron) (figure 1.4) belong to the most popular spin traps. The cyclic nitrones (e.g. DMPO, DBPMPO, OMPO) provide more distinctive data than the linear nitrones such as PBN, because cyclic nitrones have a  $\beta$ -hydrogen atom providing considerable information about the radical trapped [Hawkins and Davies 2013; Buettner 1987]. Because of their versatility, various derivatives such as DBPMPO and OMPO have been synthesized to study radicals in a more lipophilic environment and increase the half-life of the adducts [Stolze et al. 2002, 2000a, 2000b; Gamliel et al. 2008]. Spin trapping of lipid derived radicals with PBN has already been extensively studied. Unfortunately, the short half-life of PBN adducts with oxygen-centered radical spin adducts restricts its use to the detection of carbon-centered radical adducts. Furthermore, the similarity of the ESR spectra of different PBN spin adducts renders spectral identification of the trapped species rather difficult [Janzen et al. 1992; Stolze et al. 2000a]. The following spin traps were used in this study:

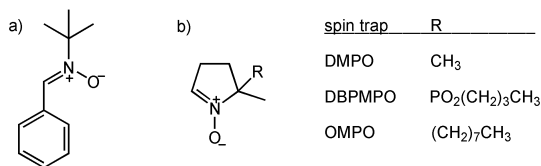


Figure 1.4: Structure of spin traps PBN (a) and DMPO derivatives (b).

### 1.4.1.3 Spin Probes

The most important class of paramagnetic tracer molecules are spin probes. These stable free radicals with the structural unit R<sub>2</sub>NO are commonly called nitroxides. They achieve their stability due to full methyl substitution in  $\beta$ -position and a delocalized spin density where approximately 40 % are on the nitrogen atom and 60 % are on the oxygen atom. The typical radical reactions like dimerization and disproportionation are inhibited. In contrast to the spin traps spin probes interact non-covalently with the system. The motion of nitroxides is strongly influenced by the dynamics and local structure of their surrounding. Therefore they can be used as tracers in the systems and indirectly de-

liver information about the internal structure of a system [Kocherginsky and Swartz 1995; Hubbell et al. 2000]. A detailed description about the characteristics of a nitroxide EPR spectrum is given in section 1.4.4. Nitroxides used were TEMPO (2,2,6,6-Tetramethyl-1-piperidinyloxy radical) and its more hydrophilic derivate TEMPOL (4-Hydroxy-2,2,6,6-tetramethyl-1-piperidinyloxy) and the lipophilic TEMPOL-benzoate (4-Hydroxy-2,2,6,6-tetramethylpiperidine-1-oxyl-benzoate) (figure 1.5):

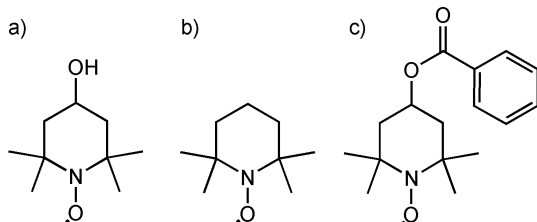


Figure 1.5: Chemical structures of TEMPOL (a), TEMPO (b) and TEMPOL-benzoate (c)

The spin scavenging ability of nitroxides is influenced by their ability to shuttle between different oxidation states [Lardinois et al. 2009]. The redox cycle of nitroxide TEMPO and its derivatives form the basis of many applications. The cycle includes the inter-conversion of TEMPO, TEMPOH (hydroxylamin) and oxoammonium ion (figure 1.6) [Soule et al. 2007; Ma et al. 2011].

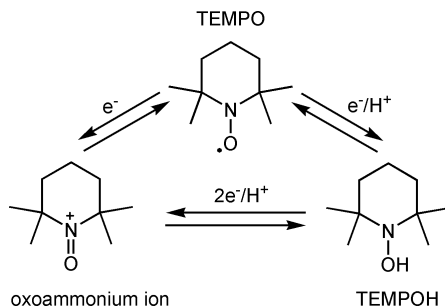


Figure 1.6: Inter-conversion of TEMPO, TEMPOH and oxoammonium salt

The inter-conversion scheme shows that only the nitroxide is of paramagnetic nature, therefore the hydroxylamine and the oxoammonium cation are not detectable with EPR (see 1.4.3) [Ma et al. 2011]. The antioxidative activity of nitroxides is widely used [Soule et al. 2007; Amorati et al. 2010; Lardinois et al. 2009]. Radical formation can be inhibited in biological matrices due to the catalytic property of nitroxides, because they can be recycled in the system without forming additional products [Lardinois et al. 2009]. The

reaction pathway of the antioxidative capability of nitroxides towards peroxy radicals is the proton-coupled electron transfer from a protonated nitroxide. However, this is only possible in acidic media when the equilibrium is directed towards the protonated form that still carries a radical. Apart from the application as spin probes and antioxidants, TEMPO and its derivatives are used i.a. as catalyst for controlled radical polymerization reactions and for controlled oxidation of primary alcohols [Amorati et al. 2010]. The Nitroxide spin scavenging technique is a powerful method to examine radical formation. Apart from determining the data on the type of radical, it is also possible to determine the exact location of the nitroxide and the radical [Hawkins and Davies 2013].

#### 1.4.1.4 Antioxidants

Apart from propyl gallate the lipophilic  $\alpha$ -Tocopherol and the hydrophilic analogue Trolox were used as antioxidants (figure 1.7). The latter is widely used as a model antioxidant due to its high activity [Oehlke et al. 2011; Shahidi and Zhong 2007; Lucio et al. 2009; Barclay et al. 1997; Friaa and Brault 2006]. The radical scavenging mechanisms and its autoxidation have been observed. Because of the structural similarity the reaction mechanisms can, to some extent, be transferred to  $\alpha$ -Tocopherol. The properties of propyl gallate have been investigated in detail in former studies [Schwarz et al. 1996; Stöckmann et al. 2000; Heins et al. 2006, 2007a; Giuffrida et al. 2007].

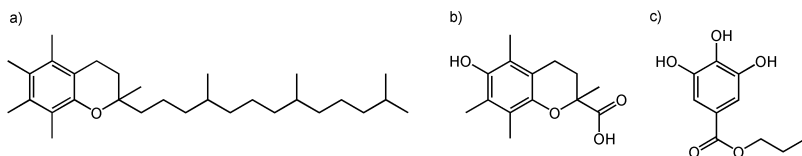


Figure 1.7: Chemical structures of  $\alpha$ -Tocopherol (a), Trolox (b) and propyl gallate (c).

### 1.4.2 Basics of EPR and NMR spectroscopy

The electron paramagnetic resonance spectroscopy (EPR), also known as electron spin resonance spectroscopy (ESR), and nuclear spin resonance (NMR) are both spectroscopic methods that require an external magnetic field. The basic principle is the absorption of electromagnetic radio-frequency of particles that align with the magnetic field. In EPR technology, the spin of an unpaired electron is the prerequisite, while the NMR technology deals with nuclear spins. The magnetic dipole moment  $\mu$  of either an electron or a nucleus is given by

$$\mu = \gamma \cdot J \quad (1.18)$$

where  $J$  is the angular momentum and  $\gamma$  is a proportionality factor, that is known as the gyromagnetic ratio in NMR spectroscopy and depends on the nucleus or, in case of EPR,

includes the Bohr magneton  $\mathfrak{B}$  and the g-factor (Landé factor). The eigenstates of both spins, from electrons and nuclei, have discrete orientations. The spin quantum number  $I$  can be half-integer or integer values. The magnetic quantum number  $m$  takes  $2I+1$  values between  $-I$  and  $+I$ . The eigenstates of the spin are degenerative. The application of an external magnetic field  $B$  leads to a distinct orientation of the spins, which is either parallel or anti-parallel to the direction of the magnetic field (Zeeman effect). The energy difference  $\Delta E$  between spin states is given by:

$$\Delta E = m \cdot \gamma \cdot \hbar \cdot B \quad (1.19)$$

for nuclei, with  $\hbar$  is the Planck's constant and:

$$\Delta E = g \cdot \beta \cdot B \quad (1.20)$$

for electrons with  $g = 2.00023$  for free electrons. The energy difference between the two states is proportional to the strength of the external magnetic field. For high resolution experiments the magnetic fields of more than 10 Tesla are required for NMR. Due to the lower mass of electrons compared to nuclei, EPR experiments of 0.3 Tesla are sufficient. The probes exist of condensed material with a great number of spins. In a thermal equilibrium the magnetic momentums in an external field distribute among the defined energy states described by the Boltzmann distribution.

$$\frac{N^-}{N^+} = \frac{(1 - E)}{(k \cdot T)} \quad (1.21)$$

Where  $N$  represents the number of spins in the lower ( $-$ , parallel) and higher ( $+$ , anti-parallel) energy state,  $k$  is the Boltzmann constant and  $T$  the absolute temperature. The application of perpendicular microwave radiation leads to resonance when the absorbed microwave energy is equal to  $\Delta E$ .

$$\Delta E = \hbar \cdot \nu \quad (1.22)$$

This energy of the distinct frequency  $\nu$  causes the transfer from the lower energy state to the higher energy state. In EPR spectroscopy a constant microwave frequency is applied and the magnetic field is scanned depending on the radical type. The common X-band spectrometers operate with a frequency from 9 to 10 GHz, while frequencies between 60 and 800 MHz are required for NMR experiments. The Fourier transform (FT) NMR spectrometer works with a constant magnetic field and varying frequencies and where short pulses of radio-frequency radiation are excited. The significant discrepancy between EPR and NMR is based on the different time scales which is caused by the distinct magnetic moments of nuclei and electrons. Apart from the different resonance frequencies the relaxation times vary from ms for nuclear  $T_1$  and  $T_2$  times in diamagnetic molecules (NMR) to ns for electronic transverse relaxation times  $T_2$  (EPR). The required NMR pulses are 10  $\mu$ s

or slower while EPR pulses are in the range of few ns or even faster [Atkins and Friedman 2011; Hawkins and Davies 2013; Lund et al. 2011; Möbius and Savitsky 2008; Weil and Bolton 2007].

### 1.4.3 EPR spectroscopy

With EPR spectroscopy paramagnetic species can be studied such as:

- free radicals in solids, liquids and gases: they can be atoms, molecules or ions.
- transition metals and rare earth ions: in these systems often multiple unpaired electrons exist.
- defects in materials: in crystals and glasses the unpaired electron occupies the empty space for an anion.
- diradicals: molecules with two unpaired electrons, which are spatially separated.
- triplet states: molecules with two interacting unpaired electrons, which are usually excited electronic states.

Studies with EPR are therefore limited to a small group of probes. That could be a disadvantage, but it is also an advantage because interferences are rare. By introducing a spin probe or spin label to a system, materials without an unpaired electron or short living radicals can be studied (Berliner, 1976). The measured spectrum is the derivative of the absorption. EPR spectra can be very complex depending on several factors, like the number of unpaired spins at the paramagnetic molecule, the chemical structure, the environment and the physical state. The unpaired electron is sensitive to its local surroundings. Therefore with EPR technique the local environment such as fluidity, viscosity and polarity as well as the molecular structure next to the unpaired electron and the molecular motion can be studied [Weil and Bolton 2007].

The g-factor: The orbital angular momentum of the electron contributes to the resonance as shown in equation 1.18. The value of the g-factor depends on the molecule structure, the physical state and the location of the unpaired electron within the molecule.

The hyperfine couplings: The nuclei of nearby atoms that have magnetic moments produce a local magnetic field at the electron. The interaction of unpaired electrons and nuclei is called hyperfine interaction and is characterized by a specific line pattern, the hyperfine coupling. The number of lines ( $l$ ) of a spectrum due to hyperfine splitting depends on the interacting nucleus:

$$l = 2 \cdot n \cdot s + 1 \tag{1.23}$$

Where  $n$  is the number of nuclei and  $s$  is the nuclear spin of the nucleus. When the value of the hyperfine splitting constant is larger than the line broadening separated peaks are observed in the EPR spectrum [Hawkins and Davies 2013]. The hyperfine splitting constant provides information about the identity and number of atoms interfering with the electron

and monitors the polarity of the molecular environment [Jores et al. 2003]. The hyperfine interactions from the protons are strongly overlapping and are unresolved. This leads to a line broadening of each peak [Kao et al. 2007].

The rotation correlation time  $\tau_c$  : In this thesis only fast isotropic motion is considered. Therefore the molecule with the unpaired electron tumbles rapidly in solution or membranes. The rotation correlation time  $\tau_c$  describes the rate of motion of the spin label in micelles and reflects the dynamic of its surroundings, which is proportional to the microviscosity [Dejanovic et al. 2008]. The spectral line shape gives information on the dynamic processes such as molecular motion and fluidity at the local environment (Freed et al., 1971; Freed & Fraenkel, 1963).

The concentration of EPR active species in a sample is related to the peak intensity, but line broadening occurs at high radical concentration. Radical concentrations of 1 mmol are more than sufficient for the spectral resolution. The radical content is given by the peak area which is determined by the double integral of the complete spectrum.

#### 1.4.4 EPR characteristics of nitroxides

The EPR method is sensitive to rotational diffusion rather than translational motion since only angular motions relative to the external magnetic field affect the magnetic interactions and the spectral line shapes. Nitroxide stable radicals show a three line pattern from the interaction of the unpaired electron, which is localized on the N-O bond, with the nitrogen, while the proton signals are unresolved. The nitrogen nucleus ( $^{14}\text{N}$ ) has a nuclear spin of 1 and, according to the quantum theory, can take three possible orientations (equation 1.23) [Hawkins and Davies 2013; Lurie and Mäder 2005; Kao et al. 2007]. If the rotation is very fast, the hyperfine couplings are an average of different directions that form an isotropic value and the spectrum consists of three equal lines. An anisotropic spectrum is obtained, if the rotational motion is prohibited e.g. in powders. The actual spectral shape depends on the time frame of the rotational diffusion and is characterized  $T_1$ . The high field peak is most strongly affected by the cumulative effect of  $g$  and  $A$  anisotropy [Lurie and Mäder 2005; Jeschke and Schlick 2006]. There are established methods used to infer  $T_1$  in the fast motion regime [Keith et al. 1970; Cimato et al. 2004; Kveder et al. 1997], but these methods break down if the spectra consist of several overlapping species. Therefore a fitting with spectral deconvolutions is necessary to obtain values for each species.

In addition to dynamics, spin probes also provide information about their local environment. The electronic structure of a nitroxide is slightly altered depending on the interaction with molecules in its surroundings. The solvent polarity influences the hyperfine coupling constants ( $a_N$ ) and  $g$ -values of a spin probe where the alterations add up at the high field line. The  $a_N$  of nitroxides is 17 G in isotropic media and 14 G in an unpolar environment. The superimposition can be noticed at the high field peak. Thus spin probes in different nanoscopic environments in dispersed systems can be distinguished and analyzed separately. The  $g$ -factor for nitroxides is  $g = 2.006$  in isotropic media.

### 1.4.5 EPR deconvolution

The structural and dynamic parameters of an EPR spectrum in a homogeneous media can be inferred by straightforward analysis. The spectrum of a paramagnetic substance in dispersed systems consists of several superimposed spectral components, complex rotational dynamics and unresolved couplings. The partitioning between the different phases divides the substance in different populations with individual spectral behavior. Deconvolution that divides the superimposed spectrum in spectral components can be carried out with EPRSIM-C software developed by Štrancar and colleagues [2005]. To separate these individual spectra from the experimental spectrum different biophysical models are used based on the following parameters: line shape (Lw), rotational correlation time ( $\tau_c$ ), relative weight (d), order parameter (S), broadening constant (W), and polarity correction factors for the g and A tensors ( $p_g$  and  $p_A$ ). Three of the models were used to describe nitroxides solubilization in micellar solutions or emulsions. A paramagnetic species that is completely solved reveals in an isotropic spectrum if the thermodynamic motion of the molecule is very fast. The first model of the EPRSIM-C software is used for an isotropic tumbling spin probe. The characteristics of the isotropic spectrum is an even line shape with symmetric narrow lines, equal widths and same heights. Another model describes a fast tumbling spin probe in a concentrated cluster in an isotropic environment. In the concentrated cluster spin exchange between the individual molecules is considered. A fast tumbling spin probe in an anisotropic environment like the headgroup or inner core of a micelle can also be simulated by a model for membrane associated substances. The spectral shape of an anisotropic spectrum gains a broad line width with stronger tendency towards the high field. Therefore, the spectral shape of each specific population in a dispersed system gives information on the microenvironment that can be defined by the biophysical parameters mentioned above [Štrancar et al. 2005, Berliner 1976; Jores et al. 2003].

### 1.4.6 NMR diffusion experiments

With the NMR spectroscopy nuclei with a spin of  $1/2$ , for example  $^1\text{H}$ ,  $^{13}\text{C}$ ,  $^{15}\text{N}$ ,  $^{19}\text{F}$ ,  $^{29}\text{Si}$  or  $^{31}\text{P}$ , which can take two energy levels corresponding to the magnetic spin quantum numbers  $1/2$  and  $-1/2$  can be studied. Due to interactions between the spin-bearing nucleus and neighboring nuclei in a molecule and the resulting signal splitting, molecule structures can be elucidated. The modern NMR instruments use impulse excitation with a subsequent Fourier transformation. Chemical shifts arise due to the interaction of the nuclear spin with electrons, which are perturbed by the static magnetic field. With pulsed field gradient (PFG) NMR the molecular diffusion can be studied. Diffusion is the random Brownian motion of molecules that is driven by internal thermal energy. The mathematical background of the diffusion process is based on Fick's first and second law of diffusion. Fick's first law



relates the diffusive flux ( $J$ ) to the change in concentration ( $\partial c$ ) across a given plane ( $\partial x$ ):

$$J = -D \frac{\partial c}{\partial x} \quad (1.24)$$

Where  $D$  is the diffusion coefficient.

Fick's second law states that the change in concentration over time ( $\partial t$ ) is equal to the change in local diffusion flux:

$$\frac{\partial c}{\partial t} = D \frac{\partial^2 c}{\partial x^2} \quad (1.25)$$

With NMR spectroscopy self-diffusion of the molecules is determined and the Stokes-Einstein equation describes the diffusion coefficient:

$$D = \frac{(k_B T)}{(6\pi \cdot \eta \cdot R)} \quad (1.26)$$

Where  $k_B$  is the Boltzmann constant,  $T$  is the temperature,  $\eta$  is the viscosity and  $R$  is the radius of the molecule. Typical self-diffusion coefficients in liquids at room temperature range from  $10^{-9} \text{ m}^2 \text{ s}^{-1}$  for small molecules in non-viscous solutions to  $10^{-12} \text{ m}^2 \text{ s}^{-1}$  for polymers in solution. In PFG experiments pulse sequences are employed to measure diffusion. The spin echo sequence was introduced by Hahn [1950], who pointed out that the echo amplitude is influenced by the Brownian motion of the molecules because of the local magnetic field fluctuations. Initially magnetization is parallel to the external field. A  $90^\circ$  pulse is then applied along the x-direction. During a period of time, each spin experiencing a slight variation in magnetic field begins to dephase. The variations in the magnetic field arise from transverse relaxation due to spin-spin interactions and inhomogeneities in the external magnetic field. It is important to make the latter reversible. At a certain time  $\tau$  a  $180^\circ$  pulse is applied along the y-direction. Thereby the spins are rotated by  $180^\circ$  around the y axis. Each spin continues to precess with its former frequency and as a result of the inverted relative position, the spins are reclustered forming an echo. The application of a magnetic field gradient during dephasing and rephrasing periods makes it possible to monitor the self-diffusion. After each pulse, field gradients of a certain length  $\delta$  and strength  $g$  are applied. These gradients cause the spin in different positions in the sample to precess differently, enhancing the dephasing process. If the spins maintain their positions throughout the experiment, they will refocus completely into a spin echo by the pulse sequence at time  $2\tau$  (figure 1.8). But if they change position during the experiment, their precession rate will change and the refocusing is incomplete. This results in a decrease of the spin echo intensity [Stilbs 1987; Levitt 2008].

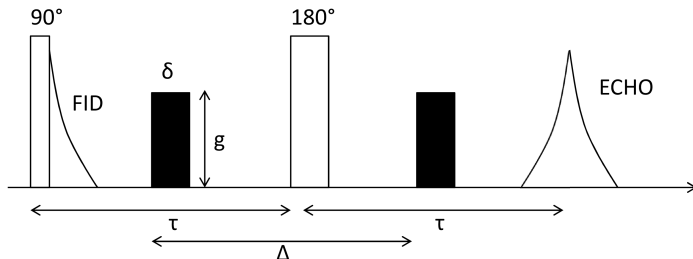


Figure 1.8: Pulse field gradient spin echo sequence. The echo appears after  $2\tau$ . After the  $90^\circ$  and  $180^\circ$  pulse are two pulse magnetic field gradients of length  $\delta$  and strength  $g$ .

## 1.4.7 Partitioning of paramagnetic substances

### 1.4.7.1 Ultrafiltration

Ultrafiltration (UF) is basically a pressure-driven separation process, governed by a membrane separation principle that depends on particle size. UF membranes are semipermeable and defined by the pore size which is given by the nominal molecular weight cut-off (MWCO). Frequent pore sizes are between 1 nm and 100 nm, thus allowing retention of compounds with a molecular weight of 300 to 500,000 Dalton. The separation efficiency is often not only influenced by the MWCO but also by interaction between the membrane and the solute. The latter is influenced by the membrane material which should be appropriate for the system to be separated. The application of a rotation force separates the filtrate that is able to pass the membrane from the remaining retentate. The application of UF in emulsions requires the separation of only a small fraction. A small volume of the aqueous phase of emulsions can be removed without interfering with the initial structure. Therefore the UF technique is qualified to determine the partitioning behavior of compounds dissolved in emulsions although it is an invasive method. The concentrations of solutes in the initial emulsion and the filtrate can be directly determined. The proportion of membrane associated nitroxides ( $d_{sol}$ ) can be calculated from the filtrate ( $c_{non-sol}$ ) and retentat ( $c_{total}$ ) concentration:

$$d_{sol} = 100 - \frac{c_{non-sol}}{c_{total}} \cdot 100 \quad (1.27)$$

The nitroxides in the collected samples were measured by EPR and the concentration was determined as relative concentrations by double integration of the signals.

### 1.4.7.2 EPRSIM-C

The deconvolution of EPR spectra is a non-invasive method to determine the partitioning of nitroxides [Grammenos et al. 2012; Abdalla and Mäder 2009; Arsov and Štrancar 2005;

Poklar Ulrich et al. 2010]. Parameters and information about the use of the EPRSIM-C software are available [Štrancar et al. 2005; Štrancar 2007; Berliner 1976]. The relative weight of different populations is given by simulation. As the  $a_N$  of individual populations depends on the polarity of the microenvironment, the location inside the membrane, aqueous phase or headgroup region can be determined. Information about the deconvolution is given above (see 1.4.5). The  $a_N$  was calculated by:

$$a_N = h_0 - h_{+1} \quad (1.28)$$

Where  $h_0$  and  $h_{+1}$  represent the  $g$  value at the maximum peak height from the middle field and the low field peak.

### 1.4.7.3 NMR diffusion

NMR diffusion measurement is another non-invasive technique to determine the partitioning of small molecules [Dupont-Leclercq et al. 2007; Sabatino et al. 2010; Wang et al. 2004; Otto et al. 2003; Kreilgaard et al. 2000]. LKO4O

$$d_{sol} = \frac{D_N - D_{mic}}{D_{Nbuffer} - D_{mic}} \cdot 100 \quad (1.29)$$

Where  $D_N$  and  $D_{Nbuffer}$  represent the self-diffusion coefficients of the sorbed nitroxides in micellar solution and the free nitroxides in buffer, and  $D_{mic}$  is the diffusion of the micelle.

The reported values for the diffusion of the micelle have been corrected to remove the contribution to the observed diffusion coefficient ( $D_{obs}$ ) from the free ( $D_{mono}$ ) detergent population using the equation after Vinogradova and colleagues [1998]:

$$D_{mic} = \frac{D_{obs} - \frac{cmc}{c_{emul}} \cdot D_{mono}}{1 - \frac{cmc}{c_{emul}}} \quad (1.30)$$

Where  $cmc$  is the critical micelle concentration and  $c_{emul}$  represents the total concentration of emulsifier.

## 1.4.8 Generation of free lipid radicals

### 1.4.8.1 Oxidation of corn oil emulsions

Lipid oxidation experiments in emulsions were carried out according to the Schaal oven test at 60 °C where typical autoxidation reactions occur [Frankel 2005; Thomsen et al. 2000]. Referring to equation 1.2 carbon-centered radicals were formed in the first step. Radical generation was measured with spin scavenging techniques as the stable nitroxide radicals react with lipid radicals. The content of EPR active nitroxides was determined by double integration of the signal prior to heating and the decrease was followed.

### 1.4.8.2 Production and decomposition of MeLOOHs

Conjugated diene hydroperoxides decompose to oxygen-centered radicals under heat treatment. They are generated during the course of fatty acid oxidation (equation 1.4-1.9). As in the first step carbon-centered radicals are formed that immediately react with the spin traps, MeLOOH were produced to measure the reaction of oxygen-centered radicals. Linoleic acid was methylated with methanol and the lewis acid bortriflouride as catalyst. The resulting fatty acid esters were oxidized at 60 °C in the dark under atmosphere oxygen until a maximum of hydroperoxides content was reached. MeLOOH were purified with column chromatography prior to use [Gardner 1975; Stolze et al. 2000a; Kadowaki et al. 2012; Ichihara and Fukubayashi 2010; Miyashita and Takagi 1986]. The hydroperoxides can be photometrically measured as they have a strong absorption maximum at 234 nm and are determined directly at this wavelength. Methyl linoleate hydroperoxide concentration  $c_{MeLOOH}$  [mmol/kg oil] was calculated using the extinction coefficient  $\varepsilon = 0.26$  [Chan and Levett 1977]:

$$c_{MeLOOH} = \frac{E \cdot d}{\varepsilon \cdot w} \quad (1.31)$$

Where  $E$  is the extinction at 234 nm,  $d$  the calculated dilution factor and  $w$  is the weighed sample. This method can only deliver reliable results in the early stage of lipid oxidation. Secondary oxidation products and polymers generated from the decomposition of lipid hydroperoxides at later stages of oxidation also absorb at 234 nm. It is also unsuitable for samples containing PUFAs [Fortier et al. 2009; Frankel 2005].

To decompose the MeLOOH to oxygen-centered radicals micellar solutions loaded with MeLOOH were heated at 100 °C to promote the degradation of hydroperoxides by breaking the O-O bonds (equation 1.4)[Roman et al. 2012].

## References

- Ahmed Abdalla and Karsten Mäder. 2009. ESR studies on the influence of physiological dissolution and digestion media on the lipid phase characteristics of SEDDS and SEDDS pellets. *International Journal of Pharmaceutics* 367, 1-2 (2009), 29-36.
- Peter M. Abuja and Riccardo Albertini. 2001. Methods for monitoring oxidative stress, lipid peroxidation and oxidation resistance of lipoproteins. *Clinica Chimica Acta* 306, 1-2 (2001), 1-17.
- Riccardo Amorati, Gian Franco Pedulli, Derek A. Pratt, and Luca Valgimigli. 2010. TEMPO reacts with oxygen-centered radicals under acidic conditions. *Chem. Commun.* 46, 28 (2010), 5139.
- Nicolas Anton and Thierry F. Vandamme. 2011. Nano-emulsions and Micro-emulsions: Clarifications of the Critical Differences. *Pharm Res* 28, 5 (2011), 978-985.
- Zoran Arsov and Janez Štrancar. 2005. Determination of Partition Coefficient of Spin Probe between Different Lipid Membrane Phases. *J. Chem. Inf. Model.* 45, 6 (2005), 1662-1671.
- Peter W. Atkins and Ronald Friedman. 2011. *Molecular quantum mechanics*. Oxford university press.
- L. R. C. Barclay, E. Crowe, and C. D. Edwards. 1997. Photo-initiated peroxidation of lipids in micelles by azaaromatics. *Lipids* 32, 3 (1997), 237-245.
- L. Ross C. Barclay and Melinda R. Vinqvist. 1994. Membrane peroxidation: Inhibiting effects of water-soluble antioxidants on phospholipids of different charge types. *Free Radical Biology and Medicine* 16, 6 (1994), 779-788.
- L. Ross C. Barclay and Melinda R. Vinqvist. 1994. Membrane peroxidation: Inhibiting effects of water-soluble antioxidants on phospholipids of different charge types. *Free Radical Biology and Medicine* 16, 6 (1994), 779-788.
- Avinoam Ben-Shaul and William M. Gelbart. 1994. Statistical thermodynamics of amphiphile self-assembly: structure and phase transitions in micellar solutions. In *Micelles, Membranes, Microemulsions, and Monolayers*. Springer, 1-104.
- L. J. Berliner. 1976. *Spin Labeling: Theory and Applications*. 1976. Academic Press, New York.
- Xavier Bernat, Emma Piacentini, Fabio Bazzarelli, Christophe Bengoa, Azael Fabregat, Enrico Drioli, Josep Font, and Lidietta Giorno. 2010. Ferrous Ion Effects on the Stability and Properties of Oil-in-Water Emulsions Formulated by Membrane Emulsification. *Industrial & Engineering Chemistry Research* 49, 8 (2010), 3818-3829.
- Claire C. Berton-Carabin, John N. Coupland, Cheng Qian, D. Julian McClements, and Ryan J. Elias. 2012. Reactivity of a lipophilic ingredient solubilized in anionic or cationic surfactant micelles. *Colloids and Surfaces A: Physicochemical and Engineering Aspects* 412, 0 (2012), 135-142.
- Caitlin S. Boon, D. Julian McClements, Jochen Weiss, and Eric A. Decker. 2009. Role of Iron and Hydroperoxides in the Degradation of Lycopene in Oil-in-Water Emulsions. *J. Agric. Food Chem.* 57, 7 (2009), 2993-2998.
- Caitlin S. Boon, Zhimin Xu, Xiaohua Yue, D. Julian McClements, Jochen Weiss, and Eric A. Decker. 2008. Factors Affecting Lycopene Oxidation in Oil-in-Water Emulsions. *J. Agric. Food Chem.* 56, 4 (2008), 1408-1414.
- Giovanni Brigati, Marco Lucarini, Veronica Mugnaini, and Gian Franco Pedulli. 2002. Determination of the substituent effect on the OH bond dissociation enthalpies of phenolic antioxidants by the EPR radical equilibration technique. *The Journal of Organic Chemistry* 67, 14 (2002), 4828-4832.
- Chrystal D. Bruce, Max L. Berkowitz, Lalith Perera, and Malcolm D. E. Forbes. 2002. Molecular dynamics simulation of sodium dodecyl sulfate micelle in water: micellar structural characteristics and counterion distribution. *The Journal of Physical Chemistry B* 106, 15 (2002), 3788-3793.
- Garry R. Buettner. 1987. Spin Trapping: ESR parameters of spin adducts 1474 1528V. *Free Radical Biology and Medicine* 3, 4 (1987), 259-303.
- C. Dunaway, S. Christian, and J. Scamehorn. 1995. Overview and history of the study of solubilization. *Solubilization in Surfactant Aggregates* 55 (1995), 3.
- Henry W.-S Chan and Gordon Levet. 1977. Autoxidation of methyl linoleate. Separation and analysis of isomeric mixtures of methyl linoleate hydroperoxides and methyl hydroxylinoleates. *Lipids*

- 12, 1 (1977), 99-104.
- Y-J Cho, J. Alamed, D. J. McClements, and E. A. Decker. 2003. Ability of Chelators to Alter the Physical Location and Prooxidant Activity of Iron in Oil-in-Water Emulsions. *Journal of Food Science* 68, 6 (2003), 1952-1957.
- Young-Je Cho, D. Julian McClements, and Eric A. Decker. 2002. Ability of Surfactant Micelles To Alter the Physical Location and Reactivity of Iron in Oil-in-Water Emulsion. *J. Agric. Food Chem.* 50, 20 (2002), 5704-5710.
- A. Cid, J. C. Mejuto, P. G. Orellana, O. López-Fernández, R. Rial-Otero, and J. Simal-Gandara. 2013. Effects of ascorbic acid on the microstructure and properties of SDS micellar aggregates for potential food applications. *Food Research International* 50, 1 (2013), 143-148.
- Alejandra N. Cimato, Lidia L. Piehl, Graciela B. Facorro, Horacio B. Torti, and Alfredo A. Hager. 2004. Antioxidant effects of water- and lipid-soluble nitroxide radicals in liposomes. *Free Radical Biology and Medicine* 37, 12 (2004), 2042-2051.
- John N. Coupland and D. Julian McClements. 1996. Lipid oxidation in food emulsions. *Trends in Food Science & Technology* 7, 3 (1996), 83-91.
- Debbie C. Crans, Christopher D. Rithner, Bharat Baruah, Bridget L. Gourley, and Nancy E. Levinger. 2006. Molecular Probe Location in Reverse Micelles Determined by NMR Dipolar Interactions. *J. Am. Chem. Soc.* 128, 13 (2006), 4437-4445.
- Xiaohong Cui, Shizhen Mao, Maili Liu, Hanzhen Yuan, and Youru Du. 2008. Mechanism of Surfactant Micelle Formation. *Langmuir* 24, 19 (2008), 10771-10775.
- Douglas G. Dalgleish. 2004. Food emulsions: their structures and properties. *Food emulsions* (2004), 1-44.
- Branka Dejanovic, Krunoslav Miroslavljevic, Vesna Noethig-Laslo, Slavko Pecar, Marjeta Sentjurg, and Peter Walde. 2008. An ESR characterization of micelles and vesicles formed in aqueous decanoic acid/sodium decanoate systems using different spin labels. *Chemistry and Physics of Lipids* 156, 1-2 (2008), 17-25.
- H. D. Dörfler. 1994. *Grenzflächen- und Kolloidchemie*. New York.
- H. D. Dörfler. 2002. *Grenzflächen und kolloid-disperse Systeme: Physik und Chemie*. Springer.
- Laurence Dupont-Leclercq, Sébastien Giroux, Bernard Henry, and Patrice Rubini. 2007. Solubilization of amphiphilic carboxylic acids in nonionic micelles: determination of partition coefficients from p K a measurements and NMR experiments. *Langmuir* 23, 21 (2007), 10463-10470.
- Sabrina Fabris, Federico Momo, Giampietro Ravagnan, and Roberto Stevanato. 2008. Antioxidant properties of resveratrol and piceid on lipid peroxidation in micelles and monolamellar liposomes. *Biophysical Chemistry* 135, 1-3 (2008), 76-83.
- J. Faeder and B. M. Ladanyi. 2000. Molecular dynamics simulations of the interior of aqueous reverse micelles. *The Journal of Physical Chemistry B* 104, 5 (2000), 1033-1046.
- Chanel A. Fortier, Bing Guan, Richard B. Cole, and Matthew A. Tarr. 2009. Covalently bound fluorescent probes as reporters for hydroxyl radical penetration into liposomal membranes. *Free Radical Biology and Medicine* 46, 10 (2009), 1376-1385.
- Mario C. Foti. 2007. Antioxidant properties of phenols. *Journal of Pharmacy and Pharmacology* 59, 12 (2007), 1673-1685.
- Patrick F. Fox and Paul L. H. McSweeney. 1998. *Physical properties of milk. Dairy chemistry and biochemistry*. Springer.
- E. N. Frankel. 1993. In search of better methods to evaluate natural antioxidants and oxidative stability in food lipids. *Trends in Food Science & Technology* 4, 7 (1993), 220-225.
- Edwin N. Frankel. 2005. *Lipid oxidation. Oily Press lipid library* (2nd. ed.). Oily Press; Lipid Technology, Bridgwater, England.
- Ouided Friaa and Daniel Brault. 2006. Kinetics of the reaction between the antioxidant Trolox and the free radical DPPH in semi-aqueous solution. *Org. Biomol. Chem.* 4, 12 (2006), 2417.
- A. Gamliel, M. Afri, and A. A. Frimer. 2008. Determining radical penetration of lipid bilayers with new lipophilic spin traps. *Free Radical Bio Med* 44, 7 (2008), 1394-1405.
- Harold W. Gardner. 1975. Decomposition of linoleic acid hydroperoxides. Enzymic reactions compared with nonenzymic. *J. Agric. Food Chem.* 23, 2 (1975), 129-136.
- C. Genot, Anne Meynier, Alain Riaublanc, and A. Kamal-Eldin. 2003. Lipid oxidation in emulsions. *Lipid oxidation pathways* (2003), 190-244.

- F. Giuffrida, F. Destailats, M. H. Egart, B. Hug, P. A. Golay, L. H. Skibsted, and F. Dionisi. 2007. Activity and thermal stability of antioxidants by differential scanning calorimetry and electron spin resonance spectroscopy. *Food Chemistry* 101, 3 (2007), 1108-1114.
- A. Grammenos, M. Fillet, M. Collodoro, S. Lecart, C. Quoilin, M.-P. Fontaine-Aupart, and M. Hoebeke. 2012. An ESR, Mass Spectrometry and Fluorescence Microscopy Approach to Study the Stearic Acid Derivatives Anchoring in Cells. *Appl Magn Reson* 43, 3 (2012), 311-320.
- K. Gunaseelan, Laurence S. Romsted, Maria-Jose Pastoriza Gallego, Elisa González-Romero, and Carlos Bravo-Díaz. 2006. Determining  $\alpha$ -tocopherol distributions between the oil, water, and interfacial regions of macroemulsions: Novel applications of electroanalytical chemistry and the pseudophase kinetic model. *Special Issue in Honor of Dr. K. L. Mittal* 123-126, 0 (2006), 303-311.
- Anne-Mette Haahr and Charlotte Jacobsen. 2008. Emulsifier type, metal chelation and pH affect oxidative stability of n-3-enriched emulsions. *European Journal of Lipid Science and Technology* 110, 10 (2008), 949-961.
- Erwin L. Hahn. 1950. Spin echoes. *Physical Review* 80, 4 (1950), 580.
- Clare L. Hawkins and Michael J. Davies. 2013. Detection and characterisation of radicals in biological materials using EPR methodology. *Biochimica et Biophysica Acta (BBA) - General Subjects* (2013).
- Anja Heins, Vasil Garamus, Bernd Steffen, Heiko Stöckmann, and Karin Schwarz. 2006. Impact of Phenolic Antioxidants on Structural Properties of Micellar Solutions. *Food Biophysics* 1, 4 (2006), 189-201.
- Anja Heins, Donald McPhail, Tobias Sokolowski, Heiko Stöckmann, and Karin Schwarz. 2007a. The Location of Phenolic Antioxidants and Radicals at Interfaces Determines Their Activity. *Lipids* 42, 6 (2007), 573-582.
- Anja Heins, Tobias Sokolowski, Heiko Stöckmann, and Karin Schwarz. 2007b. Investigating the Location of Propyl Gallate at Surfaces and Its Chemical Microenvironment by  $^1\text{H}$  NMR. *Lipids* 42, 6 (2007), 561-572.
- Dejian Huang, Boxin Ou, and Ronald L. Prior. 2005. The Chemistry behind Antioxidant Capacity Assays. *J. Agric. Food Chem.* 53, 6 (2005), 1841-1856.
- Wayne L. Hubbell, David S. Cafiso, and Christian Altenbach. 2000. Identifying conformational changes with site-directed spin labeling. *Nature Structural & Molecular Biology* 7, 9 (2000), 735-739.
- Ken'ichi Ichihara and Yumeto Fukubayashi. 2010. Preparation of fatty acid methyl esters for gas-liquid chromatography. *Journal of Lipid Research* 51, 3 (2010), 635-640.
- Edward G. Janzen, Yashige Kotake, and Randall D. Hinton. 1992. Stabilities of hydroxyl radical spin adducts of PBN-type spin traps. *Free Radical Biology and Medicine* 12, 2 (1992), 169-173.
- Gunnar Jeschke and Shulamith Schlick. 2006. Continuous Wave and Pulsed ESR Methods. *Advanced ESR methods in polymer research* (2006), 1-24.
- B. Jönsson, M. Landgren, and P. Olofsson. 1995. Solubilization of uncharged molecules in ionic micellar solution: Toward an understanding at the molecular level. *Solubilization in surfactant aggregates* 55. CRC Press, New York.
- Katja Jores, Wolfgang Mehnert, and Karsten Mäder. 2003. Physicochemical Investigations on Solid Lipid Nanoparticles and on Oil-Loaded Solid Lipid Nanoparticles: A Nuclear Magnetic Resonance and Electron Spin Resonance Study. *Pharmaceutical Research* 20, 8 (Aug. 2003), 1274-1283.
- Miguel Jorge. 2008. Molecular Dynamics Simulation of Self-Assembly of n-Decyltrimethylammonium Bromide Micelles. *Langmuir* 24, 11 (2008), 5714-5725.
- Akio Kadowaki, Satoshi Iwamoto, and Ryo Yamauchi. 2012. Reaction products of [60] fullerene during the autoxidation of methyl linoleate in bulk phase. *Chemistry and Physics of Lipids* 165, 2 (2012), 178-185.
- Joseph P. Y. Kao, Eugene D. Barth, Scott R. Burks, Philip Smithback, Colin Mailer, Kang-Hyun Ahn, Howard J. Halpern, and Gerald M. Rosen. 2007. Very-low-frequency electron paramagnetic resonance (EPR) imaging of nitroxide-loaded cells. *Magnetic Resonance in Medicine* 58, 4 (2007), 850-854.
- Alec Keith, Grahame Bulfield, and Wallace Snipes. 1970. Spin-Labeled Neurospora Mitochondria. *Biophysical journal* 10, 7 (1970), 618-629.

- Sabine Kempe, Hendrik Metz, and Karsten Mäder. 2010. Application of Electron Paramagnetic Resonance (EPR) spectroscopy and imaging in drug delivery research - Chances and challenges. *Imaging Techniques in Drug Development. European Journal of Pharmaceutics and Biopharmaceutics* 74, 1 (2010), 55-66.
- Nickolai Kochevinsky and Harold M. Swartz. 1995. Nitroxide spin labels: reactions in biology and chemistry. CRC Press.
- Mads Kreilgaard, Erik J. Pedersen, and Jerzy W. Jaroszewski. 2000. NMR characterisation and transdermal drug delivery potential of microemulsion systems. *Journal of controlled release* 69, 3 (2000), 421-433.
- Marina Kveder, Greta Pifat, Slavko Pečar, Milan Schara, Pilar Ramos, and Hermann Esterbauer. 1997. Nitroxide reduction with ascorbic acid in spin labeled human plasma LDL and VLDL. *Chemistry and Physics of Lipids* 85, 1 (1997), 1-12.
- K. R. Lange. 1999. *Surfactants: A Practical Handbook*. Hanser.
- Olivier M. Lardinois, David A. Maltby, Katalin F. Medzihradzsky, De Montellano, Paul R. Ortiz, Kenneth B. Tomer, Ronald P. Mason, and Leesa J. Deterding. 2009. Spin Scavenging Analysis of Myoglobin Protein-Centered Radicals Using Stable Nitroxide Radicals: Characterization of Oxoammonium Cation-Induced Modifications. *Chem. Res. Toxicol.* 22, 6 (2009), 1034-1049.
- Malcolm H. Levitt. 2008. *Spin dynamics: basics of nuclear magnetic resonance*. John Wiley & Sons.
- R. d. Lisi and S. Milioto. 1995. Thermodynamics of solubilization of polar additives in micellar solution. *Solubilization in surfactant aggregates* 55. CRC Press.
- Marlene Lucio, Claudia Nunes, Diana Gaspar, Helena Ferreira, Jose Lima, and Salette Reis. 2009. Antioxidant Activity of Vitamin E and Trolox: Understanding of the Factors that Govern Lipid Peroxidation Studies In Vitro. *Food Biophysics* 4, 4 (Dec. 2009), 312-320.
- Anders Lund, Masaru Shiotani, and Shigetaka Shimada. 2011. *Principles and applications of ESR spectroscopy* 76. Springer.
- David J. Lurie and Karsten Mäder. 2005. Monitoring drug delivery processes by EPR and related techniques-principles and applications. *Advanced drug delivery reviews* 57, 8 (2005), 1171-1190.
- Yun Ma, Colin Loyns, Peter Price, and Victor Chechik. 2011. Thermal decay of TEMPO in acidic media via an N-oxoammonium salt intermediate. *Organic & Biomolecular Chemistry* 9, 15 (2011), 5573-5578.
- Jennifer R. Mancuso, D. Julian McClements, and Eric A. Decker. 1999. Ability of iron to promote surfactant peroxide decomposition and oxidize  $\alpha$ -tocopherol. *Journal of Agricultural and Food Chemistry* 47, 10 (1999), 4146-4149.
- D. J. McClements and E. A. Decker. 2000. Lipid oxidation in oil-in-water emulsions: Impact of molecular environment on chemical reactions in heterogeneous food systems. *Journal of Food Science* 65, 8 (2000), 1270-1282.
- David Julian McClements. 2010. Emulsion Design to Improve the Delivery of Functional Lipophilic Components. *Annu. Rev. Food Sci. Technol.* 1, 1 (2010), 241-269.
- Longyuan Mei, D. Julian McClements, and Eric A. Decker. 1999. Lipid oxidation in emulsions as affected by charge status of antioxidants and emulsion droplets. *Journal of Agricultural and Food Chemistry* 47, 6 (1999), 2267-2273.
- Longyuan Mei, D. Julian McClements, Junnan Wu, and Eric A. Decker. 1998. Iron-catalyzed lipid oxidation in emulsion as affected by surfactant, pH and NaCl. *Food Chemistry* 61, 3 (1998), 307-312.
- U. Menge, P. Lang, and Findenegg, G. H. 1999. From Oil-Swollen Wormlike Micelles to Microemulsion Droplets: A Static Light Scattering Study of the L1 Phase of the System Water + C12E5 + Decane. *J. Phys. Chem. B* 103, 28 (1999), 5768-5774.
- Kazuo Miyashita and Toru Takagi. 1986. Study on the oxidative rate and prooxidant activity of free fatty acids. *J Am Oil Chem Soc* 63, 10 (1986), 1380-1384.
- Monica Mosca, Francesca Cuomo, Francesco Lopez, and Andrea Ceglie. 2013. Role of emulsifier layer, antioxidants and radical initiators in the oxidation of olive oil-in-water emulsions. *Food Research International* 50, 1 (2013), 377-383.
- Klaus Möbius, Anton Savitsky. 2008. *High-Field EPR Spectroscopy on Proteins and their Model Systems: Characterization of Transient Paramagnetic States*. Royal Society of Chemistry Publishing, London.



- Meysam Najafi, Kaveh Haghighi Mood, Mansour Zahedi, and Erik Klein. 2011. Study of the substituent effect on the reaction enthalpies of the individual steps of single electron transfer-proton transfer and sequential proton loss electron transfer mechanisms of chroman derivatives antioxidant action. *Computational and Theoretical Chemistry* 969, 1-3 (2011), 1-12.
- Carla D. Nuchi, Pilar Hernandez, D. Julian McClements, and Eric A. Decker. 2002. Ability of Lipid Hydroperoxides To Partition into Surfactant Micelles and Alter Lipid Oxidation Rates in Emulsions. *J. Agric. Food Chem.* 50, 19 (2002), 5445-5449.
- Kathleen Oehlke, Vasil M. Garamus, Anja Heins, Heiko Stöckmann, and Karin Schwarz. 2008. The partitioning of emulsifiers in o/w emulsions: A comparative study of SANS, ultrafiltration and dialysis. *Journal of Colloid and Interface Science* 322, 1 (2008), 294-303.
- Kathleen Oehlke, Anja Heins, Heiko Stöckmann, and Karin Schwarz. 2010. Impact of emulsifier microenvironments on acid-base equilibrium and activity of antioxidants. *Food Chemistry* 118, 1 (2010), 48-55.
- Kathleen Oehlke, Anja Heins, Heiko Stöckmann, Frank Sönnichsen, and Karin Schwarz. 2011. New insights into the antioxidant activity of Trolox in o/w emulsions. *Food Chemistry* 124, 3 (2011), 781-787.
- William H. Otto, Danny J. Britten, and Cynthia K. Larive. 2003. NMR diffusion analysis of surfactant-humic substance interactions. *Journal of Colloid and Interface Science* 261, 2 (2003), 508-513.
- Alexander Patist, S. G. Oh, R. Leung, and D. O. Shah. 2001. Kinetics of micellization: its significance to technological processes. *Colloids and Surfaces A: Physicochemical and Engineering Aspects* 176, 1 (2001), 3-16.
- Nataša Poklar Ulrih, Ajda Ota, Marjeta Šentjurs, Sandra Kure, and Veronika Abram. 2010. Flavonoids and cell membrane fluidity. *Food Chemistry* 121, 1 (2010), 78-84.
- William A. Pryor, Joseph A. Cornicelli, Larry J. Devall, Bradley Tait, B. K. Trivedi, D. T. Witiak, and Mingdan Wu. 1993. A rapid screening test to determine the antioxidant potencies of natural and synthetic antioxidants. *The Journal of Organic Chemistry* 58, 13 (1993), 3521-3532.
- Olesea Roman, Francis Courtois, Marie-Noëlle Maillard, and Anne-Marie Riquet. 2012. Kinetic Study of Hydroperoxide Degradation in Edible Oils Using Electron Spin Resonance Spectroscopy. *J Am Oil Chem Soc* (2012).
- Laurence S. Romsted and Jianbing Zhang. 2002. Kinetic Method for Determining Antioxidant Distributions in Model Food Emulsions. Distribution Constants of t-Butylhydroquinone in Mixtures of Octane, Water, and a Nonionic Emulsifier. *Journal of Agricultural and Food Chemistry* 50, 11 (2002), 3328-3336.
- Paolo Sabatino, Agnieszka Szczygiel, Davy Sinnaeve, Maryam Hakimhashemi, Hans Saveyn, José C. Martins, and Van der Meer, Paul. 2010. NMR study of the influence of pH on phenol sorption in cationic CTAB micellar solutions. *Colloids and Surfaces A: Physicochemical and Engineering Aspects* 370, 1 (2010), 42-48.
- Ashish V. Sangwai and Radhakrishna Sureshkumar. 2011. Binary Interactions and Salt-Induced Coalescence of Spherical Micelles of Cationic Surfactants from Molecular Dynamics Simulations. *Langmuir* 28, 2 (2011), 1127-1135.
- Karin Schwarz, E. N. Frankel, and J. B. German. 1996. Partition behaviour of antioxidative phenolic compounds in heterophasic systems. *Fett/Lipid* 98, 3 (1996), 115-121.
- F. Shahidi and Y. Zhong. 2007. Measurement of Antioxidant Activity in Food and Biological Systems. In *Antioxidant Measurement and Applications*. Amer Chemical Soc, Washington, 36-66.
- Benjamin P. Soule, Fuminori Hyodo, Ken-ichiro Matsumoto, Nicole L. Simone, John A. Cook, Murali C. Krishna, and James B. Mitchell. 2007. The chemistry and biology of nitroxide compounds. *Free Radical Biology and Medicine* 42, 11 (2007), 1632-1650.
- M. Sowmiya, Amit K. Tiwari, and Subit K. Saha. 2010. Fluorescent probe studies of micropolarity, premicellar and micellar aggregation of non-ionic Brij surfactants. *Journal of Colloid and Interface Science* 344, 1 (2010), 97-104.
- Peter Stilbs. 1987. Fourier transform pulsed-gradient spin-echo studies of molecular diffusion. *Progress in Nuclear Magnetic Resonance Spectroscopy* 19, 1 (1987), 1-45.
- Heiko Stöckmann, Karin Schwarz, and Tuong Huynh-Ba. 2000. The influence of various emulsifiers on the partitioning and antioxidant activity of hydroxybenzoic acids and their derivatives in

- oil-in-water emulsions. *Journal of the American Oil Chemists' Society* 77, 5 (2000), 535-542.
- K. Stolze, N. Udilova, and H. Nohl. 2000a. Lipid radicals: Properties and detection by spin trapping. *Acta Biochimica Polonica* 47, 4 (2000), 923-930.
- K. Stolze, N. Udilova, and H. Nohl. 2000b. Spin trapping of lipid radicals with DEPMPO-derived spin traps: Detection of superoxide, alkyl and alkoxy radicals in aqueous and lipid phase. *Free Radical Bio Med* 29, 10 (2000), 1005-1014.
- K. Stolze, N. Udilova, and H. Nohl. 2002. Spin adducts of superoxide, alkoxy, and lipid-derived radicals with EMPO and its derivatives. *Biological Chemistry* 383, 5 (2002), 813-820.
- Janez Štrancar. 2007. Advanced ESR Spectroscopy in Membrane Biophysics. In *ESR Spectroscopy in Membrane Biophysics*. Springer US, 49-93.
- Janez Štrancar, Tilen Koklic, Zoran Arsov, Bogdan Filipic, David Stopar, and Marcus A. Hemminga. 2005. Spin label EPR-based characterization of biosystem complexity. *Journal of chemical information and modeling* 45, 2 (2005), 394-406.
- Sharon K. Swafford, Wolfgang R. Bergmann, Kenneth G. Migliorese, and J. Leon Lichtin. 1991. Characterization of swollen micelles containing linoleic acid in a microemulsion system. *J. Soc. Cosmet. Chem.*, 42 (1991), 235-247.
- M. K. Thomsen, D. Kristensen, and L. H. Skibsted. 2000. Electron spin resonance spectroscopy for determination of the oxidative stability of food lipids. *Journal of the American Oil Chemists Society* 77, 7 (2000), 725-730.
- Olga Vinogradova, Frank Sönnichsen, and Sanders II, Charles R. 1998. On choosing a detergent for solution NMR studies of membrane proteins. *Journal of biomolecular NMR* 11, 4 (1998), 381-386.
- Junfeng Wang, Jason R. Schnell, and James J. Chou. 2004. Amantadine partition and localization in phospholipid membrane: a solution NMR study. *Biochemical and Biophysical Research Communications* 324, 1 (2004), 212-217.
- Thaddao Waraho, D. Julian McClements, and Eric A. Decker. 2011. Mechanisms of lipid oxidation in food dispersions. *Trends in Food Science & Technology* 22, 1 (2011), 3-13.
- John A. Weil and James R. Bolton. 2007. *Electron paramagnetic resonance: elementary theory and practical applications*. John Wiley & Sons.
- N. V. Yanishlieva-Maslarova, J. Pokorny, N. Yanishlieva, and M. Gordon. 2001. Inhibiting oxidation. *Antioxidants in food: Practical applications* (2001), 22-70.

## 2 The use of spintraps to detect azo-generated lipid radicals in dispersed systems

Heimke Krudopp<sup>a</sup>, Kalpana Palani<sup>a</sup>, Klaus Stolze<sup>b</sup>, Anja Steffen-Heins<sup>a</sup>

<sup>a</sup>Institute of Human Nutrition and Food Science, Kiel University, 24118 Kiel, Germany

<sup>b</sup>Institute of Pharmacology and Toxicology, Veterinary University of Vienna, Vienna, Austria

### 2.1 Abstract

Lipid radicals in dispersed systems arise from the inner core of micelles. To detect the lipid radicals with half-lives of  $\mu\text{s}$  up to ns spin traps can be used to form stable adducts with the radicals. The aim of this study was to detect lipid radicals from oxidized linoleic acid in dispersed systems. In regard to the interface barriers, a combination of hydrophilic and lipophilic radical initiators and spin traps should show where the lipid radicals are generated and trapped.

To accomplish this purpose the thermosensitive azo radical initiators AAPH, AIBN and Fenton reaction mix were used to generate lipid radicals. The spin traps DMPO, PBN, OMPO, DBPMPO have different polarities and therefore different locations in the dispersed systems where they trap radicals. In addition, we synthesized a lipophilic DMPO analog attached to stearic acid. Model systems of micellar solutions with anionic SDS, cationic CTAB, non-ionic Brij58 and Tween20 loaded with linoleic acid were used. In all systems a high content of hydroxyl radicals were detected with hydrophilic spin traps. Alkyl radicals were only detectable in systems with non-ionic emulsifiers. The spectra of more lipophilic spin trap adducts were not evaluable due to anisotropy and the lack of hyperfine couplings. The synthesis of the C17-DMPO was successful, however the application in dispersed systems is restricted due to the half-lives of the spin adducts formed with radicals.

## 2.2 Introduction

Free radicals are known to cause oxidation of lipids and proteins in food stuff leading to off-flavor and spoil foods. On one hand the nutrition value is reduced but on the other hand free radicals reaching the body cause damage to biomembranes, proteins and other biomolecules. It is suspected that the consequence of the oxidation leads to some human diseases [Halliwell 1994]. Oxygen and heat induction are known to be a possible initiator for radical formation. However, in model systems it is essential to generate free radicals at a controlled and known rate and site to study the dynamics of radical mediated oxidation. Azo-compounds generate free carbon-centered radicals by the spontaneous thermal decomposition which react with oxidizable compounds or molecular oxygen to form oxygen-centered radicals. They have been used in studies with biological systems like micelles, membranes and lipoproteins [Mojumdar et al. 2004; Krainev and Bigelow 1996; Niki 1990; Noguchi et al. 1998]. In contrast to the controlled radical initiation the Fenton reaction produces hydroxyl radicals which are known to be very reactive oxygen species [Janzen et al. 1992].

The direct detection of short living radicals is possible, but the sensitivity is most often insufficient. Chamulitrat and Mason were able to directly detect a polyunsaturated fatty acid peroxy radical [1989], Westermann and coworkers detected free radicals of undefined origin in cream cheese after light exposure [2009] and Krainev and Bigelow detected AMVN-derived peroxy radicals in dimethylsulfoxide (DMSO) solution [1996]. The development of EPR spin trapping technique enabled the detection of short living radicals as spin traps have the ability to react with transient radicals and generate persistent spin-adduct radicals. PBN and DMPO are widely used nitron spin traps. While PBN forms preferable carbon-centered spin adducts, DMPO also traps oxygen-centered radicals and give information about the structure of the radical species [Mojumdar et al. 2004; Guo et al. 2003]. With the hyperfine coupling constants of DMPO radical adducts, the trapped radical can be identified. However, the distinction between peroxy radicals and superoxide anions as well as hydroxyl and alkoxy radicals is only possible with additional identifying methods like simulation or online high performance liquid chromatography (HPLC-EPR), electrospray ionization- mass spectrometry (ESI-MS) and tandem mass spectroscopy (MS/MS) as wrong interpretations occur due to the spectral similarity [Janzen et al. 1990; Guo et al. 2003; Dikalov and Mason 2001]. Although some authors reported the detection of peroxy radical adducts [Rota et al. 1997; Davies and Slater 1986; Schaich and Borg 1988], Dikalov and Mason [2001] revealed the impossibility of peroxy radical adduct detection.

Synthesis of spin traps depending on their target use are common [Dikalov et al. 1992; Stolze et al. 2002; Becker et al. 2002; Frejavielle et al. 1995; Stolze et al. 2000a]. 5-(Diethoxyphosphoryl)-5-methyl-1-pyrroline N-oxide (DEPMPO) was synthesized to trap superoxide radicals in biological membranes. It forms more stable adducts with superoxide radicals than the commercial DMPO and the reaction kinetic towards hydroxyl radicals is twice as high, even though the partitioning coefficients are similar [Frejavielle et al. 1995]. For a higher lipophilicity Stolze and colleagues synthesized DEPMPO derivatives with in-

creasing chain length to detect lipid-derived radicals [2000a]. Becker and coworkers [2002] synthesized STAZN, used as an antioxidant and revealed a significantly enhanced potency as a chain-breaking antioxidant vs conventional nitron spin traps like PBN. That implies an improved spin trapping capability as STAZN outperforms classical phenolic antioxidants as butylhydroxytoluene and Vitamin E in a polar environment.

The preferred location of spin traps in dispersed systems is supposed to be at the lipid-water interface where they trap water-soluble peroxy radicals by single electron-transfer mechanism. The location at the interface of membranes as the major reaction site was also investigated with DMPIO, a hydrophobic DMPO analogue [Dikalov et al. 1992]. Lipophilic DMPO derivatives with alkoxy substituents with increasing chain length were also synthesized by Stolze [2002] and colleagues to form stable superoxide adducts.

The aim of this study was to generate and detect lipid radicals from linoleic acid (LA) in dispersed systems by EPR spin trapping technique. To determine the location of the radical generation and trapping, hydrophilic and lipophilic radical initiators and spin traps were used as the emulsifier interface represents a barrier between the hydrophilic and lipophilic compartment.

## 2.3 Materials and Methods

### 2.3.1 Chemicals

Acetic acid, ferrous sulphate,  $H_2O_2$ , methanol, n-hexane, SDS (sodium dodecyl sulfate, >99 %), silica gel (0.06-0.2 mm), sodium acetate (>99 %, anhydrous), Trifluoroacetic acid (TFA) and Tween20 were obtained from Carl Roth, Germany. AAPH, Brij58, CTAB (cetyl trimethyl ammonium bromide, >99 %), 4-(dimethylamino) pyridine, DMPO (5,5-dimethyl-1-pyrroline-n-oxide), linoleic acid, PBN (alpha-phenyl N-tertiary-butyl nitron), sodium tungstate and stearic acid were purchased from Sigma Aldrich, Germany. AIBN was obtained from MP Biomedicals GmbH, Germany. EDC (1-(3-dimethylaminopropyl)-3-ethylcarbodiimide hydrochloride) and BOC (1-Boc-3-hydroxypyrrolidine) were purchased from Alfa Aesar, Germany. Dichloromethane was obtained from VWR, Germany.

The spin traps DBPMPO (5-(di-n-Butoxyphosphoryl)-5-Methyl-1-Pyrroline N-Oxide) and OMPO (5-Octyl-5-Methyl-1-Pyrroline-N-Oxide) were synthesized by Stolze and coworkers [Stolze et al. 2000a, 2002].

### 2.3.2 Synthesis of C17-DMPO

The first step was the addition of stearic acid to 1-Boc-3-hydroxypyrrolidine. 1.0 g (5.35 mmol) BOC protected hydroxyl-pyrrolidine (1) and 40 ml dichloromethane was stirred on ice. To this 1.5 mg (5.28 mmol) stearic acid, 1.1 mg (5.78 mmol) EDC and few crystals of 4-(Dimethylamino) pyridine as catalyst were added and stirred for an hour. The stirring was stopped when stearic acid was no longer detectable by TLC. The product was separated by extracting with dichloromethane. Extraction was repeated three times and the combined

organic layer was washed with Brine solution and dried with anhydrous sodium sulfate. The solvent was removed under vacuum. The crude reaction mixture was dissolved in hexane and purified by silica gel column chromatography with hexane ethyl acetate (15 %) to provide the pure product 2 in 80 % yield.

To remove the protecting group 500 mg (1.04 mmol) of compound 2 was dissolved in 10 ml chloroform and cooled down on ice. After addition of 2.5 ml (32.63 mmol) TFA the reaction mixture was stirred for 2 h and the completeness was checked by TLC. The solvent was evaporated to get compound 3 in 100 % yield.

The oxidation to the nitron compound was carried out using the solid product 3 (1.04 mmol) dissolved in 10 ml methanol. The solution was cooled down on ice and 500  $\mu$ l (0.15 mmol)  $\text{H}_2\text{O}_2$  were added dropwise followed by 10 mg (3.31 mmol) of sodium tungstate. The reaction mixture was stirred at room temperature and the reaction was followed by TLC. The solvent was evaporated and the product was redissolved in 50 ml dichloromethane. The solution was washed with 10 ml water followed by 10 ml Brine solution. The organic phase was dried over anhydrous sodiumsulfate and the solvent removed under vacuum. Purification was done with silica gel column chromatography by using chloroform with increasing methanol content up to 10 %. The yield was 18 % of a yellow soft solid substance. The purity of the product 4 was assessed by LC-MS and  $^1\text{H-NMR}$ .

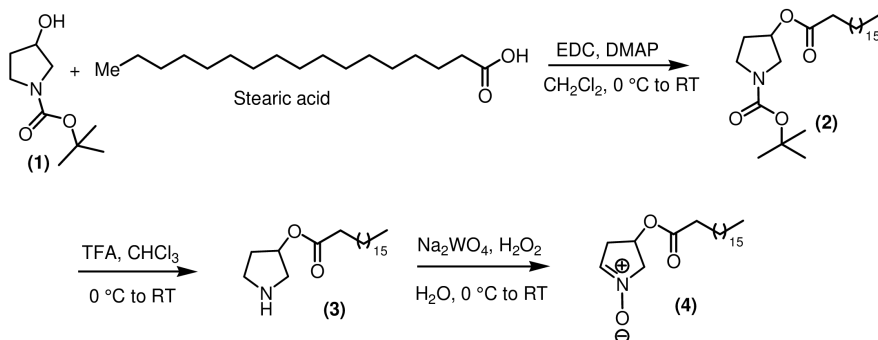


Figure 2.1: Synthesis scheme of DMPO-C17.

### 2.3.3 Preparation of dispersed systems

The systems contained 1 wt% emulsifier, 10 mmol LA, 50 mmol spin trap and 5 mmol radical generator or 1 mmol Fenton reaction mix (1 mmol  $\text{H}_2\text{O}_2$ , 1 mmol  $\text{FeSO}_4$  and 1 mmol EDTA) in acetic buffer (200 mmol, pH=5) unless otherwise stated. Stock solutions were mixed and immediately measured. Samples containing AAPH or AIBN were heated

at 46 °C for 15 min prior to measurements. Samples containing spin traps DBPMPO and OMPO were additionally measured with Desferal as a chelator or bubbled with nitrogen. Control measurements were carried out in the absence of LA. The used spin traps are shown in figure 2.2.

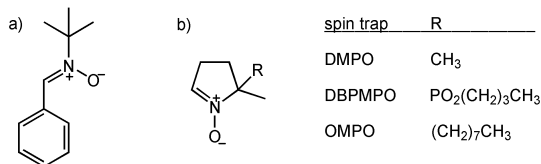


Figure 2.2: Structure of spin traps PBN (a) and DMPO derivatives (b).

### 2.3.4 EPR general setup

EPR measurements of the spin traps were carried out on a Bruker X-band EMXplus spectrometer with a PremiumX microwave bridge EMXplus and a Bruker ESP 300 E equipped with a rectangular TM110 microwave cavity at 9.7 GHz with 100 kHz modulation frequency at room temperature. Spectral simulations of DMPO adducts were performed using the EPR simulation software package XSophe.

## 2.4 Results

### 2.4.1 Detection of DMPO- and PBN-adducts

The commercially available spin traps DMPO and PBN were used as hydrophilic and lipophilic spin trap. DMPO radical adducts in micellar solution are depicted in figure 2.3. In the presence of LA, additional peaks (\*) arising from alkyl radical adducts were obtained only in Tween20 micellar solutions (figure 2.3b). All other measurements with Fenton reaction mix showed only signals of hydroxyl radical adducts like in CTAB solution (figure 2.3a). The signals in SDS and Brij58 were similar to CTAB. It has to be noticed that signal intensities in probes containing LA were decreased. The distinction of radicals type was achieved by simulations of DMPO-adduct spectra with alkyl radicals (figure 2.3c), hydroxyl radicals (figure 2.3d) and alkoxy radicals (figure 2.3e). The identification of alkyl radical adducts was possible by means of the six line pattern. Owing to the same hyperfine splitting a distinction between hydroxyl and alkoxy radical adducts was not possible.

The concentration of DMPO influences the proportions of the different adducts in Tween20 micellar solutions (Tab.1). Although the overall intensities of the peaks were higher with a concentration of 50 mmol DMPO, the formation of hydroxyl adducts is suppressed compared to the alkyl adducts when using concentrations of 10 mmol DMPO. The proportion of the different adducts were calculated for the first and second peak of each radical adduct

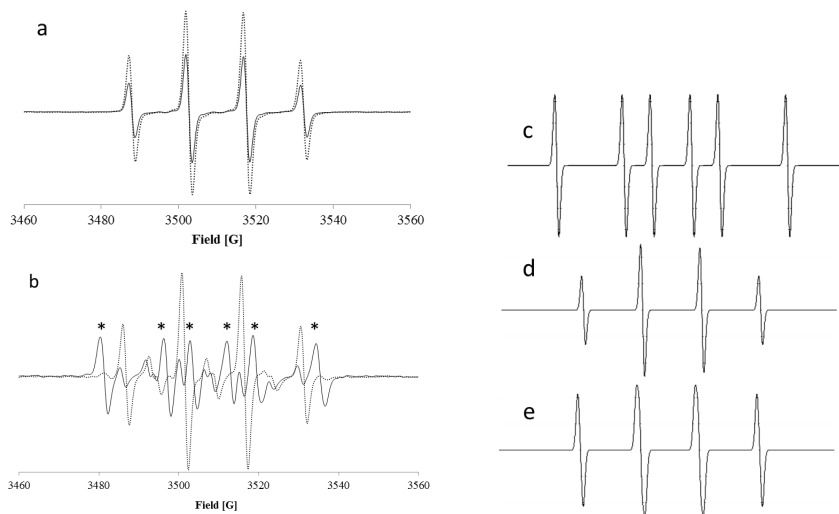
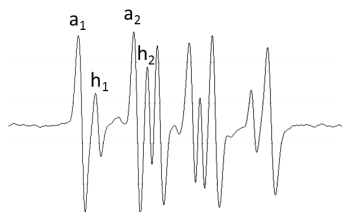


Figure 2.3: Spectra of DMPO-adducts in CTAB (a) and Tween20 (b) with Fenton reaction mix. Black lines show the samples in the presence of LA and dotted lines show the control in the absence of LA. Simulated spectra of DMPO-adducts with alkyl radicals (c), hydroxyl radicals (d) and alkoxy radicals (e). \*alkylradicals

species. Intensities were calculated as peak heights (H). With low DMPO concentrations the ratio between alkyl adducts (a) and hydroxyl adducts (h) were 3 to 4 times higher, while with higher DMPO concentrations it is one third or less.

Table 2.1: Peak heights (H) of the alkyl (a) and hydroxyl (h) adducts and their ratio ( $P_{H_a/H_h}$ ) depending on the spin trap concentration.

	$c_{\text{DMPO}} = 10 \text{ mM}$		$c_{\text{DMPO}} = 50 \text{ mM}$	
	h	$P_{H_a/H_h}$	h	$P_{H_a/H_h}$
$a_1$	0.181	3.94	0.664	0.33
$h_1$	0.046		2.034	
$a_2$	0.184	3.02	0.732	0.24
$h_2$	0.061		3.059	



To demonstrate that alkyl radicals can be trapped by DMPO, 5 % Methanol was added to a CTAB micellar solution with Fenton reaction mix. In these samples the formation of hydroxyl radical adducts is suppressed and the signals from alkyl radical adducts arise.



Fenton reaction mix oxidizes methanol and the methanol derived radicals were trapped by DMPO. In the presence of LA the overall intensity is decreased as in the other samples. In addition, we controlled the stability of the different adducts by measuring the same probes over certain time. Hydroxyl radicals were more stable than the alkyl radicals.

The use of azo-radical initiators, which is often described in literature, was not sufficient in the systems used in this work. Samples with AAPH showed lower intensities than samples with Fenton reaction mix and no alkyl radicals were detected. AAPH is not suitable for SDS micellar solutions, as a white precipitate occurred. The lipophilic AIBN showed comparable results to AAPH where again no alkyl radicals could be detected.

Literature findings revealed that the pH value influenced the spin trapping ability. Therefore an influence of the pH value was tested in solutions with both Fenton reaction mix and AAPH in buffer solutions of pH=2 (citrate buffer), pH=5 (acetate buffer), pH=7 (deionized water) and pH=9 (tris-HCL). There were no differences in the spectra of spin adducts detectable.

The spin trap PBN is known to detect carbon-centered radicals. For this reason the more lipophilic PBN was used in order to distinguish if either no alkyl radicals were formed in the core of the micelles or DMPO is not able to detect the alkyl radicals. In samples containing DMPO and LA the formation of hydroxyl radical adducts was suppressed, indicating that other reactions compete with the formation or trapping of hydroxyl radicals. The typical triplet structure of PBN adducts were not detectable in samples containing LA. Therefore, no alkyl radicals from the oxidized LA were trapped by PBN.

## 2.4.2 Detection of DBPMPO- and OMPO-adducts

The spin trapping of lipid radicals with commercially available spin traps was not successful, therefore additional lipophilic spin traps were used. The lipophilic DMPO derivatives DBPMPO and OMPO were synthesized by Stolze and colleagues [Stolze et al. 2000a, 2002]. DBPMPO was tested in micellar solution in the presence and absence of LA using Fenton reaction mix as oxidation initiator. As depicted in figure 2.4b, DBPMPO in Tween20 solution in the presence of LA shows additional peaks (\*) from the alkyl radicals. In the presence of LA, the peak intensity decreased by a factor of ten compared to the control sample (figure 2.4a) which was also found for the spin trap DMPO (see 2.3.1). The spectra recorded in Tween20 and Brij58 show the same peak shape. In ionic micellar solutions of CTAB and SDS no changes in the spectral shape between samples in the presence or absence of LA were observed, but in SDS an intensity decrease in presence of LA was observed. The addition of AIBN as a radical generator showed that no alkyl radical adduct were formed in samples in presence of LA.

The spectra of the lipophilic spin trap OMPO in Tween20 are depicted in figure 2.4c and 2.4d. In all emulsifiers tested, no additional alkyl radical adduct peaks could be measured in samples containing LA and Fenton reaction mix. However, in the presence of LA (figure 2.4d) the peak intensity decreased compared to samples in the absence of LA (figure 2.4c).

With AIBN as radical initiator the spectra in Brij58, SDS and Tween20 were the same as with Fenton reaction mix. In CTAB solution hardly any peak was detectable. To avoid oxygen and metal ion sources in the samples additional experiments were carried out with samples deoxygenated by nitrogen during incubation time and prior to measurements as well as with samples where the chelator Desferal was added. Neither the absence of oxygen nor the inhibition of metal ions led to the formation of alkyl radical adducts.

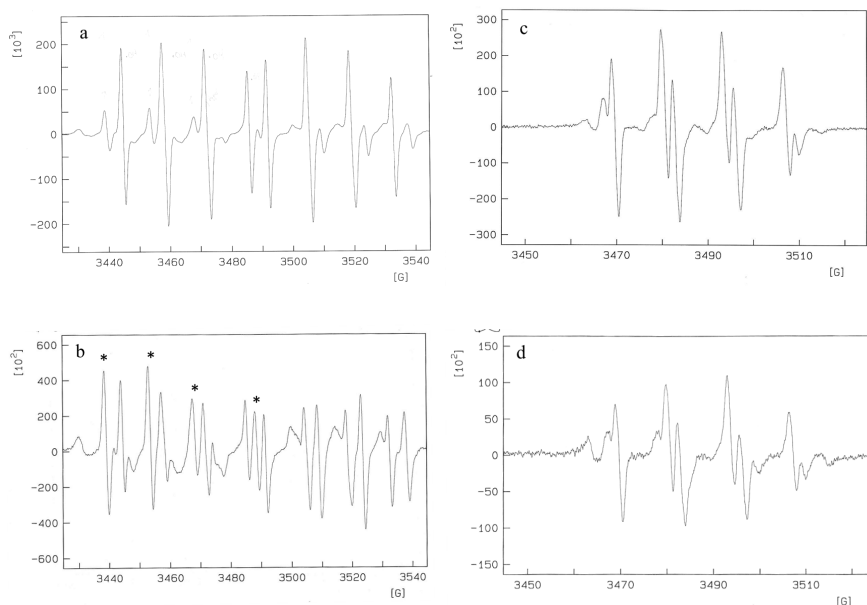


Figure 2.4: Spectra of DBPMPO (a, b) and OMPO (c, d) adducts in Tween20. Oxidation was initiated by Fenton reaction mix. LA is present in samples b and d.

### 2.4.3 C17-DMPO

The lipophilic DMPO derivatives DBPMPO and OMPO (see 2.3.2) did not show any better results than the commercially available DMPO (see 2.3.1). Therefore, a DMPO derivative attached to a stearic acid was synthesized. The theoretical partitioning-coefficient of the C17-DMPO is  $\log P=8.11$  whereas the DMPO has a  $\log P=0.88$  indicating a solubilization of C17-DMPO in the interface. The synthesis was successful and a high purity was achieved (see 2.3.2). The spectrum of C17-DMPO was recorded in chloroform with additional dimethylsulfoxide and AIBN as radical generator (figure 2.5), grey line). The solubilized

C17-DMPO in chloroform was mixed the radical containing solution and the measurement was carried out immediately. The half live of the detected adduct was too short to record a replicate measurement that directly followed. In the presence of micelles no spectrum was recorded despite the addition of all other components used in the experiment without a micellar solution. Figure 2.5 (black line) shows the measurement with Tween20 micellar solution.

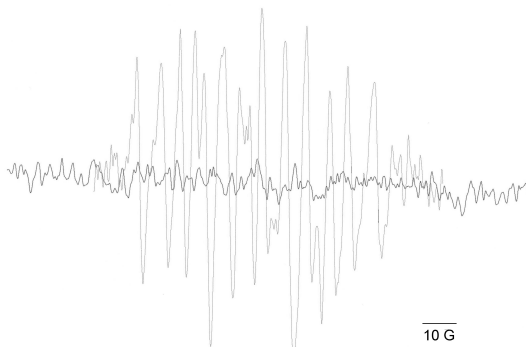


Figure 2.5: Spectra of C17-DMPO in chloroform (grey) and Tween20 (black) with AIBN and dimethylsulfoxide in chloroform as radical source.

## 2.5 Discussion

### 2.5.1 The preferred detection of hydroxyl radicals

In all micellar solutions hydroxyl radicals were trapped with every DMPO derivate tested (figure 2.3 and 2.4). Although the signal intensities in probes containing LA decreased and only in few combinations in the presence of non-ionic emulsifiers alkyl radicals were trapped, the content of hydroxyl radical adducts was predominant. In addition, we controlled the stability of the different adducts by measuring the same probes over certain time. The results showed that hydroxyl radical adducts were more stable than alkyl radical adducts. This led to the conclusion that the affinity from DMPO and its derivates towards hydroxyl radicals is much higher than to alkyl radicals and the stability of alkyl radical adducts is decreased. This is in good agreement with Dikalov and Mason [2001] who concluded that only traces of water lead to the preferred formation of DMPO  $\cdot$ OH adducts. The half live of oxygen centered radical spin adducts with DMPO is in the magnitude of several minutes [Marriott et al. 1980]. The hydroxyl radical is believed to be the most reactive species among oxygen radical intermediates and the success of its detection depends almost entirely on the stability of the hydroxyl radical spin adduct because the formation rate

of this adduct is very fast and independent from the selected spin trap [Janzen et al. 1992]. Other authors depict rate constants for the addition of radicals to DMPO as  $1.9 - 3.3 \cdot 10^9 \text{ mol}^{-1} \text{ s}^{-1}$  [Goldstein et al. 2004; Finkelstein et al. 1980; Villamena et al. 2003] and slower rate constant for alkoxy radicals as tert-butyloxy with  $9.0 \cdot 10^6 \text{ mol}^{-1} \text{ s}^{-1}$  [Bors et al. 1992] and carbon centered radicals in the range of  $2.2 - 6.8 \cdot 10^7 \text{ mol}^{-1} \text{ s}^{-1}$  [Goldstein et al. 2004; Taniguchi and Madden 1999]. Guo and coworkers [2003] also supposed that an oxygen-centred DMPO adduct is more stable than a carbon-centered adduct, which is in good agreement with our findings. Janzen [2012] postulated that spin traps do not provide completely stable spin adducts. Therefore, the intensity of the EPR spectrum may reflect a steady-state condition where the rate of formation is balanced against the rate of decay of the adducts.

### 2.5.2 The distinction between radical types

The distinction between carbon-centered and oxygen-centered radical adducts was possible (figure 2.3), but a further distinction of the oxygen-centered radicals adducts was not possible. However, the distinction between hydroxyl, alkoxy and peroxy radical is discussed controversially in literature [Dikalov and Mason 2001]. In few combinations in the presence of non-ionic emulsifiers alkyl radicals were trapped apart from hydroxyl radicals, but it was not possible to detect any other radical type such as alkoxy or peroxy radicals. It is suspected that the alkyl radicals derive from LA oxidation. However, a distinction between alkoxy and hydroxyl radicals was not possible in our experimental setup. To distinguish between hydroxyl and alkoxy radicals or other oxygen-centered radicals the proportion between the peak intensities are often used, where hydroxyl radicals show a 1:2:2:1 ratio (figure 2.3d) and alkoxy radicals approach to a 1:1:1:1 ratio (figure 2.3e) which was shown by simulation experiments which is in agreement with [Kraiev and Bigelow 1996]. From simulation experiments the fingerprint for each radical type were obtained, therefore the alkyl radicals could be identified as they show a six line pattern with distinct hyperfine couplings and same peak heights [Qian et al. 2000; Kraiev and Bigelow 1996]. Dikalov and Mason [2001] suppose that EPR spectra in aqueous solutions were often misinterpreted, because the solvent effect on the nitroxide hyperfine coupling constants is important and is often not regarded. The detection of peroxy radicals is controversial discussed in literature [Mojumdar et al. 2004; Hawkins and Davies 2013; Barclay, L Ross C and Vinqvist 2000; Dikalov and Mason 2001]. The identification of peroxy radicals in dispersed systems used in this study was not possible with the spin traps used which is in agreement with Barclay and Vinqvist [2000] who regard PBN as one of the most popular and useful spin traps. Unfortunately, and despite claims to the contrary they showed that PBN is not an active peroxy radical trapping compound. Kraiev and Bigelow [1996] investigated the differences in radical types generated from the thermal decomposition of azo compounds. They showed that AAPH produced alkoxy radical spin adducts with spin traps in aqueous media, whereas AMVN formed peroxy radicals that were detected not only by spin trapping

technique but also by direct EPR measurement. The uses of hydrophilic spin trap DMPO and lipophilic DMPIO showed that the local concentration of AAPH-derived alkoxy radicals differs in the bulk solvent and in the proximity of vesicular membranes. However, they could not trap AMVN-derived radical species in membranes, which is in agreement with our findings and we could not detect other radicals than hydroxyl radicals with lipophilic AIBN. Dikalov and Mason [2001] supposed that a detection of peroxy radicals adduct is impossible as they rearrange to alkoxy radicals and therefore only the alkoxy radicals are detectable.

### 2.5.3 Cautionary note on highly reactive free radicals from Fenton like reactions

Fenton reaction mix was used to generate small and highly reactive radicals. It was shown that the hydroxyl radicals oxidized LA in Tween20 micellar solutions, which led to the conclusion that the hydroxyl radicals can penetrate into the interface of Tween20 micelles. Nevertheless, the hydroxyl radicals were present in every sample and superimposed the spectra. The oxidation of the solvent has also been noticed by other authors [Bosnjakovic and Schlick 2006; Janzen et al. 2012]. In the presents of highly reactive free radicals such as hydroxyl radicals the spin trapping results should be interpreted with care as Janzen [2012] revealed in his review. Unpublished data from Piette and colleagues showed that in Tris buffer solutions oxidation products from water and organic buffer compounds were trapped predominantly. Spin trapping experiments with subsequent simulation from Bosnjakovic and Schlick [2006] showed that DMPO in methanol trapped different radicals from the oxidized solvent. Stolze and colleagues [2000a] discussed the use of Fenton reaction mix critically as the iron ions of the Fenton reaction mix can attack the spin adducts. To prevent spin adducts the addition of chelators is useful. Another method is to interrupt the reaction by extracting the spin adducts with organic solvents as metal ions remain in the aqueous phase. However, as control measurements in the absence of LA were carried out under the same conditions showing no alkyl radical adducts, the alkyl adducts detected must be generated from LA oxidation. In addition the pH stability of the systems were tested between pH 2 and 9 were no differences occurred which is in contrast to literature findings [Janzen et al. 1992; He et al. 2012]. He and colleagues [2012] could not detect hydroxyl radicals with DMPO above pH 7.4 in a Fenton like system with silver nanoparticles as metal source. Janzen and colleagues [1992] also found an influence of the pH value, as the half-lives of hydroxyl spin adducts with PBN decreased with increasing pH value.

### 2.5.4 Cautionary note on azo-initiator generated radicals

The targeted generation of radicals was performed using the hydrophilic AAPH and the lipophilic AIBN. These were chosen because their partitioning in the aqueous phase (AAPH) and micellar phase (AIBN) was assumed which would have led to radical generation either

in the continuous phase or in the interface. However, this purpose could not be verified as only hydroxyl radicals were trapped (see 2.4.1). Findings in the literature were contrary about the generation of radicals with azo-initiators [Krainev and Bigelow 1996; Mojumdar et al. 2004]. Mojumdar and colleagues [2004] reported to generated peroxy radicals using azo initiators such as AIBN, AMVN and AAPH. Krainev and Bigelow [1996] investigated the differences of AAPH and AMVN, where AAPH produced alkoxy radical spin adducts in aqueous media and AMVN formed peroxy radicals (see also 2.4.2). Although AAPH is widely used as a radical initiator, in our experiments a white precipitate occurred in SDS micelles due to the reaction of negatively charged SDS and positively charged AAPH. Freyaldenhofen and colleagues [1998] as well as Mojumdar and colleagues [2004] used SDS micelles with incorporated methyl linoleate in combination with AAPH but they did not mention any precipitation. A reduced effective radical initiation from AAPH in SDS micelles due to charge effects is reported from Dai and colleagues [2009]. The purpose of the experiments with hydrophilic AAPH and lipophilic AIBN was to show that radicals were generated depending on the lipophilicity of the radical initiator. Even with AIBN no other radicals but hydroxyl radicals were trapped. This implies that the azo compounds oxidized the water immediately after their decomposition and neither the LA was oxidized and trapped nor the decomposition products could be trapped.

### 2.5.5 Further investigations to trap alkyl radicals

The signal intensities in all probes containing LA were decreased compared to the control samples even when no other radicals but hydroxyl radicals were detectable. That implies that there was a correlation between the presence of LA and the reduced content of hydroxyl radical adducts. It seemed reasonable that the radicals reacted with LA, but it was not possible to trap the oxidized LA radicals. A reduction of the hydroxyl adduct content was also observed with lower DMPO concentrations, while in case of Tween20 micellar solutions the alkyl adduct content showed a lower reduction. The hydroxyl radicals were trapped less when using concentrations of 10 mmol DMPO compared to 50 mmol DMPO. Same results were shown from Guo and co-workers [2003], who observed a shift of different adduct contents which were additionally identified by LC-MS. They also mentioned that the identification of carbon-centered radical adducts was not possible, because the half-lives were too short for the LC-MS measurement duration.

Bosnjakovic and Schlick [2006] showed that alkyl radicals were formed by the oxidation of methanol. They used a system with DMPO and Fenton reaction mix in pure methanol and determined the identification and content alkyl radical adducts by simulation. In this study methanol was added to a CTAB micellar solution with Fenton reaction mix and it was demonstrated that alkyl radicals in the continuous phase can be trapped by DMPO in CTAB micellar solution. Therefore, it could be shown that the emulsifier did not influence the spin trapping ability, but hindered the DMPO to trap carbon-centered radicals from the lipophilic core.

To determine whether DMPO is not suitable to detect LA oxidized alkyl radicals or no alkyl radicals were formed in the core of the micelles, the more lipophilic PBN was used as is known for its selectivity towards trapping carbon-centered radical species [Stolze et al. 2000b; Novakov et al. 2001] as oxygen centered radical PBN adducts have short half-lives [Janzen et al. 1992]. PBN alkyl adducts were not detectable in the presence of LA. Therefore, no alkyl radicals from the oxidized LA were trapped by PBN. This might be due to the presence of oxygen-centered LA radicals that could be formed by hydroxyl radicals and LA under oxygen atmosphere. Although, findings from Heins and colleagues [2007] indicated the absence of oxygen in the core of micellar solutions. They studied the spin interactions of galvinoxyl, a lipophilic stable radical, in different solutions and showed the missing spin interactions of galvinoxyl solubilized in micelles and deoxygenated solutions.

### 2.5.6 Synthesis of spin traps

Due to the lack of commercially available spin traps with appropriate characteristics many working groups synthesized spin traps for their specific target use [Stolze et al. 2002; Krainev and Bigelow 1996; Mojumdar et al. 2004; Stolze et al. 2000a; Becker et al. 2002]. As shown above, the commercially available DMPO (figure 2.3b) and its lipophilic derivate DBPMPO, synthesized by Stolze and colleagues [2000a], (figure 2.4b), were capable to detect alkyl radicals in Tween20 solutions but not in other micellar solutions. This is supposed to be due to different locations between spin trap and radical. Therefore, a highly lipophilic DMPO derivate (C17-DMPO) was synthesized (2.3.2).

To ensure that the spin trap is located in proximity to LA we synthesized a DMPO derivate with a stearic acid chain. Unfortunately, no C17-DMPO spin adducts could be detected in dispersed systems. However, in homogenous control measurements in chloroform the spin trapping ability was approved. It is most likely possible that the detection of C17-DMPO radical adducts was not achieved due to the localization of the spin trap. It is assumed that the stearic acid chain aligns with the hydrophobic emulsifier chain and the spin trapping active ring structure is in the headgroup region, where the DMSO derived radicals should have access.

The synthesis of lipophilic spin traps is required for studies in dispersed systems or biological systems with membranes as the interfacial region is the favored location for spin traps in these systems. Therefore and apart from others, Stolze and colleagues [2000a] synthesized DEPMPO derivatives with increasing chain length; Becker, Mojumdar and co-workers [2004; 2002] synthesized STAZN, a stilbazulenyl-bis-nitron, which is supposed to be at the lipid- water interface; Krainev and Bigelow [1996] investigated the hydrophobic DMPO analogue DMPIO same as by Stolze and colleagues [2002] with DMPO derivatives with alkoxy substituents with increasing chain length.

DMSO is widely used to produce methyl radicals [Dikalov et al. 1992; Krainev and Bigelow 1996; Liu et al. 2008]. The trapping of free radicals with the C17-DMPO in chloroform was successful (figure 2.5). The spectrum could be recorded immediately after

adding the radical containing mixture to the C17-DMPO solution, but the short half-life of the adduct restricted additional measurements. However, in the presence of interfaces no adduct could be detected. It has to be noticed that the mobility of the C17-DMPO in dispersed systems was restricted which could be a reason for the reduced trapping ability in micellar solution. The short half-life might be due to a lack of adduct-stabilizing substituents. The stability of cyclic radicals is given by methyl substituents in  $\alpha$ -position [Soule et al. 2007] as most spin traps show [Stolze et al. 2011; Krainev and Bigelow 1996] and which is a main characteristic for stable spin probes [Balog et al. 2007].

## 2.6 Outlook

Spin trapping of LA derived lipid radicals is not suitable in aqueous solutions with the radical initiators used. The hydroxyl radicals from water oxidation dominate the spectra. In Tween20 dispersed systems it was possible to detect alkyl radicals, but not in other solutions. As the signal intensities were equal to the amount of radicals it is concluded that in the presence of LA less hydroxyl radicals were trapped, but in all samples but Tween20 we could not detect any other kind of radicals.

Further studies of lipid radicals in aqueous dispersed solutions should include an alternative for the preparation of lipid radicals. Furthermore, the lipophilicity and the radical trapping ability of the spin traps were not sufficient. In dispersed systems, the location of a spin trap is prerequisite to detect the lipid radicals arising from the inner core of a micelle. As the radicals are short living species the spin trap should be in distinct location with the radical origin. The knowledge of the distinct location in dispersed systems is important for further studies and should be investigated.

Due to the difficulties in trapping lipid radicals spin probes could be used as an alternative approach to detect free lipid radicals. The advantage of spin probes is their sensitivity towards the microenvironment and therefore the determination of the location should be possible. In addition these stable nitroxide radicals can react with lipid radicals and with antioxidants due to a redox cycle between nitroxide, hydroxylamine and oxoammonium ion.

### Acknowledgement

We thank Dr. Philipp Kurz and his colleagues from the Institute of Inorganic Chemistry, Kiel University, for the introduction to EPR measurements.



## References

- Maria Balog, Christoph Abe, Tamas Kalai, Heinz-Juergen Steinhoff, Jozsef Jeko, and Kalman Hideg. 2007. Synthesis of new paramagnetic fatty acids and lipophilic spin labels. *Synthesis-Stuttgart*, 11 (2007), 1663–1670.
- Barclay, L Ross C and Melinda R. Vinqvist. 2000. Do spin traps also act as classical chain-breaking antioxidants? a quantitative kinetic study of phenyl tert-butyl nitron (PBN) in solution and in liposomes. *Free Radical Biology and Medicine* 28, 7 (2000), 1079–1090.
- David A. Becker, James J. Ley, Luis Echegoyen, and Robert Alvarado. 2002. Stilbazulenyl nitron (STAZN): a nitronyl-substituted hydrocarbon with the potency of classical phenolic chain-breaking antioxidants. *Journal of the American Chemical Society* 124, 17 (2002), 4678–4684.
- Wolf Bors, Christa Michel, and Kurt Stettmaier. 1992. Radical species produced from the photolytic and pulse-radiolytic degradation of tert-butyl hydroperoxide. An EPR spin trapping investigation. *J. Chem. Soc., Perkin Trans. 2*, 9 (1992), 1513–1517.
- A. Bosnjakovic and S. Schlick. 2006. Spin trapping by 5,5-dimethylpyrroline-N-oxide in Fenton media in the presence of Nafion perfluorinated membranes: Limitations and potential. *Journal of Physical Chemistry B* 110, 22 (2006), 10720–10728.
- W. Chamulitrat and R. P. Mason. 1989. Lipid peroxy radical intermediates in the peroxidation of polyunsaturated fatty acids by lipoxygenase. Direct electron spin resonance investigations. *Journal of Biological Chemistry* 264, 35 (1989), 20968–20973.
- F. Dai, W. F. Chen, B. Zhou, L. Yang, and Z. L. Liu. 2009. Antioxidative Effects of Curcumin and its Analogues against the Free-radical-induced Peroxidation of Linoleic Acid in Micelles. *Phytotherapy Research* 23, 9 (2009), 1220–1228.
- Michael J. Davies and Trevor F. Slater. 1986. Studies on the photolytic breakdown of hydroperoxides and peroxidized fatty acids by using electron spin resonance spectroscopy. Spin trapping of alkoxy and peroxy radicals in organic solvents. *Biochem. J* 240 (1986), 789–795.
- S. I. Dikalov, I. A. Kirilyuk, I. A. Grigor'ev, and L. B. Volodarskii. 1992. 2H-imidazole-N-oxides as spin traps. *Russ Chem Bull* 41, 5 (1992), 834–837.
- S. I. Dikalov and R. P. Mason. 2001. Spin trapping of polyunsaturated fatty acid-derived peroxy radicals: Reassignment to alkoxy radical adducts. *Free Radical Biology and Medicine* 30, 2 (2001), 187–197.
- Eli Finkelstein, Gerald M. Rosen, and Elmer J. Rauckman. 1980. Spin trapping. Kinetics of the reaction of superoxide and hydroxyl radicals with nitrones. *J. Am. Chem. Soc.* 102, 15 (1980), 4994–4999.
- Claudine Frejaville, Hakim Karoui, Beatrice Tuccio, Francois Le Moigne, Marcel Culcasi, Sylvia Pietri, Robert Lauricella, and Paul Tordo. 1995. 5-(Diethoxyphosphoryl)-5-methyl-1-pyrroline N-oxide: A New Efficient Phosphorylated Nitron for the in Vitro and in Vivo Spin Trapping of Oxygen-Centered Radicals. *Journal of Medicinal Chemistry* 38, 2 (1995), 258–265.
- M. A. Freyaldenhoven, P. A. Lehman, T. J. Franz, R. V. Lloyd, and V. M. Samokyszyn. 1998. Retinoic acid-dependent stimulation of 2,2'-azobis(2-amidinopropane)-initiated autoxidation of linoleic acid in sodium dodecyl sulfate micelles: A novel prooxidant effect of retinoic acid. *CHEM RES TOXICOL* 11, 2 (1998), 102–110.
- Sara Goldstein, Gerald M. Rosen, Angelo Russo, and Amram Samuni. 2004. Kinetics of Spin Trapping Superoxide, Hydroxyl, and Aliphatic Radicals by Cyclic Nitrones. *The Journal of Physical Chemistry A* 108, 32 (2004), 6679–6685.
- Qiong Guo, Steven Y. Qian, and Ronald P. Mason. 2003. Separation and identification of DMPO adducts of oxygen-centered radicals formed from organic hydroperoxides by HPLC-ESR, ESI-MS and MS/MS. *Journal of the American Society for Mass Spectrometry* 14, 8 (2003), 862–871.
- B. Halliwell. 1994. Free radicals, antioxidants, and human disease: curiosity, cause, or consequence? Originally published as Volume 2, Issue 8924 344, 8924 (1994), 721–724.
- Clare L. Hawkins and Michael J. Davies. 2013. Detection and characterisation of radicals in biological materials using EPR methodology. *Biochimica et Biophysica Acta (BBA) - General Subjects*

- (2013).
- Weiwei He, Yu-Ting Zhou, Wayne G. Wamer, Mary D. Boudreau, and Jun-Jie Yin. 2012. Mechanisms of the pH dependent generation of hydroxyl radicals and oxygen induced by Ag nanoparticles. *Biomaterials* 33, 30 (2012), 7547–7555.
- Anja Heins, Donald McPhail, Tobias Sokolowski, Heiko Stöckmann, and Karin Schwarz. 2007. The Location of Phenolic Antioxidants and Radicals at Interfaces Determines Their Activity. *Lipids* 42, 6 (2007), 573–582.
- Edward G. Janzen, Yashige Kotake, and Randall D. Hinton. 1992. Stabilities of hydroxyl radical spin adducts of PBN-type spin traps. *Free Radical Biology and Medicine* 12, 2 (1992), 169–173.
- Edward G. Janzen, Peter H. Krygsmann, David A. Lindsay, and D. Larry Haire. 1990. Detection of alkyl, alkoxy, and alkyperoxy radicals from the thermolysis of azobis(isobutyronitrile) by ESR/spin trapping. Evidence for double spin adducts from liquid-phase chromatography and mass spectroscopy. *Journal of the American Chemical Society* 112, 23 (Nov. 1990), 8279–8284.
- Edward G. Janzen, Stable Free Radicals, Diamagnetic Traps, and A. Historical. 2012. A critical review of spin trapping. *Free radicals in biology* 4 (2012), 115.
- Arkadi G. Krainev and Diana J. Bigelow. 1996. Comparison of 2,2'-azobis(2-amidinopropane) hydrochloride (AAPH) and 2,2'-azobis(2,4-dimethylvaleronitrile) (AMVN) as free radical initiators: a spin-trapping study. *J. Chem. Soc., Perkin Trans. 2*, 4 (1996), 747–754.
- Jie Liu, Steven Y. Qian, Qiong Guo, JinJie Jiang, Michael P. Waalkes, Ronald P. Mason, and Maria B. Kadiiska. 2008. Cadmium generates reactive oxygen- and carbon-centered radical species in rats: Insights from in vivo spin-trapping studies. *Free Radical Biology and Medicine* 45, 4 (2008), 475–481.
- Paul R. Marriott, Perkins, M. John, and David Griller. 1980. Spin trapping for hydroxyl in water: a kinetic evaluation of two popular traps. *Can. J. Chem.* 58, 8 (1980), 803–807.
- Subhash C. Mojumdar, David A. Becker, Gino A. DiLabio, James J. Ley, L. Ross C. Barclay, and K. U. Ingold. 2004. Kinetic Studies on Stilbazulenyl-bis-nitron (STAZN), a Nonphenolic Chain-Breaking Antioxidant in Solution, Micelles, and Lipid Membranes. *The Journal of Organic Chemistry* 69, 9 (2004), 2929–2936.
- Etsuo Niki. Free radicals initiators as source of water-or lipid-soluble peroxy radicals. *Methods in enzymology* 186 (1990), 100–108. Noriko Noguchi, Hiromasa Yamashita, Naohiro Gotoh, Yuko Yamamoto, Rika Numano, and Etsuo Niki. 1998. 2,2'-Azobis (4-Methoxy-2,4-Dimethylvaleronitrile), a New Lipid-Soluble Azo Initiator: Application to Oxidations of Lipids and Low-Density Lipoprotein in Solution and in Aqueous Dispersions. *Free Radical Biology and Medicine* 24, 2 (1998), 259–268.
- Christo P. Novakov, Dennis Feerman, Arthur I. Cederbaum, and Detcho A. Stoyanovsky. 2001. An ESR and HPLC-EC Assay for the Detection of Alkyl Radicals. *Chemical Research in Toxicology* 14, 9 (2001), 1239–1246.
- S. Y. Qian, H. P. Wang, F. Q. Schafer, and G. R. Buettner. 2000. EPR detection of lipid-derived free radicals from PUFA, LDL, and cell oxidations. *Free Radical Bio Med* 29, 6 (2000), 568–579.
- Cristina Rota, D. Barr, M. Martin, F. Guengerich, Aldo Tomasi, and R. Mason. 1997. Detection of free radicals produced from the reaction of cytochrome P-450 with linoleic acid hydroperoxide. *Biochem. J* 328 (1997), 565–571.
- K. M. Schaich and D. C. Borg. 1988. Fenton reactions in lipid phases. *Lipids* 23, 6 (1988), 570–579.
- Benjamin P. Soule, Fuminori Hyodo, Ken-ichiro Matsumoto, Nicole L. Simone, John A. Cook, Murali C. Krishna, and James B. Mitchell. 2007. The chemistry and biology of nitroxide compounds. *Free Radical Biology and Medicine* 42, 11 (2007), 1632–1650.
- K. Stolze, N. Udilova, and H. Nohl. 2000a. Spin trapping of lipid radicals with DEPMPO-derived spin traps: Detection of superoxide, alkyl and alkoxy radicals in aqueous and lipid phase. *Free Radical Bio Med* 29, 10 (2000), 1005–1014.
- K. Stolze, N. Udilova, and H. Nohl. 2002. Spin adducts of superoxide, alkoxy, and lipid-derived radicals with EMPO and its derivatives. *Biol Chem* 383, 5 (2002), 813–820.
- Klaus Stolze, Natascha Rohr-Udilova, Anjan Patel, and Thomas Rosenau. 2011. Synthesis and characterization of 5-hydroxymethyl-5-methyl-pyrroline N-oxide and its derivatives. *Bioorganic & Medicinal Chemistry* 19, 2 (2011), 985–993.
- Klaus Stolze, Natascha Udilova, and Hans Nohl. 2000b. Lipid radicals: Properties and detection by

- spin trapping. *Acta Biochimica Polonica* 47, 4 (2000), 923–930.
- Hitoshi Taniguchi and Keith P. Madden. 1999. An in situ radiolysis time-resolved ESR study of the kinetics of spin trapping by 5, 5-dimethyl-1-pyrroline-N-oxide. *Journal of the American Chemical Society* 121, 50 (1999), 11875–11879.
- Frederick A. Villamena, Christopher M. Hadad, and Jay L. Zweier. 2003. Kinetic Study and Theoretical Analysis of Hydroxyl Radical Trapping and Spin Adduct Decay of Alkoxy carbonyl and Dialkoxylphosphoryl Nitrones in Aqueous Media. *J. Phys. Chem. A* 107, 22 (2003), 4407–4414.
- Signe Westermann, Dagmar A. Brüggemann, Karsten Olsen, and Leif H. Skibsted. 2009. Light-induced formation of free radicals in cream cheese. *Food Chemistry* 116, 4 (2009), 974–981.



# 3 Partitioning of nitroxides in dispersed systems investigated by ultrafiltration, EPR and NMR spectroscopy

Heimke Krudopp<sup>a</sup>, Frank D. Sönnichsen<sup>b</sup> and Anja Steffen-Heins<sup>a</sup>

<sup>a</sup>Institute of Human Nutrition and Food Science, Kiel University, 24118 Kiel, Germany

<sup>b</sup>Otto Diels Institute for Organic Chemistry, Kiel University, 24118 Kiel, Germany

Journal of Colloid and Interface Science, 2015, Aug 15;452:15-23.

doi: 10.1016/j.jcis.2015.03.001

## 3.1 Abstract

*Hypothesis:* The partitioning behavior of paramagnetic nitroxides in dispersed systems can be determined by deconvolution of electron paramagnetic resonance (EPR) spectra giving equivalent results with the validated methods of ultrafiltration techniques (UF) and pulsed-field gradient nuclear magnetic resonance spectroscopy (PFG-NMR).

*Experiments:* The partitioning behavior of nitroxides with increasing lipophilicity was investigated anionic, cationic and nonionic micellar systems and 10 % o/w emulsions. Apart from EPR spectra deconvolution, the PFG-NMR was used in micellar solutions as a non-destructive approach, while UF based on separation of very small volume of the aqueous phase.

*Findings:* As a function of their substituent and lipophilicity, the proportions of nitroxides that were solubilized in the micellar or emulsion interface increased with increasing nitroxide lipophilicity for all emulsifier used. Comparing the different approaches, EPR deconvolution and UF revealed comparable nitroxide proportions that were solubilized in the interfaces. Those proportions were higher than found with PFG-NMR. For PFG-NMR self-diffusion experiments the reduced nitroxides were used revealing a high dynamic of hydroxylamines and emulsifiers. Deconvolution of EPR spectra turned out to be the preferred method for measuring the partitioning behavior of paramagnetic molecules as it enables distinguishing between several populations at their individual solubilization sites.

## 3.2 Introduction

Today, paramagnetic nitroxides are used in several fields of research [Borbat 2001; Soule et al. 2007; Keana 1978] i.e. in controlled free radical polymerization [Farcet et al. 2000], or as spin probes in pharmaceutical research. In this field, nitroxides are used to observe the release of drug compounds from micellar structures [Wang et al. 2004; Qian et al. 2000] or from solid lipid nanoparticles [Jores et al. 2003, 2003] and to monitor lipid oxidation at its early stage [Cimato et al. 2004; Voest et al. 1993]. Owing to their lipophilicity and chemical structure, nitroxides partition into the distinct phases in dispersed systems such as emulsions and micellar solutions [Aliaga et al. 2012]. The type of the emulsifier thereby ascertain the proportion and distinct location of nitroxides within the dispersed phase which is crucial for the nitroxides function and reactivity [Berton-Carabin et al. 2013a, 2013b]. Thus, the knowledge of the influence of emulsifiers on the partitioning and function of nitroxides is crucial prior to application of nitroxides as spin probe into foods or pharmaceutical products for monitoring lipid oxidation, antioxidant effectiveness or releases of bioactive compounds.

There are different methods available to determine the partitioning of small molecules in dispersed systems which are minimally invasive. Romsted and Zhang [2002] developed a pseudophase kinetic model to determine the distribution constants of antioxidants in microemulsions. Ultrafiltration (UF) is often used to study the solubilization of small molecules in micellar aggregates [Oehlke et al. 2010], whereas separation of only a small proportion of the continuous phase from the initial emulsion does not interfere with the partitioning equilibrium of the emulsifiers [Stöckmann and Schwarz 1999]. The chemical shift specificity of pulsed-field gradient nuclear magnetic resonance (PFG-NMR) technique allows the simultaneous measurement of the diffusion coefficients of the individual species [Otto et al. 2003] without perturbing aggregation equilibria. This method is well known to study the partition of small molecules in micelles in the past decade [Kreilgaard et al. 2000; Wang et al. 2004; Otto et al. 2003; Dupont-Leclercq et al. 2007] as for instance to obtain the solubilized fraction of phenol in CTAB micelles [Sabatino et al. 2010].

Investigating paramagnetic molecules, the electron paramagnetic resonance spectroscopy (EPR) may be a good alternative to determine the partitioning of e.g. stable radicals [Aliaga et al. 2012]. The benefit of EPR is that the internal structure of the emulsions is not influenced and EPR spectra additionally give a variety of information on the molecule environment. The hyperfine splitting constants are indicative of the polarity of the molecular environment [Jores et al. 2003] by which the partition of different populations of nitroxides between the interface and bulk water can be monitored [Lucarini et al. 2005]. The partitioning between buffer and interface may be calculated as the ratio between the signal intensities of the high field peak, which is only possible with e.g. TEMPO (2,2,6,6-tetramethylpiperidine-1-oxyl) when the hyperfine splitting constants of superimposed spectra lead to the separation of the high field peak [Kveder et al. 1997]. As hydrophilic ascorbic acid is supposed to reduce the nitroxide proportion only in the water phase, it can be used to

solely monitor the nitroxide proportion that is intercalated into the dispersed phase [Jores et al. 2003; Dejanovic et al. 2008; Kveder et al. 1997; Ahlin et al. 2000]. The rotational correlation time describes a restricted motion in micelles and reflects the dynamics of the surrounding which is proportional to the microviscosity [Ahlin et al. 2003; Lewińska et al. 2012; Dejanovic et al. 2008]. Together with the spectral shape they are determined by the molecular mobility of the nitroxide and are therefore indicative for the location of the spin probe. Almeida and colleagues [1998] studied the localization of TEMPO and TEMPOL (2,2,6,6-tetramethyl-4-piperidinol-1-oxyl) in the interface of CTAC, SDS, HPS and Triton X-100 micellar solutions and proposed that both nitroxides had the equal solubilization site but were different orientated.

However, considering the combination of spectral information, it is possible to calculate the partitioning of the individual spin probe populations and their characteristics from the deconvolution of the recorded spectrum. The Štrancar group [2005] investigated the simulation software EPRSIM-C to enable the different spectral populations of a spin probe that differ in site, micro polarity and molecular tumbling to be distinguished.

The aim of the study was to find out the most suitable approach for determination of the partitioning behavior of paramagnetic molecules in dispersed systems. The knowledge on the partitioning and location of paramagnetic molecules in dispersed systems as a function of different interface properties allow to applicate those nitroxides as probes to characterize interface properties on a molecular level. Just to name a few applications, nitroxides could be used to investigate their reactions with antioxidants or free radicals at the interfaces of food systems. Applications of probes for nano carriers are also conceivable to test interferences with encapsulates, coating material or other interfacial active matrix compounds such as proteins. Studies on release of probes from nano carriers may be also suitable for storage or in vitro digestion tests.

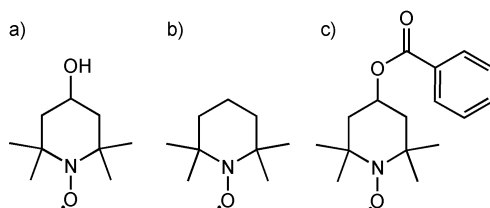


Figure 3.1: Paramagnetic nitroxides TEMPOL (a), TEMPO (b) and TB (c).

To the best of our knowledge this is the first time that different methods were compared to investigate the partitioning behavior of paramagnetic small molecules in micelles and emulsions. Thus, ultrafiltration of dispersed systems and EPR detection of nitroxides within the permeate as well as EPR spectra of the entire dispersed system that was simulated for individual spin probe population [Štrancar et al. 2005] and PFG-NMR technique were compared to validate the methods. TEMPOL, TEMPO and TEMPOL-benzoate (TB,

2,2,6,6-tetramethyl-4-piperidinol-1-oxylbenzoate) (3.1) were used as nitroxides in micellar solutions and emulsions that contain anionic SDS, cationic CTAB or non-ionic Brij58 as emulsifier. Therefore, different interfaces were produced to show the influence of different environments on the partitioning of the spin probes used in this study.

### 3.3 Materials and Methods

#### 3.3.1 Chemicals

SDS (sodium dodecylsulfate, >99 %), sodium acetate (>99 %, anhydrous), acetic acid, ascorbic acid and n-hexane were obtained from Carl Roth, Germany. CTAB (hexadecyltrimethylammonium bromide, >99 %), Brij58 (Polyethylene glycol hexadecyl ether), aluminum oxide, TEMPO (2,2,6,6-tetramethyl-4-piperidinol-1-oxyl) TEMPOL (4-Hydroxy-2,2,6,6-tetramethylpiperidine 1-oxyl) and TEMPOL-benzoate (2,2,6,6-tetramethyl-4-piperidinol-1-oxyl benzoate) were purchased from Sigma Aldrich, Germany. Deuterated sodium acetate (99 %) and deuterated acetic acid (99,5 %) were purchased from Deutero, Germany. Corn oil was purchased at the local market and purified according to Lampi and Kamal-Eldin [1998]. All chemicals were of analytical grade and used without further purification.

#### 3.3.2 Preparation of micellar solutions

The micellar solutions contained 1wt % emulsifier in acetic acid buffer solution (0.05 mol, pH 5.0). Nitroxide stock solutions of TEMPO and TEMPOL in buffer were added to micellar solution and well mixed. TB was dissolved in ether and the solvent was evaporated under nitrogen. The micellar solution was added to the re-crystallized nitroxide and placed in ultrasonic bath. The solutions were diluted with buffer solution to the final nitroxide concentration of 1 mmol. For control measurements in pure buffer solution in case of TB the supernatant was used for further experiment due to poor solubility.

#### 3.3.3 Preparation of emulsions

The oil-in-water emulsions consisted of 10 wt% commercial corn oil in acetic acid buffer solution (0.05 mol, pH 5.0) with 1 wt% emulsifier. For EPR measurements batches of 5 ml were prepared. 0.5 g oil was weighted into plastic sample tubes followed by 2 ml emulsifier solution (2.5 wt%). Stock solutions of nitroxides TEMPO and TEMPOL in buffer was added and the pre-emulsion was formed by shaking. In case of TB a stock solution of the nitroxide in ether was transferred to the sample tube on ice. The solvent was evaporated under nitrogen and the re-crystallized nitroxide remained in the sample tube for the emulsion preparation as described above. The pre-emulsion was sonicated for 180 sec (cycle 9, 40 % power, Bandelin sonopuls HD 2200). After 30 s the remaining buffer was added stepwise within 30 s. For UF experiments batches of 12 ml were prepared as described above.



### 3.3.4 Preparation of NMR samples

Micellar solutions for NMR experiments were prepared in deuterated acetic acid buffer solution (0.05 mole, pH 5.0). Prior to the measurements the nitroxides were reduced by ascorbic acid to their hydroxylamines [Kveder et al. 1997; Jores et al. 2003]. Emulsifier concentrations were 0.1 wt% for CTAB and Brij58 and 0.7 wt% for SDS, which were well above the individual critical micellar concentrations. Stock solutions of nitroxides TEMPO and TEMPOL in deuterated buffer were mixed with equal molar ascorbic acid stock solution. TEMPOL-benzoate was dissolved in ether and the solvent was evaporated under nitrogen. Micellar stock solution was added to the re-crystallized nitroxide and placed in ultrasonic bath. Ascorbic acid stock solution was added in equal molar ratio. Reduction of nitroxides was monitored by EPR. Prior to the measurements 50  $\mu$ l TSP/D<sub>2</sub>O was added to 500  $\mu$ l sample. The solution was transferred to a 5 mm NMR tube.

### 3.3.5 Determination of critical micellar concentration

Critical micellar concentration (cmc) was determined by dye micellization method at room temperature. In the presence of increasing emulsifier concentration the reduced absorbance of eosin y was measured in triplicate for SDS and Brij58 at 542 nm (eosin y concentration 0.019 mM) [Patist et al.2000] and for CTAB at 526 nm (eosin y concentration 0.005 mM) [Suradkar et al. 2006] on Genesys 10S UV-Vis spectrophotometer (Thermo Scientific, Braunschweig, Germany). Absorbance was plotted against common logarithm of emulsifier concentration and fitted with a step function in Origin 8.0 to calculate the point of deflection according to Heins and colleagues [2006].

### 3.3.6 EPR based partitioning behavior

Electron paramagnetic spin resonance (EPR) measurements of the nitroxides were carried out on a Bruker Elexsys II E500 spectrometer (Rheinstetten, Germany) operating with X-band at 9.85 GHz at room temperature. EPR settings were as followed: modulation frequency: 100 kHz; modulation amplitude: 1.2 G; sweep width: 66.7 G; microwave power: 0.2 mW; time constant: 41 ms; conversion time: 20 ms and center field: 3512 G.

#### 3.3.6.1 Ultrafiltration probes

Ultrafiltration experiments were carried out at room temperature according to Oehlke and colleagues [2008]. Centrifugal devices (Merck Millipore, Germany, 3 kDa) were used to separate a small volume of the aqueous phase containing emulsifier monomers and non-solubilized nitroxides from the micellar solution or emulsion without phase segregation. Prior to the separation the membranes were flushed with buffer for 30 min at 2000 g. Containing 2 ml emulsion or micellar solution centrifugation was applied for 5 min at 2000 g, in case of Brij58 at 300 g in order to separate approx. 30  $\mu$ l – 50  $\mu$ l aqueous phase. The first two centrifugation steps were used to equilibrate the membrane as the

filtrate concentration increased. The following three centrifuge permeates were measured. All experiments were carried out in duplicates with three sampling steps each, so that the results were the mean of six individual values. The experiments were performed at room temperature. EPR spectra were acquired from the entire sample to determine the total nitroxides content ( $c_{total}$ ) and from the permeates after each centrifugation step to determine the non-solubilized nitroxide content from permeates after each centrifugation step to determine the non-solubilized nitroxide content ( $c_{non-sol}$ ). The nitroxide contents were calculated by double integration of the entire EPR spectrum given as the area under the curve. The proportion of the solubilized nitroxide ( $d_{sol}$ ) in the micellar phase, the oil phase or the interface was calculated by equation 3.1,

$$d_{sol} = 100 - \frac{c_{non-sol}}{c_{total}} \cdot 100 \quad (3.1)$$

### 3.3.6.2 Deconvolution of superimposed spectra with EPRSIM-C

The partitioning behavior of nitroxides was analyzed by deconvolution of the individual probe populations using EPRSIM-C software for nitroxide fitting developed by Štrancar and colleagues [2005]. To proof the best fit parameters of the spectra different numbers and kinds of models were evaluated and proofed for lowest value of chi-squared test of goodness of fit as well as for minimum difference after subtraction of fitted from measured spectra. To separate these individual spectra from the experimental spectrum three biophysical models were used based on the following parameters: line shape (Lw), rotational correlation time ( $\tau_c$ ), relative weight (d), order parameter (S), broadening constant (W), and polarity correction factors for the g and A tensors ( $p_g$  and  $p_A$ ). The first model was used for an isotropic tumbling spin probe within an isotropic environment (population 1). Regarding the polarity of population 2, as the second model either a concentration of the nitroxide spin probes in an isotropic environment was assumed, in which spin exchange was considered or a fast tumbling spin probe in an anisotropic environment like the head group or inner core of a micelle was adopted. Population 3 was simulated by considering the anisotropic environment. The g tensors for TB and TEMPO are  $g_{xx}=2.0103$ ,  $g_{yy}=2.0069$ ,  $g_{zz}=2.0030$  and the A tensors are  $A_{xx}=7.60$ ,  $A_{yy}=6.00$ ,  $A_{zz}=31.80$ . For TEMPOL tensors were  $g_{xx}=2.0095$ ,  $g_{yy}=2.0064$ ,  $g_{zz}=2.0027$  for g tensors and  $A_{xx}=7.60$ ,  $A_{yy}=6.00$ ,  $A_{zz}=31.80$  for A tensors [Berliner 1976]. The spectral parameters for the superimposed spectra were calculated from the simulated spectrum and given as the mean of three individual samples. The overall micro polarity of the spin probe was calculated by means of the hyperfine splitting parameter  $a_N$  and was given as the distance between low field peak ( $h_{+1}$ ) and middle field peak ( $h_0$ ).

### 3.3.7 NMR based partitioning behavior

$^1\text{H}$ -NMR spectra using a  $90^\circ$  pulse and excitation sculpting for water suppression were recorded on a Bruker 600 MHz NMR controlled by Topspin 3.2 spectrometer operating

software (Bruker) at 295 K. A spectral width of 16 ppm, 2 s acquisition time and a relaxation delay of 2 s were used. Self-diffusion coefficients were measured with a pseudo 2D-sequence using stimulated echo, bipolar gradient pulses for diffusion, a spectral width of 14 ppm, 2 seconds acquisition time, 1.5 s relaxation delay and 32 experiments with linearly varying gradient strength. Reduced nitroxides show fast exchange between aqueous and micellar phase. Hence, the measured diffusion coefficients of nitroxides in presence of emulsifiers were weighted averages of the contributions from non-solubilized and solubilized nitroxides. By measuring the diffusion coefficient of reduced nitroxides in buffer solution ( $D_{Nbuffer}$ ) and in micellar solution ( $D_N$ ) and of the unloaded micelle ( $D_{mic}$ ) the proportion of solubilized nitroxide in the micellar phase ( $d_{sol}$ ) was calculated by equation 3.2,

$$d_{sol} = \frac{D_N - D_{Nbuffer}}{D_{mic} - D_{Nbuffer}} \cdot 100 \quad (3.2)$$

The reported values for the diffusion of the micelle ( $D_{obs}$ ) have been corrected to remove the contribution of the emulsifier monomers ( $D_{mono}$ ) to the observed self-diffusion coefficient ( $D_{obs}$ ) using the equation by Vinogradova and colleagues [1998],

$$D_{mic} = \frac{D_{obs} - \frac{cmc}{c_{emul}} \cdot D_{mono}}{1 - \frac{cmc}{c_{emul}}} \quad (3.3)$$

where cmc is the critical micelle concentration and  $c_{emul}$  represents the total concentration of emulsifier.

Deviations of replicate assessments were proofed fivefold for TEMPO in SDS micellar solution and were generally very small below  $< 5\%$ . Therefore diffusion coefficients were determined by single experiments and the relative experimental error for all diffusion measurements were estimated to about 5%.

## 3.4 Results and discussion

### 3.4.1 Diffusion rates of hydroxylamines

NMR self-diffusion measurements are not suitable for paramagnetic substances because this technique requires slowly relaxing proton signals [Furtado et al. 2011]. Proton resonances from paramagnetic substances completely relax within microseconds, while the NMR's time scale for acquisition is in the range of milliseconds to seconds. In contrast, the EPR's time scale is nanosecond, and thus suited for studying faster dynamics [Borbat 2001]. Therefore we used the reduced form of the nitroxides, the hydroxylamines, for this NMR study. Nevertheless, it has to be noted that the lipophilicity of reduced nitroxides is expected to be somewhat lower than that of the paramagnetic molecules.

Diffusion coefficients were calculated from peaks at 1.41 ppm ( $\text{CH}_3$  substituents in  $\alpha$ -position) for TEMPOL-H and TEMPO-H and 8.05 ppm (H in C2-position of benzene ring) for TB-H. The determination of diffusion coefficients of compounds with weak resonances

located in the foot of strong signals was rather difficult [Kreilgaard et al. 2000], which was the case with reduced nitroxides in micellar buffer solution. To avoid the strong signals of buffer components, deuterated acetic acid and sodium acetate were used. While an increase of the the nitroxide relative to detergent concentration would have increased integral accuracy in the remaining overlapp situations, this was not pursued in order to prevent an overload of molecules in the micellar interface. The accuracy of the determined diffusion coefficient of signals on foot of strong signals was determined in comparison to the other signals, for example the methylene groups of the benzene ring. Nevertheless, the determinations of diffusion coefficients in a few probes were difficult. The diffusion rates of TEMPO-H in CTAB and TB-H in Brij58 as well as Brij58 monomers were difficult to obtain. Because of small peaks or difficult resolution of a peak next to an intense peak the curve progression showed greater variability than in the other samples.

Table 3.1: Critical micellar concentration (cmc) and self-diffusion coefficients ( $D_N$ ) of hydroxylamines TEMPOL-H, TEMPO-H and TB-H in micelles of SDS, CTAB and Brij58 emulsifier monomers ( $D_{\text{mono}}$ ) and unloaded micelles ( $D_{\text{mic}}$ ).

	self-diffusion coefficients ( $D \pm 5\%$ ) <sup>a</sup>						
	in the absence of nitroxides				in the presents of nitroxides		
	cmc mM	$D_{\text{mono}}$ $10^{-10} \text{ m}^2 \text{ s}^{-1}$	$D_{\text{obs}}$ $10^{-10} \text{ m}^2 \text{ s}^{-1}$	$D_{\text{mic}}^b$ $10^{-10} \text{ m}^2 \text{ s}^{-1}$	$D_N$ TEMPOL $10^{-10} \text{ m}^2 \text{ s}^{-1}$	$D_N$ TEMPO $10^{-10} \text{ m}^2 \text{ s}^{-1}$	$D_N$ TB $10^{-10} \text{ m}^2 \text{ s}^{-1}$
buffer solution	-				6.8	7.2	5.6
CTAB	$0.101 \pm 0.00$	5.5	1.3	1.3	6.5	2.7	3.2
SDS	$6.930 \pm 0.21$	6.3	1.7	2.3	1.4	1.1	1.0
Brij58	$0.013 \pm 0.00$	4.9	0.6	0.7	6.8	6.4	4.1

<sup>a</sup>Single experiments with relative experimental error for all diffusion measurements

<sup>b</sup> $D_{\text{mic}}$  was calculated by equation 3.3

Diffusion rates of hydroxylamines in buffer solution were  $6.8 \cdot 10^{-10} \text{ m}^2 \text{ s}^{-1}$  for TEMPOL-H,  $7.2 \cdot 10^{-10} \text{ m}^2 \text{ s}^{-1}$  for TEMPO-H and  $5.6 \cdot 10^{-10} \text{ m}^2 \text{ s}^{-1}$  for TB-H (table 3.1). TB-H had lower diffusion rates due to the increased size of the benzene ring. In SDS solutions diffusion rates of all reduced nitroxides decreased by a factor of about 5 to 6 down to  $1.0\text{-}1.4 \cdot 10^{-10} \text{ m}^2 \text{ s}^{-1}$ , which was even considerably lower than the diffusion rate of the SDS micelle with  $2.3 \cdot 10^{-10} \text{ m}^2 \text{ s}^{-1}$ . In CTAB and Brij58 diffusion rates of TEMPOL-H were similar to buffer solution. Strong influence was shown for TEMPO-H in CTAB ( $2.7 \cdot 10^{-10} \text{ m}^2 \text{ s}^{-1}$ ) while it was moderate in Brij58 ( $6.4 \cdot 10^{-10} \text{ m}^2 \text{ s}^{-1}$ ). TB-H showed diffusion rates of  $3.2 \cdot 10^{-10} \text{ m}^2 \text{ s}^{-1}$  in CTAB and  $4.1 \cdot 10^{-10} \text{ m}^2 \text{ s}^{-1}$  in Brij58. With the exception of lower values of nitroxides in SDS micelles, the diffusion coefficient in the magnitude of  $10^{-10} \text{ m}^2 \text{ s}^{-1}$  indicated only a moderate incorporation of the nitroxides. Indeed, the diffusion coefficients from the hydroxylamines in SDS micelles ( $D_N$ ) were lower than those of the unloaded SDS micelles ( $D_{\text{obs}}$ ), and considerably after the application of the correction factor (equation 3.3) ( $D_{\text{mic}}$ ) with  $2.3 \cdot 10^{-10} \text{ m}^2 \text{ s}^{-1}$ . This may be due to the amount of SDS monomeres ( $D_{\text{mono}} = 6.3 \cdot 10^{-10} \text{ m}^2 \text{ s}^{-1}$ ) that was still high. The cmc of SDS micelles was

high with  $6.93 \pm 0.21$  mmol indicating that the SDS is a weak detergent and the concentration of SDS was only 4 times the cmc. The low diffusion coefficients of the nitroxides in SDS micellar solutions ( $D_N$ ) indicate that they have a great affinity towards the micelles so that all hydroxylamines applied were completely solubilized in the micellar phase.

SDS self-diffusion rates were almost determined in several studies [Nilsson and Lindman 1984; Söderman et al. 2004; Aizawa et al. 1979; Vinogradova et al. 1998] whereas the emulsifier concentrations used were often higher than in this study resulting in lower diffusion rate of the micelles, i.e.  $0.7 \cdot 10^{-10} \text{ m}^2 \text{ s}^{-1}$  for 8 wt% SDS micellar solutions [Vinogradova et al. 1998]. Söderman and colleagues [2004] determined the self-diffusion of SDS monomers in  $D_2O$  to be  $4.3 \cdot 10^{-10} \text{ m}^2 \text{ s}^{-1}$  which decreased to  $0.28 \cdot 10^{-10} \text{ m}^2 \text{ s}^{-1}$  in micelles. They determined the cmc of SDS in  $D_2O$  with 0.2 wt%, which was higher than the cmc used to calculate the 30fold cmc. On the other hand, the diffusion rates of the monomers were higher in the acetic acid buffer with 10 %  $D_2O$  than in pure  $D_2O$  solution. The obtained self-diffusion coefficient for Brij58 with  $0.6 \cdot 10^{-10} \text{ m}^2 \text{ s}^{-1}$  was also slightly higher compared to the findings of Dupont-Leclercq and colleagues [2007], who determined a self-diffusion coefficient of  $0.3 \cdot 10^{-10} \text{ m}^2 \text{ s}^{-1}$  for Brij58 micelles.

To the best of our knowledge, self-diffusion coefficients for nitroxides and hydroxylamines are rare in literature. Aizawa and colleagues [1979] determined self-diffusion coefficients of  $2 \cdot 10^{-11} \text{ m}^2 \text{ s}^{-1}$  for TB in SDS 4-7 wt% by EPR spin exchange interactions which disagreed with our results. While Furtado and colleagues [2011] determined the self-diffusion coefficient for TEMPO in homogenous aqueous solution with  $6.7 \cdot 10^{-10} \text{ m}^2 \text{ s}^{-1}$  by paramagnetic relaxation enhancement (PRE) NMR which is in same magnitude with  $7.2 \cdot 10^{-10} \text{ m}^2 \text{ s}^{-1}$  for TEMPO-H obtained by PFG-NMR.

However, PFG-NMR is often used to determination the diffusion coefficients of small molecules in dispersed systems [Dupont-Leclercq et al. 2007; Fischer et al. 2009; Kreilgaard et al. 2000]. Kreilgaard and colleagues [2000] determined diffusion coefficients for microemulsions of Labrasol, Plurol Isostearique and isostearylic isostearate in magnitude of  $10^{-12} \text{ m}^2 \text{ s}^{-1}$  indicating an inclusion of the emulsifiers to conjugated frame-like structures. The incorporation of lipophilic lidocaine and hydrophilic prilocaine hydrochloride was by diffusion coefficients in the range of  $10^{-11} \text{ m}^2 \text{ s}^{-1}$  and therefore the presumed association of both compounds to the surfactant structure was confirmed. Fischer and colleagues [2009] investigated the diffusion coefficients from fragrances in micellar solutions. They found that the diffusion coefficient for fragrances decreased in the range of  $\log P = 2.5-3.5$  down to the level of the diffusion coefficients of the surfactant micelles, which proves an incorporation of fragrance molecules into the micelles. Dupont-Leclercq and colleagues [2007] showed that the structure of a molecule including the polarities influences the solubilization properties of octanoic and octylamidotartaric acid in Brij58 and TritonX-100 micelles. The acidic form was located in the micelle to a higher amount whereas the basic form was mainly solved in the aqueous phase. As all probes were carried out in buffer solution at  $\text{pH} = 5$  there was no influence of polarities so the comparison of the individual probes was given.

### 3.4.2 Different microenvironments of spin probes

Nitroxides in dispersed systems give rise to the detection of the coexistence of different rotational motions and polarities of probe populations, which results in spin probe spectra composed of several superimposed spectral components. These superimposed spectra were simulated to calculate the hyperfine splitting ( $a_N$ ), proportion ( $d$ ) and rotational correlation time ( $\tau_c$ ), for each spectral population which are indicative for a characteristic solubilization site in micellar solutions (table 3.2) and emulsions (table 3.2). Deconvolutions were carried out by adoption of different biophysical models as a function of the population polarity by using the software EPRSIM-C of Štrancar and colleagues [2005].

The deconvolution of superimposed nitroxide spectra in micellar solutions and emulsions revealed three different spectral domains for all nitroxides (figure 3.2) which was also found for TB deconvolution in other lipid based structures such as solid lipid nanoparticles [Jores et al. 2003] or liposomes [Frenzel and Steffen-Heins 2014].

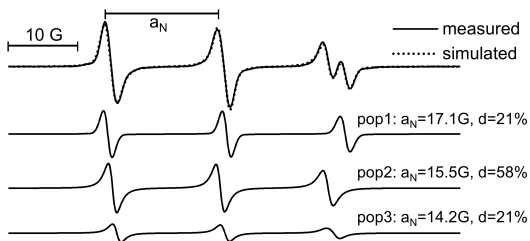


Figure 3.2: Measured and simulated spectra of TEMPO in SDS emulsion. Best fit simulation of superimposed spectra ended up with three individual TEMPO populations with different solubilization sites.

Thereby one population resembled an isotropic spectrum of a free tumbling nitroxide (figure 3.2, population 1), which was indicated by a low  $\tau_c < 0.03$  ns and the hyperfine splitting constants in range of  $a_N = 17.2$ - $16.8$  G (table 1). This range of  $a_N$  for the different nitroxides depends on the substituents on the nitroxide, which lower  $a_N$  of TB and TEMPOL compared with TEMPO [Windle 1981]. As the rotational correlation time  $\tau_c$  describes the rate of motion of the nitroxide as a function of its micro environment  $\tau_c$  is proportional to the microviscosity [Dejanovic et al. 2008], which is very low when solubilized in the bulk water phase as found for population 1. The obtained  $\tau_c$  were in line with findings from Ahlin and colleagues [2003] who found  $\tau_c = 0.04$  ns for TEMPOL in the bulk water phase of solid lipid nanoparticles. To simulate the population 3, a fast tumbling nitroxide population in an anisotropic environment was assumed that is accounted by the interface and /or the oil phase (figure 3.2) with  $\tau_c \gg 0.1$  ns and  $a_N \ll 16.5$  G. To obtain the best fit of the superimposed spectra two possible simulation models for populations 2 were concerned. The most reasonable limit for the model decision was set on  $a_N = 16.5$  G. For  $a_N > 16.5$  G,

population 2 was simulated as concentrated nitroxide spin probes in an isotropic environment, for  $a_N < 16.5$  a fast tumbling nitroxide in an anisotropic environment was adopted. In the case of concentrated nitroxide in a polar environment,  $a_N$  was in the range of 16.5 - 16.8 G also associated with reduction of molecular motion as indicated by  $\tau_c > 0.1$  ns.

Referring  $a_N$  to the micro environmental polarity, tables 3.2 and 3.3 gave two rough ranges of  $a_N$  for the individual population between  $15 \text{ G} < a_N < 16.5 \text{ G}$  for the hydrocarbon phase/interface resembling a variety of solvents with low to medium dielectric constants [Knauer and Napier 1976] and below  $a_N = 15 \text{ G}$  for the oil phase as also found by Mäder for TB in MCT oil [2006]. These different microenvironments were in line with the observations of Jores and colleagues [2003] who identify  $a_N$  values for TB populations of  $a_N = 17.2 \text{ G}$  for the aqueous phase,  $a_N = 16.5\text{-}16.8 \text{ G}$  for high concentrated nitroxides at the surface and  $a_N = 15.1\text{-}15.8 \text{ G}$  for the lipophilic environment in solid lipid nanoparticles and emulsions.

Table 3.2: EPRSIM-C deconvolution of rotational correlation time ( $\tau_c$ ), hyperfine coupling ( $a_N$ ) and proportion of populations 1-3 of the nitroxides TEMPOL, TEMPO and TB in micellar solutions of SDS, CTAB and Brij58.

	TEMPOL			TEMPO			TB		
	CTAB	SDS	Brij58	CTAB	SDS	Brij58	CTAB	SDS	Brij58
	mean $\pm$ SD	mean $\pm$ SD	mean $\pm$ SD	mean $\pm$ SD	mean $\pm$ SD	mean $\pm$ SD	mean $\pm$ SD	mean $\pm$ SD	mean $\pm$ SD
$\tau_{c1}$ [ns] <sup>a</sup>	0.02 $\pm$ 0.006	0.04 $\pm$ 0.025	0.02 $\pm$ 0.007	0.07 $\pm$ 0.003	0.04 $\pm$ 0.006	0.02 $\pm$ 0.010	0.05 $\pm$ 0.015	0.09 $\pm$ 0.138	0.03 $\pm$ 0.006
$a_{N1}$ [G]	16.90 $\pm$ 0.080	16.89 $\pm$ 0.085	16.88 $\pm$ 0.118	17.08 $\pm$ 0.096	17.10 $\pm$ 0.102	17.17 $\pm$ 0.028	17.01 $\pm$ .024	16.75 $\pm$ 0.069	16.86 $\pm$ 0.056
$d_1$ [%]	56 $\pm$ 5.0	58 $\pm$ 2.0	74 $\pm$ 1.0	39 $\pm$ 3.5	35 $\pm$ 4.6	49 $\pm$ 1.5	2 $\pm$ 0.8	4 $\pm$ 1.0	11 $\pm$ 1.2
$\tau_{c2}$ [ns] <sup>b</sup>	0.27 $\pm$ 0.158	0.45 $\pm$ 0.200	0.12 $\pm$ 0.021	0.10 $\pm$ 0.000	0.11 $\pm$ 0.012	0.17 $\pm$ 0.127	0.54 $\pm$ 0.025	0.29 $\pm$ 0.058	0.34 $\pm$ 0.410
$a_{N2}$ [G]	16.73 $\pm$ 0.102	16.62 $\pm$ 0.075	16.75 $\pm$ 0.053	16.74 $\pm$ 0.175	16.67 $\pm$ 0.056	16.87 $\pm$ 0.025	15.86 $\pm$ 0.074	16.11 $\pm$ 0.138	16.11 $\pm$ 0.352
$d_2$ [%]	31 $\pm$ 4.2	33 $\pm$ 6.1	17 $\pm$ 3.0	20 $\pm$ 1.5	19 $\pm$ 4.9	17 $\pm$ 1.5	67 $\pm$ 2.6	56 $\pm$ 4.0	42 $\pm$ 2.9
$\tau_{c3}$ [ns] <sup>c</sup>	0.16 $\pm$ 0.095	0.10 $\pm$ 0.000	0.13 $\pm$ 0.095	0.16 $\pm$ 0.067	0.10 $\pm$ 0.000	0.13 $\pm$ 0.029	0.31 $\pm$ 0.025	0.28 $\pm$ 0.018	0.07 $\pm$ 0.053
$a_{N3}$ [G]	15.58 $\pm$ 1.330	16.11 $\pm$ 0.586	15.36 $\pm$ 0.095	16.16 $\pm$ 0.067	16.47 $\pm$ 0.141	16.25 $\pm$ 0.291	15.41 $\pm$ 0.199	15.72 $\pm$ 0.138	15.89 $\pm$ 0.282
$d_3$ [%]	13 $\pm$ 3.5	9 $\pm$ 5.2	9 $\pm$ 2.0	42 $\pm$ 1.7	46 $\pm$ 1.2	33 $\pm$ 3.1	31 $\pm$ 2.5	40 $\pm$ 3.2	47 $\pm$ 2.6

<sup>a</sup>Population 1 was simulated by EPRSIM-C adopting an fast tumbling nitroxide in an isotropic environment.

<sup>b</sup>For  $a_N > 16.5$ , population 2 was simulated by EPRSIM-C adopting an concentrated nitroxide spin probes in isotropic environment, for  $a_N < 16.5$  for population 2 an fast tumbling nitroxide in an anisotropic environment was adopted.

<sup>c</sup>Population 3 was simulated by EPRSIM-C adopting an fast tumbling in an anisotropic environment.

Values of nitroxide populations in pure buffer solutions were simulated as: TEMPOL ( $a_{N1}=17.06\pm 0.05$ ,  $\tau_c=0.01\pm 0.00$ ,  $d_1=55\pm 1.6$ ;  $a_{N2}=16.81\pm 0.05$ ,  $\tau_c=0.14\pm 0.01$ ,  $d_2=45\pm 1.6$ ); TEMPO ( $a_{N1}=17.28\pm 0.00$ ,  $\tau_c=0.01\pm 0.00$ ,  $d_1=55\pm 1.2$ ;  $a_{N2}=17.09\pm 0.05$ ,  $\tau_c=0.1\pm 0.00$ ,  $d_2=45\pm 1.2$ ) and TB ( $a_{N1}=17.00\pm 0.07$ ,  $\tau_c=0.03\pm 0.00$ ,  $d_1=67\pm 1.6$ ;  $a_{N2}=16.78\pm 0.05$ ,  $\tau_c=0.17\pm 0.01$ ,  $d_2=33\pm 1.6$ ).

In pure buffer solution 1 mmol TEMPO and TEMPOL possessed a free tumbling ( $d_1 = 55$  %) and a concentrated cluster population ( $d_2 = 45$  %). The TB proportion that was solubilized in water, which was below 0.1 mmol, showed a free tumbling population of  $d_1 = 67$  %. Indicated by  $a_N$  and  $\tau_c$  values in micellar solutions (table 3.2), TEMPOL and TEMPO adapted three different spectral domains with two populations in the aqueous phase, where one was a clustered and the second one was a free tumbled population. The third population was solubilized in the hydrocarbon/interface. Thereby, the major content of hydrophilic TEMPOL that was free tumbling resembled the free population in pure buffer solution. The clustered population was lower since a third population could be solubilized in the hydrocarbon/interface. In contrast in Brij58 micellar solution the isotropic population was higher. More of the nitroxide TEMPO was solubilized in the hydrocarbon/interphase

being in the range  $\text{SDS} > \text{CTAB} > \text{Brij58}$  thereby reducing the clustered population to only 20 % and the free tumbling to round about 40 %. Only a very small proportion of TB by 2-11 % was solubilized in the aqueous phase, whereas two populations intercalated in the interface that slightly differ in polarity.

Table 3.3: EPRSIM-C deconvolution of rotational correlation time ( $\tau_c$ ), hyperfine coupling ( $a_N$ ) and proportion of populations 1-3 of the nitroxides TEMPOL, TEMPO and TB in emulsions of SDS, CTAB and Brij58.

	TEMPOL			TEMPO			TB		
	CTAB	SDS	Brij58	CTAB	SDS	Brij58	CTAB	SDS	Brij58
	mean $\pm$ SD	mean $\pm$ SD	mean $\pm$ SD	mean $\pm$ SD	mean $\pm$ SD	mean $\pm$ SD	mean $\pm$ SD	mean $\pm$ SD	mean $\pm$ SD
$\tau_{c1}$ [ns] <sup>a</sup>	0.01 $\pm$ 0.010	0.02 $\pm$ 0.012	0.02 $\pm$ 0.014	0.09 $\pm$ 0.017	0.09 $\pm$ 0.006	0.03 $\pm$ 0.002	0.41 $\pm$ 0.018	0.24 $\pm$ 0.036	0.45 $\pm$ 0.012
$a_{N1}$ [G]	17.00 $\pm$ 0.000	16.98 $\pm$ 0.038	17.02 $\pm$ 0.038	17.22 $\pm$ 0.038	17.11 $\pm$ 0.038	17.26 $\pm$ 0.000	16.81 $\pm$ 0.000	16.91 $\pm$ 0.038	16.44 $\pm$ 0.075
$d_1$ [%]	65 $\pm$ 5.5	59 $\pm$ 3.5	56 $\pm$ 1.4	12 $\pm$ 1.6	21 $\pm$ 0.6	17 $\pm$ 0.0	7 $\pm$ 0.1	4 $\pm$ 1.2	11 $\pm$ 2.1
$\tau_{c2}$ [ns] <sup>b</sup>	0.60 $\pm$ 0.298	0.54 $\pm$ 0.231	0.14 $\pm$ 0.049	0.13 $\pm$ 0.007	0.11 $\pm$ 0.012	0.11 $\pm$ 0.006	0.17 $\pm$ 0.014	0.22 $\pm$ 0.021	0.13 $\pm$ 0.015
$a_{N2}$ [G]	16.65 $\pm$ 0.235	16.61 $\pm$ 0.113	16.74 $\pm$ 0.065	15.55 $\pm$ 0.075	15.50 $\pm$ 0.616	15.59 $\pm$ 0.038	15.37 $\pm$ 0.000	15.46 $\pm$ 0.038	15.41 $\pm$ 0.038
$d_2$ [%]	18 $\pm$ 7.5	32 $\pm$ 7.2	34 $\pm$ 4.2	66 $\pm$ 1.5	58 $\pm$ 2.3	71 $\pm$ 1.0	65 $\pm$ 2.0	71 $\pm$ 3.5	62 $\pm$ 1.5
$\tau_{c3}$ [ns] <sup>c</sup>	0.13 $\pm$ 0.025	0.57 $\pm$ 0.535	0.56 $\pm$ 0.300	0.42 $\pm$ 0.061	0.48 $\pm$ 0.164	0.10 $\pm$ 0.000	0.33 $\pm$ 0.031	0.29 $\pm$ 0.012	0.25 $\pm$ 0.015
$a_{N3}$ [G]	14.66 $\pm$ 1.564	14.31 $\pm$ 0.359	14.22 $\pm$ 1.760	14.44 $\pm$ 0.038	14.24 $\pm$ 0.209	15.39 $\pm$ 0.075	14.24 $\pm$ 0.136	14.40 $\pm$ 0.172	14.18 $\pm$ 0.038
$d_3$ [%]	18 $\pm$ 6.8	9 $\pm$ 3.8	10 $\pm$ 2.1	22 $\pm$ 2.6	21 $\pm$ 2.3	12 $\pm$ 1.0	28 $\pm$ 2.0	25 $\pm$ 3.8	27 $\pm$ 1.5

<sup>a</sup>Population 1 was simulated by EPRSIM-C adopting an fast tumbling nitroxide in an isotropic environment.

<sup>b</sup>For  $a_N > 16.5$ , population 2 was simulated by EPRSIM-C adopting an concentrated nitroxide spin probes in isotropic environment, for  $a_N < 16.5$  for population 2 an fast tumbling nitroxide in an anisotropic environment was adopted.

<sup>c</sup>Population 3 was simulated by EPRSIM-C adopting an fast tumbling in an anisotropic environment.

Values of nitroxide populations in pure buffer solutions were simulated as: TEMPOL ( $a_{N1}=17.06 \pm 0.05$ ,  $\tau_c=0.01 \pm 0.00$ ,  $d_1=55 \pm 1.6$ ;  $a_{N2}=16.81 \pm 0.05$ ,  $\tau_c=0.14 \pm 0.01$ ,  $d_2=45 \pm 1.6$ ), TEMPO ( $a_{N1}=17.28 \pm 0.00$ ,  $\tau_c=0.01 \pm 0.00$ ,  $d_1=55 \pm 1.2$ ;  $a_{N2}=17.09 \pm 0.05$ ,  $\tau_c=0.10 \pm 0.00$ ,  $d_2=45 \pm 1.2$ ) and TB ( $a_{N1}=17.00 \pm 0.07$ ,  $\tau_c=0.03 \pm 0.00$ ,  $d_1=67 \pm 1.6$ ;  $a_{N2}=16.78 \pm 0.05$ ,  $\tau_c=0.17 \pm 0.01$ ,  $d_2=33 \pm 1.6$ ).

In emulsion systems, the third population revealed a much lower  $a_N < 15$  G and a  $\tau_c > 0.3$  ns indicating a solubilization in the oil phase for all nitroxide-emulsifier combinations (table 3.3) [Jores et al. 2003]. The two populations of the hydrophilic TEMPOL in the aqueous phase showed identical properties as in micellar solutions. However, TEMPO lost its clustered population and partitions into the oil and the interface while the free tumbling proportion in the aqueous phase was reduced to 10-20 % as a function of the emulsifier used. The increase of populations 2 + 3 in emulsions compared to micellar solutions was accompanied with an increase of the surface area. Therefore more nitroxide molecules can be solubilized at the surface, which was the favored environment in dispersed systems [Heins et al. 2007]. The major population of TB was solubilized in the interface and 30 % in the oil phase. In emulsions, the TB population in the aqueous phase was very small and hindered in its tumbling indicating a close proximity to the surface of oil droplets as found in a lower  $a_N$  and an enhanced  $\tau_c$  relative to the micellar solutions.

### 3.4.3 Partitioning behavior of nitroxides into the micellar and emulsion interface determined by different methods

As a function of their substituent and lipophilicity, the proportions of nitroxides that were solubilized in the micellar (table 3.4) or emulsion (table 3.5) interface increased in the range



TEMPOL < TEMPO < TB for all emulsifier used.

In SDS dispersed systems, the content of the nitroxides solubilized in the emulsion or micellar interface were the highest, followed by CTAB and Brij58. TB was solubilized in the micellar phase to more than 90 %, while in emulsions it was almost completely solubilized in the emulsifier interphase/inner core. The hydrophilic TEMPOL was solubilized in the micellar phase up to 15 - 20 % in micelles and emulsions. Considering all methods used for the determination of the partitioning behavior, the solubilized proportions of TEMPO varied the most between the emulsifiers, ranging from 12 - 33 % in Brij58, 42 - 76 % in CTAB to 46 - 65 % in SDS micelles (table 3.4). However, in emulsions the proportion was around 80 % for all nitroxides with only slight differences between the emulsifiers (table 3.5).

Table 3.4: Solubilized proportion ( $d_{sol}$ ) of the nitroxides TEMPOL, TEMPO and TEMPOL-benzoate in SDS, CTAB and Brij58 micellar solutions determined by ultrafiltration technique (UF), NMR and deconvolution of EPR spectra (EPR).

		Solubilized proportion of nitroxides ( $d_{sol}$ ), % in the micellar interface		
		TEMPOL	TEMPO	TB
		mean $\pm$ SD	mean $\pm$ SD	mean $\pm$ SD
UF	CTAB	14.8 $\pm$ 3.56	46.1 $\pm$ 2.03	89.4 $\pm$ 7.52
	SDS	15.5 $\pm$ 0.99	64.8 $\pm$ 0.95	98.9 $\pm$ 0.32
	Brij58	4.6 $\pm$ 1.67	18.6 $\pm$ 1.12	93.1 $\pm$ 2.07
NMR	CTAB	5 $\pm$ 0.3	76 $\pm$ 3.8	56 $\pm$ 2.8
	SDS	100 <sup>a</sup>	100 <sup>a</sup>	100 <sup>a</sup>
	Brij58	0 $\pm$ 0.1	12 $\pm$ 0.6	30 $\pm$ 1.675
EPR	CTAB	13 $\pm$ 3.5 <sup>b</sup>	42 $\pm$ 1.7 <sup>b</sup>	97 $\pm$ 0.0 <sup>c</sup>
	SDS	9 $\pm$ 5.2 <sup>b</sup>	46 $\pm$ 1.2 <sup>b</sup>	96 $\pm$ 1.0 <sup>c</sup>
	Brij58	9 $\pm$ 2.0 <sup>b</sup>	33 $\pm$ 3.1 <sup>b</sup>	89 $\pm$ 1.2 <sup>c</sup>

<sup>a</sup>Hydroxylamines were completely solubilized in SDS micelles.

<sup>b</sup>Including only the nitroxide proportion of population 3.

<sup>c</sup>Including the nitroxide proportion of populations 2+3. *Please see text for further explanation.*

With the exception of TEMPO-H in CTAB micelles, the partitioning behavior of hydroxylamines in micelles calculated by NMR diffusion coefficients were lower than calculated by UF or EPR deconvolution. The intercalation of TB-H into CTAB micelles was calculated by 56 % and into Brij58 micelles by 30 %. It was not possible to determine the partitioning of hydroxylamines in SDS micellar solutions as the self-diffusion coefficients of hydroxylamines ( $D_N$ ) were even lower than those of the micelle ( $D_{mic}$ ) resulting in an solubilized proportion of all hydroxylamines of more than 100 %.

The self-diffusion coefficients decreased in micellar solution compared to those measured in buffer solution (table 3.1). The decrease for TEMPO-H was higher than for TEMPOL-H which was due to the increased incorporation of TEMPO-H in the micelles. TB-H showed a moderate incorporation that was lower than expected based on its more lipophilic structure. Estimation of theoretically lipophilicities (logP) by software Chemdraw Ultra 8.0 indicated

Table 3.5: Solubilized proportion ( $d_{\text{sol}}$ ) of TEMPOL, TEMPO and TEMPOL-benzoate in SDS, CTAB and Brij58 emulsions determined by ultrafiltration technique (UF) and deconvolution of EPR spectra (EPR).

		Solubilized proportion of nitroxides ( $d_{\text{sol}}$ ), % in the emulsion phase		
		TEMPOL mean $\pm$ SD	TEMPO mean $\pm$ SD	TB mean $\pm$ SD
UF	CTAB	7.5 $\pm$ 1.62	77.8 $\pm$ 0.70	99.7 $\pm$ 0.67
	SDS	9.1 $\pm$ 0.54	81.2 $\pm$ 0.70	99.2 $\pm$ 0.51
	Brij58	0.6 $\pm$ 1.11	75.8 $\pm$ 0.93	99.6 $\pm$ 0.65
EPR	CTAB	18 $\pm$ 6.8 <sup>a</sup>	88 $\pm$ 1.6 <sup>b</sup>	97 $\pm$ 0.6 <sup>b</sup>
	SDS	9 $\pm$ 3.8 <sup>a</sup>	79 $\pm$ 0.6 <sup>b</sup>	96 $\pm$ 1.2 <sup>b</sup>
	Brij58	10 $\pm$ 2.1 <sup>a</sup>	83 $\pm$ 1.0 <sup>b</sup>	89 $\pm$ 2.1 <sup>b</sup>

<sup>a</sup>Including only the nitroxide proportion of population 3.

<sup>b</sup>Including the nitroxide proportion of populations 2+3. *Please see text for further explanation.*

lower lipophilicities of the hydroxylamines (TEMPOL-H: -0.1, TEMPO-H: 2.0, TB: 2.8) relative to the nitroxides (TEMPOL: 1.0, TEMPO: 3.0, TB: 3.8), which might interfere with the partitioning behavior.

The NMR diffusion model is based on the equilibrium of a substance between two populations, the dissolved and the ligated solutes [Momot and Kuchel 2003]. The diffusion rate between those two populations was determined to calculate the partitioning behavior [Fischer et al. 2009]. As we know from the EPR deconvolution we had three different populations, where the ligated proportion was divided into the clustered and the interfacial population. If this downstream diffusion between the interfacial and the clustered population is much slower than the diffusion between the dissolved and the ligated, it is not possible to monitor this second equilibrium. However, it will influence the first equilibrium.

Proportions of solubilized nitroxides in the interfaces of emulsions or micellar solutions determined by EPR were obtained from EPR line shape deconvolution. The proportions of TEMPOL and TB solubilized in the interface of micelles were comparable with those proportions obtained from UF experiments, but the proportion of TEMPOL in CTAB and Brij58 emulsions was found to be higher calculated by EPR deconvolution. The proportions of TEMPO in micellar solutions were given by the proportion of population 3. However, in emulsions the sum of the proportions of population 2 and 3 was used for calculation of the partitioning behavior as both populations were solubilized in an anisotropic environment indicated by  $a_N < 16.5$  G (see 3.4.2). Regardless of the emulsifier, the shift of population 2 from the isotropic environment into the anisotropic environment was due to the increase of the interfacial area and led to an increased proportion of nitroxides solubilized in the interface.

The higher proportion of TEMPO solubilized in the interface of SDS micellar solution determined by UF (65 %) compared to EPR (46 %) might be due to the retention of the

clustered population (19 %) by the UF membrane.

As the UF technique is a validated separation method a few things need to be taken into account. It is still common to completely separate the emulsion although other studies disapprove of such an application as the total separation leads to a conversion of the system [Stöckmann et al. 2000; Stöckmann and Schwarz 1999].

An influencing parameter is the adsorption of emulsifier monomers [Oehlke et al. 2008] and nitroxides to the membrane surface. This would lead to a decreased concentration in the filtrate and therefore to an overestimation of the intercalated proportion of the spin probe. However, the UF membranes used in this study were already tested in CTAB systems [Oehlke et al. 2008], and proofed not to interfere with the emulsifiers used. As the adsorption of the nitroxides to the membrane cannot be neglected, the membranes were equilibrated with the initial disperse system before use. After the equilibration steps no further change in the filtrate concentration occurred. Therefore it was concluded that no further adsorption occurred during the following measurements.

By using the EPR method to quantify the nitroxides proportions in the filtrate and the in the entire dispersed system, the shape of the nitroxides spectra became more isotropic in the aqueous filtrate relative to those in the micellar solution or emulsion (spectra not shown) indicating the presents of only one free tumbling population. Thus, the absence of micelles or oil droplets in the filtrate was proofed.

Comparing these different methods it is important to distinguish between the UF technique as an invasive method and PFG-NMR and EPR deconvolution that represent non-invasive methods. The spectroscopic measurements underlie different methods to record a spectrum in dynamic in the systems. While the fast measurement duration in EPR experiments give a superimposition of the spectra from the different populations, the NMR technique records an averaged spectrum of the fast replacing components over a long time scale. Therefore, the required time scale for paramagnetic molecules is given by the EPR technique in range of nanoseconds [Borbat 2001].

With UF and PFG-NMR equilibrium between two populations is preconditioned where additional populations influence this equilibrium, but cannot be characterized. Nevertheless, the UF method is a quick and easy method to determine the partition behavior between aqueous and micellar phase for most applications [Oehlke et al. 2008]. PFG-NMR is widely used to obtain partitioning data [Fischer et al. 2009], but, as it is unsuitable for paramagnetic substances [Furtado et al. 2011], it required the use of hydroxylamines. The proportions determined were only comparable with the other methods to a limited extent. However, knowledge about the dynamic within the systems is beneficial for further characterization of nitroxides in dispersed systems.

Deconvolution of EPR spectra is the preferred method to determine the partitioning of paramagnetic molecules in dispersed systems as this method benefit from short experimental time and further information on the solubilization site of the different coexisting populations [Štrancar et al. 2005].

### 3.5 Conclusion

To figure out the most accurate and sensitive approach for the determination of the partitioning behavior of paramagnetic substances in dispersed systems, results investigated by means of ultrafiltration technique (UF), pulsed-field gradient nuclear magnetic resonance spectroscopy (PFG-NMR) and deconvolution of electron paramagnetic resonance spectroscopy (EPR) spectra by EPRSIM-C were compared.

UF is an accurate method for investigating the partitioning of small molecules, as the equilibrium was not interfered [Stöckmann et al. 1999, Oehlke et al. 2009], and give comparable results with EPR deconvolution. The high dynamic of the studied systems was demonstrated by PFG-NMR as the diffusion rates show the relocation of molecules between two populations in equilibrium [Fischer et al. 2009, Momot and Kuchel 2003], resulting in lower partitioning data as found with the other two methods. However, results from deconvolution of EPR spectra revealed three domains for stable nitroxide radicals in dispersed systems. In the aqueous phase an isotropic free tumbling population and a clustered population that is slightly hindered in tumbling could be found, while a third population was located in an anisotropic environment such as the interface which is comparable with literature findings [Jores et al. 2003, Frenzel and Steffen-Heins 2015].

As a function of the required time scale for paramagnetic molecules which is given by the EPR technique in range of nanoseconds [Borbat 2001], EPR measurements result in a superimposition of the spectra from the different populations, however, the NMR technique records an averaged spectrum of the fast replacing components over a long time scale. With UF and PFG-NMR equilibrium between two populations is preconditioned where additional populations influence this equilibrium, but cannot be characterized. Data thus obtained that deconvolution of EPR spectra turned out to be the preferred method for measuring the partitioning behavior of paramagnetic molecules as it enables distinguishing between several populations at their individual solubilization sites [Štrancar et al. 2005].

The nitroxides TEMPOL, TEMPO and TB differed in polarity and solubilized to different extents into the discrete phases, however, their solubilization site in the palisade layer of the interface seemed to be comparable which is also in line with other observations [Almeida 1998]. The knowledge of the nitroxide partitioning behavior is the prerequisite for investigating their reactions in dispersed systems, which can be applied as an important approach to understand the reactions of free lipid radicals and antioxidants in complex food matrices we focus on in our further studies.

#### Acknowledgement

We are grateful to Marion Höftmann and Gitta Kohlmeier-Yilmaz of the Otto Diels Institute for Organic Chemistry, Kiel, for the technical assistance of NMR measurements and to Annegret Rösen of the Institute of Human Nutrition and Food Science for the measurement of the critical micellar concentration.

## References

- P. Ahlin, J. Kristl, S. Pecar, J. Strancar, and M. Sentjerc. 2003. The effect of lipophilicity of spin-labeled compounds on their distribution in solid lipid nanoparticle dispersions studied by electron paramagnetic resonance. *Journal of Pharmaceutical Sciences* 92, 1 (2003), 58–66.
- P. Ahlin, J. Kristl, M. Sentjerc, J. Strancar, and S. Pecar. 2000. Influence of spin probe structure on its distribution in SLN dispersions. *International Journal of Pharmaceutics* 196, 2 (2000), 241–244.
- Masayuki Aizawa, Tsuyoshi Komatsu, and Tsurutaro Nakagawa. 1979. Electron Spin-Spin Interaction and Translational Diffusion of Nitroxide Radicals in Sodium Dodecyl Sulfate Micelles. *Bulletin of the Chemical Society of Japan* 52, 4 (1979), 980–983.
- C. Aliaga, P. Torres, F. Silva, A simple method for the determination of the partitioning of nitroxide probes in microheterogeneous media, *Magnetic Resonance in Chemistry* 50 (2012) 779–783.
- L. Almeida. 1998. Different Micellar Packing and Hydrophobicity of the Membrane Probes TEMPO and TEMPOL Influence Their Partition Between Aqueous and Micellar Phases Rather than Location in the Micelle Interior. *Journal of Colloid and Interface Science* 203, 2 (1998), 456–463.
- L. J. Berliner. 1976. Spin labeling. Theory and applications. Molecular biology (21st. ed.). Academic Press Inc JNL-Comp Subscriptions, New York.
- Claire C. Berton-Carabin, John N. Coupland, and Ryan J. Elias. 2013a. Effect of the lipophilicity of model ingredients on their location and reactivity in emulsions and solid lipid nanoparticles. *Colloids and Surfaces A: Physicochemical and Engineering Aspects* 431 (2013), 9–17.
- Claire C. Berton-Carabin, Ryan J. Elias, and John N. Coupland. 2013b. Reactivity of a model lipophilic ingredient in surfactant-stabilized emulsions: Effect of droplet surface charge and ingredient location. *Colloids and Surfaces A: Physicochemical and Engineering Aspects* 418, 0 (2013), 68–75.
- P. P. Borbat. 2001. Electron Spin Resonance in Studies of Membranes and Proteins. *Science* 291, 5502 (2001), 266–269.
- Alejandra N. Cimato, Lidia L. Piehl, Graciela B. Facorro, Horacio B. Torti, and Alfredo A. Hager. 2004. Antioxidant effects of water- and lipid-soluble nitroxide radicals in liposomes. *Free Radical Biology and Medicine* 37, 12 (2004), 2042–2051.
- Branka Dejanovic, Krunoslav Miroslavljevic, Vesna Noethig-Laslo, Slavko Pecar, Marjeta Sentjerc, and Peter Walde. 2008. An ESR characterization of micelles and vesicles formed in aqueous decanoic acid/sodium decanoate systems using different spin labels. *Chemistry and Physics of Lipids* 156, 1-2 (2008), 17–25.
- Laurence Dupont-Leclercq, Sébastien Giroux, Bernard Henry, and Patrice Rubini. 2007. Solubilization of amphiphilic carboxylic acids in nonionic micelles: determination of partition coefficients from p K a measurements and NMR experiments. *Langmuir* 23, 21 (2007), 10463–10470.
- C. Farcet, M. Lansalot, B. Charleux, R. Pirri, and Vairon, J. P. 2000. Mechanistic Aspects of Nitroxide-Mediated Controlled Radical Polymerization of Styrene in Miniemulsion, Using a Water-Soluble Radical Initiator. *Macromolecules* 33, 23 (2000), 8559–8570.
- Elmar Fischer, Wolfgang Fieber, Charles Navarro, Horst Sommer, Daniel Benczédi, Maria Inés Velazco, and Monika Schönhoff. 2009. Partitioning and localization of fragrances in surfactant mixed micelles. *Journal of surfactants and detergents* 12, 1 (2009), 73–84.
- Monika Frenzel and Anja Steffen-Heins. 2014. Whey protein coating increased bilayer rigidity and stability of liposomes in food like matrices. *Food Chemistry*, 173 (2015) 1090–1099.
- Filipe Furtado, Petrik Galvosas, Frank Stallmach, Ulf Roland, Jörg Kärger, and Frank-Dieter Kopinke. 2011. Paramagnetic Relaxation Enhancement (PRE) as a Tool for Probing Diffusion in Environmentally Relevant Porous Media. *Environ. Sci. Technol.* 45, 20 (2011), 8866–8872.
- Anja Heins, Vasil Garamus, Bernd Steffen, Heiko Stöckmann, and Karin Schwarz. 2006. Impact of Phenolic Antioxidants on Structural Properties of Micellar Solutions. *Food Biophysics* 1, 4 (2006), 189–201.
- Anja Heins, Donald McPhail, Tobias Sokolowski, Heiko Stöckmann, and Karin Schwarz. 2007. The Location of Phenolic Antioxidants and Radicals at Interfaces Determines Their Activity. *Lipids* 42, 6 (2007), 573–582.

- Katja Jores, Wolfgang Mehnert, and Karsten Mäder. 2003. Physicochemical Investigations on Solid Lipid Nanoparticles and on Oil-Loaded Solid Lipid Nanoparticles: A Nuclear Magnetic Resonance and Electron Spin Resonance Study. *Pharmaceutical Research* 20, 8 (Aug. 2003), 1274–1283.
- John F. W. Keana. 1978. Newer aspects of the synthesis and chemistry of nitroxide spin labels. *Chemical reviews* 78, 1 (1978), 37–64.
- Bruce R. Knauer and James J. Napier. 1976. The nitrogen hyperfine splitting constant of the nitroxide functional group as a solvent polarity parameter. The relative importance for a solvent polarity parameter of its being a cybotactic probe vs. its being a model process. *J. Am. Chem. Soc.* 98, 15 (1976), 4395–4400.
- Mads Kreilgaard, Erik J. Pedersen, and Jerzy W. Jaroszewski. 2000. NMR characterisation and transdermal drug delivery potential of microemulsion systems. *Journal of controlled release* 69, 3 (2000), 421–433.
- Marina Kveder, Greta Pifat, Slavko Pečar, Milan Schara, Pilar Ramos, and Hermann Esterbauer. 1997. Nitroxide reduction with ascorbic acid in spin labeled human plasma LDL and VLDL. *Chemistry and Physics of Lipids* 85, 1 (1997), 1–12.
- Anna-Maija Lampi and Afaf Kamal-Eldin. 1998. Effect of  $\alpha$ - and  $\gamma$ -tocopherols on thermal polymerization of purified high-oleic sunflower triacylglycerols. *J Amer Oil Chem Soc* 75, 12 (1998), 1699–1703.
- Agnieszka Lewińska, Kazimiera A. Wilk, and Adam Jezierski. 2012. Characterization of the Microenvironments of Alkylamidoamine-N-oxide Surfactant Aggregates by the EPR Spin Labeling Method. *J Solution Chem* 41, 7 (2012), 1210–1223.
- Marco Lucarini, Paola Franchi, Gian Franco Pedulli, Cristina Gentilini, Stefano Polizzi, Paolo Pengo, Paolo Scrimin, and Lucia Pasquato. 2005. Effect of core size on the partition of organic solutes in the monolayer of water-soluble nanoparticles: an ESR investigation. *J Am Chem Soc* 127, 47 (2005), 16384–16385.
- Karsten Mäder (Ed.). 2006. *Nanotechnologies for the Life Sciences. Characterization of nanoscaled drug delivery systems by Electron Spin Resonance (ESR). Nanosystem Characterization Tools in the Life Sciences.* Chapter 7, 241–258. Wiley-Vch Verlag.
- Konstantin I. Momot and Philip W. Kuchel. 2003. *Concept. Magn. Reson.* 19A (2003) 51–64.
- Per Gunnar Nilsson and Bjoern Lindman. 1984. Mixed micelles of nonionic and ionic surfactants. A nuclear magnetic resonance self-diffusion and proton relaxation study. *J. Phys. Chem.* 88, 22 (1984), 5391–5397.
- Kathleen Oehlke, Vasil M. Garamus, Anja Heins, Heiko Stöckmann, and Karin Schwarz. 2008. The partitioning of emulsifiers in o/w emulsions: A comparative study of SANS, ultrafiltration and dialysis. *Journal of Colloid and Interface Science* 322, 1 (2008), 294–303.
- Kathleen Oehlke, Anja Heins, Heiko Stöckmann, and Karin Schwarz. 2010. Impact of emulsifier microenvironments on acid-base equilibrium and activity of antioxidants. *Food Chemistry* 118, 1 (2010), 48–55.
- William H. Otto, Danny J. Britten, and Cynthia K. Larive. 2003. NMR diffusion analysis of surfactant–humic substance interactions. *Journal of Colloid and Interface Science* 261, 2 (2003), 508–513.
- A. Patist, S.S. Bhagwat, K.W. Penfield, P. Aikens, D.O. Shah, On the measurement of critical micelle concentrations of pure and technical grade nonionic surfactants. *Journal of Surfactants and Detergents* 3 (2000) 53–58.
- S. Y. Qian, H. P. Wang, F. Q. Schafer, and G. R. Buettner. 2000. EPR detection of lipid-derived free radicals from PUFA, LDL, and cell oxidations. *Free Radical Biology and Medicine* 29, 6 (2000), 568–579.
- Laurence S. Romsted and Jianbing Zhang. 2002. Kinetic Method for Determining Antioxidant Distributions in Model Food Emulsions: Distribution Constants of t-Butylhydroquinone in Mixtures of Octane, Water, and a Nonionic Emulsifier. *Journal of Agricultural and Food Chemistry* 50, 11 (2002), 3328–3336.
- Paolo Sabatino, Agnieszka Szczygiel, Davy Sinnaeve, Maryam Hakimhashemi, Hans Saveyn, José C. Martins, and Van der Meer, Paul. 2010. NMR study of the influence of pH on phenol sorption in cationic CTAB micellar solutions. *Colloids and Surfaces A: Physicochemical and*

- Engineering Aspects 370, 1-3 (2010), 42–48.
- Olle Söderman, Peter Stilbs, and William S. Price. 2004. NMR studies of surfactants. *Concepts Magn. Reson.* 23A, 2 (2004), 121–135.
- Benjamin P. Soule, Fuminori Hyodo, Ken-ichiro Matsumoto, Nicole L. Simone, John A. Cook, Murali C. Krishna, and James B. Mitchell. 2007. The chemistry and biology of nitroxide compounds. *Free Radical Biology and Medicine* 42, 11 (2007), 1632–1650.
- Heiko Stöckmann and Karin Schwarz. 1999. Partitioning of Low Molecular Weight Compounds in Oil-in-Water Emulsions. *Langmuir* 15, 19 (1999), 6142–6149.
- Heiko Stöckmann, Karin Schwarz, and Tuong Huynh-Ba. 2000. The influence of various emulsifiers on the partitioning and antioxidant activity of hydroxybenzoic acids and their derivatives in oil-in-water emulsions. *Journal of the American Oil Chemists' Society* 77, 5 (2000), 535–542.
- Janez Štrancar, Tilen Koklic, Zoran Arsov, Bogdan Filipic, David Stopar, and Marcus A. Hemminga. 2005. Spin label EPR-based characterization of biosystem complexity. *Journal of chemical information and modeling* 45, 2 (2005), 394–406.
- Y.R. Suradkar, S.S. Bhagwat, CMC Determination of an Odd Carbon Chain Surfactant (C 13 E 20 ) Mixed with Other Surfactants Using a Spectrophotometric Technique, *Journal of Chemical & Engineering Data* 51 (2006) 2026-2031
- Olga Vinogradova, Frank Sönnichsen, and Sanders II, Charles R. 1998. On choosing a detergent for solution NMR studies of membrane proteins. *Journal of biomolecular NMR* 11, 4 (1998), 381–386.
- Emile E. Voest, Ernst van Faassen, and Marx, Joannes J. M. 1993. An electron paramagnetic resonance study of the antioxidant properties of the nitroxide free radical tempo. *Free Radical Biology and Medicine* 15, 6 (1993), 589–595.
- Junfeng Wang, Jason R. Schnell, and James J. Chou. 2004. Amantadine partition and localization in phospholipid membrane: a solution NMR study. *Biochemical and Biophysical Research Communications* 324, 1 (2004), 212–217.
- J. J. Windle. 1981. Hyperfine coupling constants for nitroxide spin probes in water and carbon tetrachloride. *Journal of Magnetic Resonance* (1969) 45, 3 (1981), 432–439.





# 4 EPR study on the solubilization side of nitroxide in multiphase systems and its relevance to the reduction capacity of antioxidants

Heimke Krudopp<sup>a</sup>, Frank Sönnichsen<sup>b</sup> and Anja Steffen-Heins<sup>a</sup>

<sup>a</sup> Institute of Human Nutrition and Food Science, Kiel University, 24118 Kiel, Germany

<sup>b</sup> Otto Diels Institute for Organic Chemistry, Kiel University, 24119 Kiel, Germany

## 4.1 Abstract

The interfaces in foods play a major role concerning oxidation processes, chemical and physical stability and half-lives of foods. To systematically evaluate the reactions of antioxidants and radicals at interfaces as a function of their solubilization site, the stable nitroxides with increasing lipophilicity TEMPOL < TEMPO < TEMPOL-benzoate were investigated in micellar solutions of SDS, CTAB and Brij58. EPR spectra of nitroxides in the presence and absence of micellar solutions were analyzed concerning the hyperfine splitting constants  $a_N$  and the rotational correlation time  $\tau_c$  to deduce the nitroxide solubilization site which is supported by determination of their NMR  $T_1$ -relaxation times.

The antioxidant kinetic to reduce the different nitroxides by propyl gallate, Trolox and  $\alpha$ -tocopherol were measured as a function of the nitroxide solubilization site. TEMPO was reduced the fastest by all antioxidants compared with TEMPOL and TB which may be due to a different alignment of the nitroxides. TEMPO may align with the NO moiety to the more hydrophilic part of the interface being then in optimal proximity to the antioxidants. The anionic interface of SDS micelles turned out to accelerate nitroxides reduction by antioxidants, as TEMPO may quickly diffuse into the SDS Stern layer. Here it was reduced to the corresponding hydroxylamine by the antioxidants present and could afterwards be exchanged with nitroxide radical solubilized in the aqueous phase.

## 4.2 Introduction

Oxidation stability of food is governed by the interface properties in structurally and compositionally heterogeneous matrices. Several studies have been performed on the properties of dispersed systems and the antioxidants that are used to minimize e.g. lipid oxidation, to clarify how significant the antioxidant potency is influenced [McClements 2010; Schwarz et al. 2000; Heins et al. 2007a; Oehlke et al. 2010]. Although former studies focused on the solubilisation site of antioxidant at designed interfaces [Losada-Barreiro et al. 2014; Stöckmann et al. 2000; Oehlke et al. 2010; Heins et al. 2007b; Oehlke et al. 2011], a localization of free radicals in multiphase systems has not been done before.

To investigate processes on a nanometer scale like micelles, spectroscopic methods are used to develop methods that allow a systematically approach focusing on interfaces. Electron paramagnetic resonance experiments (EPR) make it possible to estimate the potency of hydrogen atom donation of antioxidants in various systems measuring the reaction rate with stable radicals [Aliaga et al. 2008; Kocherginsky and Swartz 1995] or unstable radicals in the presence of spin trapping probes [Dikalov and Mason 2001].

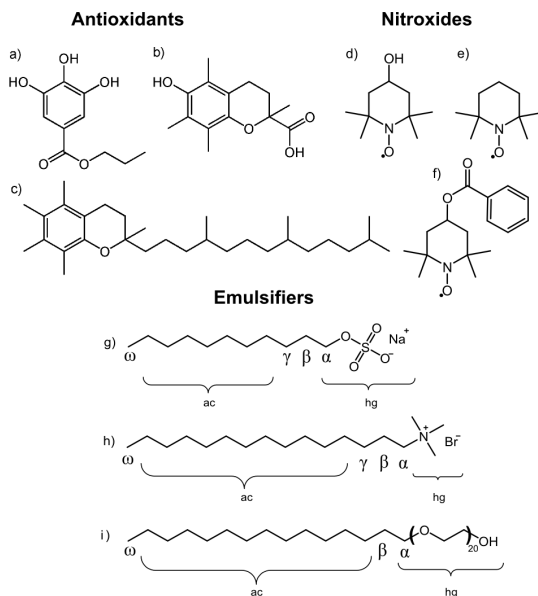


Figure 4.1: Chemical structure of the antioxidants  $\alpha$ -tocopherol (a), Trolox (b), propyl galate (c), of the nitroxides TEMPOL (d), TEMPO (e) and TB (f), and of emulsifiers SDS (g), CTAB (h) and Brij58 (i). Nomenclature of emulsifier proton signals are given for NMR measurements (hg: head group, ac: acyl chain,  $\alpha$ ,  $\beta$ ,  $\gamma$ :  $\alpha$ -CH<sub>2</sub>,  $\beta$ -CH<sub>2</sub>,  $\gamma$ -CH<sub>2</sub> and  $\omega$ :  $\omega$ -CH<sub>3</sub>)

EPR spin probing technique is a prominent approach to circumvent the difficult detection of short living free radicals. Since nitroxides are very sensitive to their chemical microenvironment (polarity), the individual partitioning of nitroxides as well as their reaction with antioxidants or lipid radicals are indicated by the alteration of the isotropic hyperfine splitting. Previous studies on stable radical behavior showed that the interfacial properties determine the antioxidants behavior and therefore the potency to reduce radicals or may even hinder the reaction by forming a steric barrier by the emulsifier used [Heins et al. 2007a]. However these radicals were charged and therefore not applicable for all micellar systems.

The three types of rings that are most commonly used for nitroxide spin-probes are piperidine, pyrrolidine and doxyl rings. Nitroxides are commercially available and offer different properties, e.g. they are more or less stable/reactive (e.g., doxyl rings are more stable than piperidines), hydrophilic (TEMPO) or lipophilic (doxyl stearates), charged (Cat1-H) or neutral and therefore applicable for various EPR spin-probing experiments in redox research [Kocherginsky and Swartz 1995]. The reduction of nitroxides by ascorbic acid is known for a long time [Jores et al. 2003; Paleos and Dais 1977; Kveder et al. 1997] and it is used to locate spin probes in lipid membranes [Kocherginsky and Swartz 1995].

Nitroxides can be reduced by (biological) antioxidants and oxidized by oxygen species due to their interconversion between the EPR-active nitroxyl radical and the EPR-silent hydroxylamine or oxoammonium ion [Kishioka et al. 2002]. Indeed, oxygen is able to reoxidize hydroxylamines to nitroxyl radicals in biological systems, but as previous results showed for the spectral pattern of galvinoxyl, which is completely dissolved in SDS, Brij58 and CTAB micelles, the micellar oxygen concentration can be neglected [Heins et al. 2007a]. This is in accordance with the findings of Berberan-Santos and colleagues [1992] estimating that 98 % of the SDS micelles are oxygen free under atmospheric conditions. The prerequisite for our approach is the reaction between antioxidants and the spin probes. The reaction kinetic of phenolic antioxidants or tocopherols and its analogues towards doxyl spin probes like 5- or 12-DSA is too slow (data not shown). However, nitroxides are only slowly reduced by phenolic antioxidants and even faster by  $\alpha$ -tocopherol and its water-soluble analogue Trolox.

As spin probes are sensitive to their microenvironment the relative anisotropy observed in an ESR spectrum is directly related to the rotational mobility of the probe, and can be correlated with the probe's microenvironment [Bahri et al. 2006]. The rotational correlation time ( $\tau_c$ ) represents the time needed to rotate one radian as an average reflecting the mobility of the probe and the rigidity due to the microenvironment. An increased  $\tau_c$  indicates a reduced mobility of the spin probe [Yoshioka et al. 2006]. Incorporation of the lipophilic spin probe PTMIO into SDS or DTAB micelles showed an alteration in reducing by ascorbic acid. Negatively charged ascorbic acid showed a greater reduction capacity towards PTMIO in positively charged DTAB than in negatively charged SDS [Berton-Carabin et al. 2012] this may not be the truth due to the importance of hydrogen abstraction which is prior to the negatively ascorbyl radical.

The aim of this study was to correlate the solubilization site of stable nitroxide radicals in micellar solutions with different interfacial properties with the efficiency of different antioxidants (4.1). Nitroxides used according to their increasing lipophilicity were TEMPOL (4-Hydroxy-2,2,6,6-tetramethylpiperidine 1-oxyl,  $\log P = 0.62$ ,  $P_{w/o} = 6.64$ ) < TEMPO (2,2,6,6-Tetramethyl-1-piperidinyloxy,  $\log P = 1.77$ ,  $P_{w/o} = 59.4 - 64.6$ ) < TEMPOL-benzoate (TB; 4-Hydroxy-2,2,6,6-tetramethylpiperidine 1-oxyl benzoate,  $\log P = 2.46$ ,  $P_{w/o} > 100$ ) [Kroll 1999; Rube 2006; Ahlin et al. 2000; Rosen et al. 1982; Cimato et al. 2004]. Antioxidants used were the phenolic propyl gallate (PG) showing strong interaction with the emulsifiers as a function of its different solubilization sites in the micellar phases of SDS, CTAB and Brij58 [Heins et al. 2007b]. Trolox and  $\alpha$ -tocopherol were showing much lower interactions towards emulsifiers, where Trolox showed equivalence in solubilization site with PG. For the first time, the influence of antioxidants on the solubilization site of nitroxides were investigated by  $\tau_c$  and  $T_1$  relaxation times and correlated with the antioxidant kinetic to reduce the different nitroxides.

## 4.3 Materials and Methods

### 4.3.1 Chemicals

Cationic CTAB (cetyltrimethylammonium bromide), anionic SDS (sodium dodecyl sulphate), non-ionic Brij58 (polyoxyethylene-20-cethyl ether), propyl gallate, Trolox,  $\alpha$ -tocopherol, TEMPO, TEMPOL and TB were obtained from Sigma-Aldrich, Germany and used without further purification.

### 4.3.2 Sample preparation

The micellar solutions contained 1 wt% emulsifier in acetic acid buffer solution (0.05 mol, pH = 5). Nitroxide stock solutions of TEMPO and TEMPOL were prepared in buffer solution, added to each micellar solution and mixed well. TEMPOL-benzoate was dissolved in ether which was evaporated under nitrogen. For sample preparation, micellar solution was added to the re-crystallized nitroxide and placed in ultrasonic bath. For the control sample, the same procedure was repeated using only buffer solution resulting in a concentration below 0.1 mmol. The antioxidant stock solution of propyl gallate was prepared in buffer solution, added to each micellar solution and mixed well. Trolox and  $\alpha$ -tocopherol were dissolved in ethanol, evaporated under nitrogen and redissolved in each micellar solution. Micellar solutions containing antioxidants and those containing nitroxides were mixed ending up with an equimolar antioxidant and nitroxide concentration of 1mmol for all sample solutions.

### 4.3.3 Partitioning behavior

Proportions of nitroxides solubilized in the interfaces were calculated according to chapter 3 where the nitroxide proportion was determined by EPRSIM-C [Štrancar et al. 2005]. The

partitioning of antioxidants were investigated by Heins [2005] who measured the antioxidant proportion solubilized in the interface by ultrafiltration and HPLC detection as described by Stöckmann and colleagues [2000].

### 4.3.4 EPR analysis

Electron paramagnetic spin resonance (EPR) measurements were carried out on a Bruker Elexys II E500 spectrometer operating with X-band at 9.85 GHz at room temperature using a modulation frequency of 100 kHz; a modulation amplitude of 1.2 G; and a microwave power of 0.2 mW. Spectra were optimized using a center field of 3510 G, a sweep width of 66.7 g, a time constant of 81.92 ms, a conversion time of 39.16 ms and a receiver gain of 60 dB. The overall micro polarity of the spin probes was calculated by means of the hyperfine splitting parameter  $a_N$  and was given as the distance between low field peak ( $H_{+1}$ ) and middle field peak ( $H_0$ ).

#### 4.3.4.1 Calculation of the rotational correlation time ( $\tau_c$ ) of superimposed spectra

From the first derivative EPR spectra the rotational correlation time  $\tau_c$  [ns] was calculated by equation 4.1 for isotropic high mobility regime measurements at X band [Beghein et al. 2007]:

$$\tau_c = 6.51 \cdot 10^{-10} \cdot \Delta H_0 \left( \sqrt{\frac{h_0}{h_{-1}}} + \sqrt{\frac{h_0}{h_{+1}}} - 2 \right) \quad (4.1)$$

Where  $\Delta H_0$  [G] is the peakwidth of the central line of the EPR spectrum and the peak amplitudes are given by  $h_{+1}$ , (low-field peak),  $h_0$  (central peak) and  $h_{-1}$  (high-field peak). The factor is customarily used for X band experiments taken into account the magnetic field, the anisotropic  $g$  value and the hyperfine coupling  $a_N$  [Keith et al. 1970]. This equation is valid for isotropic motions ( $\tau_c < 10^{-9}$  s) where the spectra display  $g$  and  $A$  tensors as an average of the principle components [Schreier et al. 1978]. The increase in the value of  $\tau_c$  means a decrease of the rotational motion of the nitroxides due to higher spin concentrations or microviscosity.  $\tau_c$  were depicted as the mean and the standard deviation of triplicates. Statistical analysis of  $\tau_c$  was carried out with GraphPad Prism 6.0, using a two-way ANOVA and Bonferroni correction for multiple comparisons. Significance was accepted at  $p \leq 0.05$ .

#### 4.3.4.2 Calculation of the antioxidative capacity

To compare the reduction capacities of antioxidants towards the nitroxides used, the EPR spectra of individual nitroxides were acquired after 5 min of incubation with antioxidants and repeated as a function of the reaction kinetic every 5 to 15 min in a period of 2 to 20 h. These spectra were recorded in the presence or absence of SDS, CTAB or Brij58

micellar solutions and the double integrals of the entire spectra were plotted against the time. Decay curves were fitted by a first order exponential decay (eq.4.2):

$$f(t) = (aoc)e^{bt} + n \quad (4.2)$$

where aoc [%] is the antioxidative capacity or the maximum reduction potential, respectively, b is the reaction kinetic and n is the nonreduced nitroxide residuum. The half-life (hl) [h] that is referred to as the time needed to reach 50 % of the maximum reduction potential was calculated by equation 4.3.

$$hl = \frac{-\ln(2)}{b} \quad (4.3)$$

Decays of nitroxides with very slow reaction kinetics did not correspond to an exponential decay within the 20 h of investigation. In this case as an antioxidative capacity of 100 % was assumed and the half-life goes to infinity the coefficient of determination of was found of  $R^2 < 0.6$ , and reactions were referred to as no reduction of nitroxides proceeded.

### 4.3.5 NMR analysis: $T_1$ relaxation time

#### 4.3.5.1 Antioxidants

The performance of NMR-measurements of antioxidants is previously described in detail [Heins et al. 2007b]. Experimental errors were calculated for each proton signal and were set on 10 %. The individual emulsifier protons with their respective nomenclatures for the specific headgroup region (hg), the alkyl chain (ac) as well as for the individual methylene and methyl protons that split into a single multiplet ( $\alpha, \beta, \gamma$  and  $\omega$ ) are shown in figure 4.1.

#### 4.3.5.2 Nitroxides

$T_1$  relaxation time in the presence and absence of nitroxides were acquired on a Bruker DRX spectrometer operating at a proton resonance frequency of 500 MHz ( $B_0 = 11.75$  T). Typical parameters of 1D- $^1\text{H}$  experiments were 16 scans acquired at 27 °C with a pulsewidth of 14.2  $\mu\text{s}$ , a spectral width of 16 ppm, an acquisition time of 2 s and a repetition delay of 2 s were averaged. The water resonance was suppressed with an excitation sculpting suppression scheme [Hwang and Shaka 1995].

Identical parameters were used for the determination of  $T_1$  relaxation times using an inversion recovery experiment with espg water suppression. A series of 22 relaxation time delays ranging from 1 ms to 2 s were measured with 4 scans each, and the relaxation rates/times determined using the analysis module in the Bruker processing software Topspin 1.3. Accuracies of  $T_1$  relaxation time measurements were 5 %. Provided that the free mobility is the same for the portion of antioxidants and nitroxides in the aqueous phase of the micellar solution as for those in buffer solution ( $T_{1,obs}$ ) the relaxation rate for antioxidants/nitroxides solubilized in the micellar phase ( $T_{1,eff}$ ) was calculated considering the

individual partitioning behavior ( $P_{AO}/P_N$ ) by [Heins et al. 2007b]:

$$\frac{1}{T_{1,obs}} = \frac{1-P}{T_{1,con} \cdot 100} + \frac{P}{T_{1,eff} \cdot 100} \quad (4.4)$$

The  $T_1$  relaxation ratio was used to compare the effective relaxation times of the antioxidant/nitroxides solubilized in micelles  $T_{1,eff}$  with the relaxation times of the freely movable antioxidant/nitroxides in the aqueous phase  $T_{1,con}$ .

## 4.4 Results and Discussion

### 4.4.1 Solubilization site of antioxidants and nitroxides

The partitioning behavior due to lipophilicity and the chemical structure of solutes is an important factor to understand the spectroscopic parameter and to interpret the differences in antioxidant activity. Nearly the entire proportion of antioxidants used ( $P_{AO}$ ) partitioned into CTAB micellar phase (table 4.1).  $\alpha$ -Tocopherol could not be measured in the aqueous phase. Thus, it was assumed that  $\alpha$ -tocopherol completely partitioned into all micellar phases. For Trolox and PG the proportion of antioxidants solubilized in the micellar phase decreases in the order CTAB > Brij > SDS, where PG is solubilized to a higher extent than Trolox. Differences in partitioning are accompanied with different localizations of the

Table 4.1: Partitioning of nitroxides ( $P_N$ ) and antioxidants ( $P_{AO}$ ) into the micellar phases of different micellar solutions

	$P_N, \%^a$			$P_{AO}, \%^b$		
	TEMPOL mean $\pm$ s.d.	TEMPO mean $\pm$ s.d.	TB mean $\pm$ s.d.	PG mean $\pm$ s.d.	Trolox mean $\pm$ s.d.	$\alpha$ -tocopherol
CTAB	13 $\pm$ 3.5	42 $\pm$ 1.7	97 $\pm$ 0.0	99 $\pm$ 0.0	97 $\pm$ 0.4	100*
SDS	9 $\pm$ 5.5	46 $\pm$ 1.2	96 $\pm$ 1.0	74 $\pm$ 0.2	38 $\pm$ 1.0	100*
Brij 58	9 $\pm$ 2.0	33 $\pm$ 3.1	89 $\pm$ 1.2	90 $\pm$ 0.2	50 $\pm$ 0.8	100*

<sup>a</sup>Proportion of nitroxides in the micellar phase calculated by EPR simulation (chapter 3)

<sup>b</sup>Proportion of antioxidants in the micellar phase detected by HPLC after ultrafiltration.

\* $\alpha$ -Tocopherol could not be measured in the aqueous phase. Thus, it was assumed that  $\alpha$ -tocopherol partitioned to 100% into the micellar phase.

antioxidants in the micellar phase leading to influences of different chemical microenvironments and the formation of different strength of interactions between the antioxidant and emulsifier molecules [Heins et al. 2007b; Heins et al. 2006]. The changes in chemical shifts of individual emulsifier proton signals in the presents of the antioxidants compared with

their absence giving information on the solubilization site of the antioxidants (table 4.2).

Table 4.2:  $^1\text{H}$ -NMR parameter for localization of the antioxidants propyl gallate (PG), Trolox and  $\alpha$ -tocopherol in the micellar phase of CTAB, SDS and Brij58 micellar solutions

		$\Delta\delta_{\text{HDO}=2.00} \pm 0.003$ [ppm] of single emulsifier protons in presence of antioxidants			$T_1$ relaxation ratio ( $T_{1,\text{sol}}/T_{1,\text{con}} \pm 0.1$ of emulsifier proton signals)		
		PG	Trolox	$\alpha$ -tocopherol	PG	Trolox	$\alpha$ -tocopherol
CTAB	a-CH <sub>2</sub>	0.108	0.072	0.014	0.71	1.05	0.98
	hg	0.049	0.061	0.006	0.78	0.97	0.96
	$\beta$ -CH <sub>2</sub>		0.048	0.022	0.80	1.04	0.99
	ac	0.062	0.047	0.035	0.95	0.98	0.96
	w-CH <sub>3</sub>	0.000	0.030	0.042	1.10	0.95	0.86
SDS	a-CH <sub>2</sub> (hg)	-0.002	0.016	0.017	1.06	1.10	0.94
	$\beta$ -CH <sub>2</sub>		0.018	0.028	0.80	1.03	0.92
	ac	0.023	0.027	0.022	1.03	0.93	0.94
	w-CH <sub>3</sub>	0.023	0.024	0.058	1.04	1.41	0.77
Brij 58	hg	-0.018	0.012	0.003	0.97	1.05	1.00
	$\beta$ -CH <sub>2</sub>				0.82	1.44	1.02
	ac	0.026	0.028	0.018	1.01	1.29	0.97
	w-CH <sub>3</sub>	0.016	0.025	0.014	1.05	0.99	1.06

Chemical shift differences showed positive values in case of a higher chemical shift in the presence than in the absence of antioxidants indicating a higher electron density around individual emulsifier protons, when antioxidants are solubilized [Heins et al. 2007b]. Highest differences in the chemical shift were found for PG and Trolox in CTAB for the headgroup proton signals and for  $\alpha$ -tocopherol for the alkyl chain and stronger for the  $\omega$ -methyl group signal. These shifts indicated that  $\alpha$ -tocopherol was located in the micellar interior of CTAB, whereas PG and Trolox were located in the palisade layer close to the headgroup around the  $\alpha$ -CH<sub>2</sub> group. In SDS micelles,  $\alpha$ -tocopherol was located around the  $\omega$ -CH<sub>3</sub> while PG and Trolox showed only low positive chemical shift difference indicating their solubilization in the Stern layer of SDS [Heins et al. 2007b]. In Brij58 low shifts in chemical shift was found for the alkyl chain signals of all emulsifiers in the presence of all antioxidants, whereas the headgroup region of Brij58 showed only a very small increase of electron density. Summarized and compared with further data [Heins et al. 2007b], PG and Trolox showed a similar localization in the micellar phases, while  $\alpha$ -tocopherol was located in the micellar interior.

However, the interactions arising at the individual solubilization site that can be indicated by the  $T_1$  relaxation times is very different. While PG showed a strong reduction of the  $T_1$  relaxation time for the emulsifier headgroup protons and the two adjacent methyl group protons indicating strong interactions with CTAB, Trolox showed no interference of the CTAB protons indicated by a  $T_1$  relaxation ratio close to 1. This is also true for Trolox



in SDS and Brij58 systems. PG showed no interactions with SDS protons but with the first methyl group of the alkyl chain of Brij58.  $\alpha$ -Tocopherol reduced the  $T_1$  relaxation time of the  $\omega$ -CH<sub>3</sub> proton of SDS and CTAB due to interactions arising. The stronger the interactions are the lower is the antioxidant efficiency.

The proportion of nitroxides ( $P_N$ ) solubilized in the micellar phase of all emulsifiers increased with increasing lipophilicity of TEMPOL > TEMPO > TB (table 4.1). For all nitroxides used, SDS showed the highest solubilization capacity. A lower extent of nitroxides was solubilized in CTAB and least amounts were solubilized in Brij58 micelles. While TB was solubilized in the micellar phase to over 90 %, the water-soluble TEMPOL was only solubilized in the micellar phase to 9-13 %, with equal proportions in micellar solutions. The widest range of partitioning was found for TEMPO ranging from 33 % in Brij58 to 46 % in SDS micelles.

To determine the solubilization site of nitroxides in the different micellar environments, <sup>1</sup>H-NMR was carried out to measure the  $T_1$  relaxation times of the emulsifier protons in the presence and absence of the nitroxides (figure 4.2) as it was already done for the stable radicals Fremy's salt and galvinoxyl [Heins et al. 2007a]. Unlike to these stable radicals or the antioxidants investigated, the nitroxides concentrations used in the study showed very strong reduction of the  $T_1$  relaxation times to an equal extent of all emulsifier protons which may be a result of strong hydrogen-bonding interactions of the NO moiety [Pyter et al. 1982]. This is also true for all emulsifier used, when taking into account the individual partitioning behaviors of the nitroxides into the different micelles ( $T_{1,eff}$ ). Therefore, the strongest reduction of  $T_1$  relaxation time ( $T_1$ ) that was found e.g. in SDS micellar solution in the range TB > TEMPO > TEMPOL (table 4.3) is only an effect of the different nitroxide contents in the micellar phases.

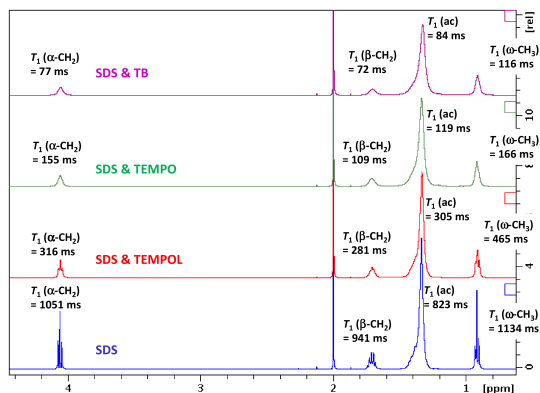


Figure 4.2: <sup>1</sup>H-NMR spectra of SDS in the absence and the presence of TEMPOL, TEMPO and TB. In  $T_1$ -relaxation times of individual emulsifier proton signals are included.

The NO moiety strongly enhances the magnetic relaxation of the neighboring protons leading to an overall enhanced relaxation time. Comparing the  $T_1$  relaxation ratios, there is a tendency, that the palisade protons  $\alpha$  and  $\beta$  show slight stronger reduction of the  $T_1$  relaxation in the presence of the NO moiety of all nitroxides. Pyter and colleagues [1982] also postulated a predominant solubilization of nitroxides in the headgroup region of micelles regardless of the nitroxide lipophilicities. These observations were conformed with the works of Oakes [1972] and Almeida and co-workers [1998]. Almeida and co-workers also showed that TEMPO has a higher binding constant for CTAC, SDS and Triton X-100 micelles than TEMPOL. They correlate a higher binding constant of the radicals with the micellar environment with the higher packing of the emulsifier monomers in the micelle indicated also by a higher cmc. The concentrations at which micelles were formed in the used study systems were  $0.8 \pm 0.07$  mmol for SDS,  $0.095 \pm 0.005$  mmol for CTAB and  $0.004 \pm 2.5 \cdot 10^{-5}$  mmol for Brij58 [Heins et al. 2006]. These cmc would also be correlated with a reduced partitioning of TEMPO into the micellar phases in the range of SDS > CTAB > Brij58 supporting the findings from Almeida and colleagues [1998].

Table 4.3:  $T_1$ -relaxation ratio of individual emulsifier proton signals of CTAB, SDS and Brij58 in the presence of micellar TEMPOL, TEMPO and TEMPOL-benzoate

		$T_1$ relaxation ratio ( $T_{1,eff}/T_{1,con}$ ) of emulsifier proton signals		
		TEMPOL	TEMPO	TEMPOL-benzoate
CTAB	hg	0.11	0.07	0.09
	$\alpha$ -CH <sub>2</sub>	0.07	0.04	0.06
	$\beta$ -CH <sub>2</sub>	0.07	0.05	n.d.
	ac	0.09	0.07	0.07
	$\omega$ -CH <sub>3</sub>	0.17	0.09	0.09
SDS	$\alpha$ -CH <sub>2</sub> (hg)	0.04	0.08	0.07
	$\beta$ -CH <sub>2</sub>	0.03	0.05	0.07
	ac	0.04	0.06	0.08
	$\omega$ -CH <sub>3</sub>	0.08	0.08	0.11
Brij	hg	0.22	0.26	0.19
	$\alpha$ -CH <sub>2</sub>	0.02	n.d.	n.d.
	$\beta$ -CH <sub>2</sub>	0.08	n.d.	n.d.
	ac	0.11	0.07	0.05
	$\omega$ -CH <sub>3</sub>	0.14	0.07	0.05

n.d.: Not detectable

Regardless of their different lipophilicity both nitroxides have their paramagnetic fragments localized in the same micelle region, in the palisade layer. However, Almeida and co-workers [1998] suppose that the orientation of TEMPO and TEMPOL differs in the micellar phase. While TEMPOL may be orientated with its additional hydroxyl group in the more polar region and the NO moiety is aligned to the more nonpolar region, TEMPO may be accommodated with the NO moiety in the more hydrophilic region. This is also in line with the work of Oakes [1972]. Brigati and colleagues [2002] suggested that it might be very difficult for nitroxides with a polar OH group to pass the micellar interface and to



Table 4.4: Hyperfine splitting constants of nitroxides in buffer and micellar solutions (n=3)

		Hyperfine splitting constants $a_N$ , G			
		no antioxidant	PG	Trolox	$\alpha$ -Tocopherol
		mean $\pm$ s.d.	mean $\pm$ s.d.	mean $\pm$ s.d.	mean $\pm$ s.d.
TEMPOL	Buffer Solution	16.89 $\pm$ 0.075 <sup>ab,i</sup>	17.00 $\pm$ 0.000 <sup>a,j</sup>	17.00 $\pm$ 0.000 <sup>a,j</sup>	n.d.
	CTAB	16.94 $\pm$ 0.000 <sup>b,i</sup>	16.92 $\pm$ 0.046 <sup>a,i</sup>	16.86 $\pm$ 0.088 <sup>b,j</sup>	16.97 $\pm$ 0.048 <sup>b,j</sup>
	SDS	16.80 $\pm$ 0.065 <sup>a,i</sup>	16.93 $\pm$ 0.000 <sup>a,ii</sup>	16.93 $\pm$ 0.000 <sup>ab,ii</sup>	16.82 $\pm$ 0.038 <sup>a,ii</sup>
	Brij 58	16.83 $\pm$ 0.096 <sup>ab,i</sup>	16.98 $\pm$ 0.050 <sup>a,ii</sup>	16.98 $\pm$ 0.050 <sup>ab,ii</sup>	16.89 $\pm$ 0.096 <sup>ab,ii</sup>
TEMPO	Buffer Solution	17.19 $\pm$ 0.000 <sup>a,i</sup>	17.22 $\pm$ 0.048 <sup>a,i</sup>	17.08 $\pm$ 0.127 <sup>a,i</sup>	n.d.
	CTAB	16.89 $\pm$ 0.082 <sup>b,i</sup>	16.21 $\pm$ 0.047 <sup>b,ii</sup>	16.95 $\pm$ 0.188 <sup>a,j</sup>	16.92 $\pm$ 0.170 <sup>a,j</sup>
	SDS	16.94 $\pm$ 0.000 <sup>b,i</sup>	16.97 $\pm$ 0.096 <sup>c,i</sup>	17.05 $\pm$ 0.048 <sup>a,j</sup>	16.97 $\pm$ 0.096 <sup>a,j</sup>
	Brij 58	17.08 $\pm$ 0.127 <sup>a,i</sup>	17.06 $\pm$ 0.177 <sup>a,i</sup>	17.08 $\pm$ 0.050 <sup>a,i</sup>	17.05 $\pm$ 0.048 <sup>a,i</sup>
TEMPOL- benzoate	Buffer Solution	16.92 $\pm$ 0.048 <sup>a,i</sup>	16.92 $\pm$ 0.048 <sup>a,i</sup>	16.90 $\pm$ 0.048 <sup>a,i</sup>	n.d.
	CTAB	16.19 $\pm$ 0.000 <sup>c,i</sup>	16.19 $\pm$ 0.000 <sup>b,i</sup>	16.14 $\pm$ 0.127 <sup>c,i</sup>	16.14 $\pm$ 0.096 <sup>c,i</sup>
	SDS	16.35 $\pm$ 0.094 <sup>c,i</sup>	16.46 $\pm$ 0.047 <sup>b,ii</sup>	16.47 $\pm$ 0.022 <sup>b,j</sup>	16.46 $\pm$ 0.022 <sup>b,j</sup>
	Brij 58	16.70 $\pm$ 0.125 <sup>b,i</sup>	16.73 $\pm$ 0.000 <sup>a,i</sup>	16.49 $\pm$ 0.141 <sup>b,ii</sup>	16.43 $\pm$ 0.236 <sup>b,ii</sup>

n.d.: Not detectable due to low solubility in water.

<sup>a-d</sup> Emulsifier effect: Values of one column with different letters indicate statistically significant differences (n=3, p<0.05, Bonferroni)

<sup>i-ii</sup> Antioxidant effect: Values of one row with different roman numbers indicate statistically significant differences (n=3, p<0.05, Bonferroni)

solubilization in a less polar environment (table 4.4), thereby more favoring the resonance structure I. The reduction of  $a_N$  was higher for TB than for TEMPO and for both nitroxides stronger pronounced in CTAB and SDS micelles than in Brij 58 micelles. These findings indicate a concentration effect of nitroxides in the micellar phase with increasing lipophilicity which is also in accordance to the NMR (table 4.3) and partitioning data (table 4.1).

The microenvironment viscosity and specific interactions led to changes in the rotational mobility indicated by the alteration of the peak width and peak intensities of the nitroxides spectra which make it possible to calculate the  $\tau_c$  [Tedeschi et al. 2002]. To take into account the spectral changes when nitroxides are solubilized in the micellar phase the  $\tau_c$  is calculated giving an overview about the chemical microenvironment at the solubilization site (table 4.5). In buffer solution, the presence of the antioxidants PG and Trolox did not influence the  $\tau_c$  of the nitroxides TEMPO, TEMPOL and TB.  $\alpha$ -tocopherol was not soluble in pure buffer solution, so that a control of  $\tau_c$  could not be measured but it would be reasonable that the isotropic free tumbling ( $\tau_c < 0.3$  ns) found for TEMPOL and TEMPO and slight reduced tumbling of TB ( $\tau_c = 0.6$  ns) could be also assumed in the presence of  $\alpha$ -tocopherol. With the exception of TEMPOL in Brij58 micellar solution, the  $\tau_c$  of all nitroxides significantly increased in micellar solution relatively to the pure buffer solution. This is due to a concentration effect of nitroxides that lead to spin-spin interaction with

Table 4.5: Rotational correlation times of nitroxides in the absence and presents of different antioxidants

		Rotational correlation time, ns			
		no antioxidant mean $\pm$ s.d.	PG mean $\pm$ s.d.	Trolox mean $\pm$ s.d.	$\alpha$ -Tocopherol mean $\pm$ s.d.
TEMPOL	Buffer Solution	0.03 $\pm$ 0.006 <sup>a,i</sup>	0.03 $\pm$ 0.002 <sup>a,i</sup>	0.03 $\pm$ 0.001 <sup>a,i</sup>	n.d.
	CTAB	0.07 $\pm$ 0.002 <sup>b,i</sup>	0.07 $\pm$ 0.002 <sup>b,i</sup>	0.08 $\pm$ 0.018 <sup>b,i</sup>	0.06 $\pm$ 0.000 <sup>b,i</sup>
	SDS	0.09 $\pm$ 0.019 <sup>b,i</sup>	0.08 $\pm$ 0.001 <sup>b,i</sup>	0.07 $\pm$ 0.016 <sup>b,i</sup>	0.07 $\pm$ 0.019 <sup>b,i</sup>
	Brij 58	0.04 $\pm$ 0.003 <sup>a,i</sup>	0.04 $\pm$ 0.003 <sup>a,i</sup>	0.05 $\pm$ 0.017 <sup>a,i</sup>	0.04 $\pm$ 0.003 <sup>a,i</sup>
TEMPO	Buffer Solution	0.02 $\pm$ 0.001 <sup>a,i</sup>	0.02 $\pm$ 0.001 <sup>a,i</sup>	0.04 $\pm$ 0.037 <sup>a,i</sup>	n.d.
	CTAB	0.24 $\pm$ 0.095 <sup>c,i</sup>	0.59 $\pm$ 0.012 <sup>c,ii</sup>	0.25 $\pm$ 0.074 <sup>c,i</sup>	0.21 $\pm$ 0.111 <sup>b,i</sup>
	SDS	0.11 $\pm$ 0.027 <sup>b,i</sup>	0.11 $\pm$ 0.027 <sup>b,i</sup>	0.12 $\pm$ 0.007 <sup>b,i</sup>	0.13 $\pm$ 0.009 <sup>b,i</sup>
	Brij 58	0.06 $\pm$ 0.021 <sup>a,i</sup>	0.06 $\pm$ 0.014 <sup>a,i</sup>	0.06 $\pm$ 0.008 <sup>a,i</sup>	0.04 $\pm$ 0.008 <sup>a,i</sup>
TEMPOL- benzoate	Buffer Solution	0.06 $\pm$ 0.003 <sup>a,i</sup>	0.06 $\pm$ 0.006 <sup>a,i</sup>	0.06 $\pm$ 0.007 <sup>a,i</sup>	n.d.
	CTAB	0.61 $\pm$ 0.029 <sup>d,i</sup>	0.58 $\pm$ 0.014 <sup>d,i</sup>	0.63 $\pm$ 0.049 <sup>c,i</sup>	0.62 $\pm$ 0.020 <sup>d,i</sup>
	SDS	0.42 $\pm$ 0.004 <sup>c,i</sup>	0.43 $\pm$ 0.004 <sup>c,i</sup>	0.41 $\pm$ 0.028 <sup>b,i</sup>	0.51 $\pm$ 0.060 <sup>c,ii</sup>
	Brij 58	0.18 $\pm$ 0.038 <sup>b,i</sup>	0.21 $\pm$ 0.004 <sup>b,i</sup>	0.36 $\pm$ 0.062 <sup>b,ii</sup>	0.26 $\pm$ 0.080 <sup>b,ii</sup>

n.d.: Not detectable due to low solubility in water.

<sup>a-d</sup> Emulsifier effect: Values of one column with different letters indicate statistically significant differences (n=3, p<0.05, Bonferroni)

<sup>i-ii</sup> Antioxidant effect: Values of one row with different roman numbers indicate statistically significant differences (n=3, p<0.05, Bonferroni)

showing in a reduced tumbling of the spin probes as also found in the studies of Jolicoeur and Freidman [1978].

While TEMPOL is solubilized in Brij58 micelles to such a low extent (table 4.1) that the tumbling of TEMPOL was not interfered, it had comparable  $\tau_c$  in CTAB and SDS micellar solutions which is due to a similar partitioning behavior of nitroxides into SDS and CTAB micelles. However, in CTAB micellar solution TEMPO had a twice as high  $\tau_c$  compared with SDS micellar solution although their partitioning was equivalent. The same relation was also found for TB.

In all combinations of antioxidants and nitroxides,  $\tau_c$  of nitroxides in Brij58 micellar solution were the lowest which may be due to the bigger particle size of Brij58 relative to the ionic emulsifiers [Heins et al. 2006]. Although PG was nearly complete solubilized in the CTAB micellar phase, it showed no influence on the  $\tau_c$  of TEMPOL and TB, but significantly increased the  $\tau_c$  of TEMPO in CTAB to  $0.59 \pm 0.012$  ns which was also accompanied with a very strong reduction of  $a_N$  to  $16.21 \pm 0.047$  G (table 4.4). This indicated that PG interfered with TEMPO at the same solubilization site which might result in a displacement of TEMPO from the palisade layer into the micellar core which is accompanied with an increased sterical hindrances of TEMPO.

However, the same solubilization site was true for the total content of TB and a low content of TEMPOL but without any interferences of PG. This might be due to the different alignment of the NO moiety of TEMPO that has no substituent compared with TB and TEMPOL that possess polar substituents (see 4.4.1). An alignment of the NO moiety to the more hydrophilic part of the micelle may result in formation of H-bondings [Pyter et al. 1982; Shenderovich et al. 1997] with the H-donating group of the phenolic antioxidant PG [Heins et al. 2007b]. The similar observation could be made in Brij58 micellar solutions where only in the presence of TB the antioxidants Trolox and  $\alpha$ -tocopherol resulted in an increase of  $\tau_c$  (table 4.5) and a reduction of  $a_N$  (table 4.4).

All antioxidants induced a higher  $a_N$  for TEMPOL when solubilized in CTAB and SDS micellar solutions (table 4.4), indicating that the proportion of TEMPOL solubilized in the micellar phase would be displaced by the antioxidants. As  $a_N$  values and  $\tau_c$  is calculated for the superimposed spectra it is not possible to observe the antioxidant effect on the nitroxides population that is solubilized in the micellar solutions. However, with deconvolution of the superimposed spectra using EPRSIM-C the distinction between different spectral domains influencing the nitroxide populations, the calculation of the partitioning behavior as well as  $a_N$  and  $\tau_c$  for the individual nitroxides populations are possible (chapter 3) [Frenzel and Steffen-Heins 2014].

### 4.4.3 Antioxidant capacity to reduce micellar nitroxides

Nitroxides are stable radicals that are directly reducible by antioxidants via hydrogen donation transfer forming cyclic hydroxylamines [Damiani et al. 2004]. Together with a possible electron transfer the nitroxide radical is in equilibrium with the cyclic hydroxylamine and the oxoammoniumion, which are EPR-silent [Amorati et al. 2010]. The decay of the three different nitroxides of different lipophilicity was observed in the three micellar solutions and in the presence of the antioxidants Trolox,  $\alpha$ -tocopherol and PG (figure 4.4). To compare the antioxidant capacities to reduce the used nitroxides in different micellar solutions, the decay of the nitroxides was measured during 2-20h reaction time and fitted by a first order exponential decay. Table 4.6 depict the fitting parameters for all sample combinations regarding the antioxidant capacity (aoc) which is given by the maximum of nitroxide reduction and the half-life which is given by the time in hours that is needed to reach 50 % of the aoc. Decays of nitroxides with very slow reaction kinetics did not correspond to an exponential decay within the 20h of investigation, so that these scenarios indicated that no reduction of nitroxides occurred.

Comparing the decay of TEMPOL, TEMPO and TB by PG in buffer solution no reduction of the nitroxides could be observed (figure 4.4a and table 4.6). Further no reduction was investigated of TEMPOL by PG or  $\alpha$ -tocopherol in micellar solutions of Brij58. This is due to the very low concentration of TEMPOL in the Brij58 micelle while these antioxidants are solubilized in the Brij58 micelle to more than 90 % (table 4.1), so that they do not meet for reaction [Heins et al. 2007a]. The combination of TB and  $\alpha$ -tocopherol in Brij58 or

CTAB micellar solution also did not result in a reduction of TB, although both reactants were nearly completely solubilized in the micellar phase. This may be explained by the possible alignment of the NO moiety of TB to the micellar core.

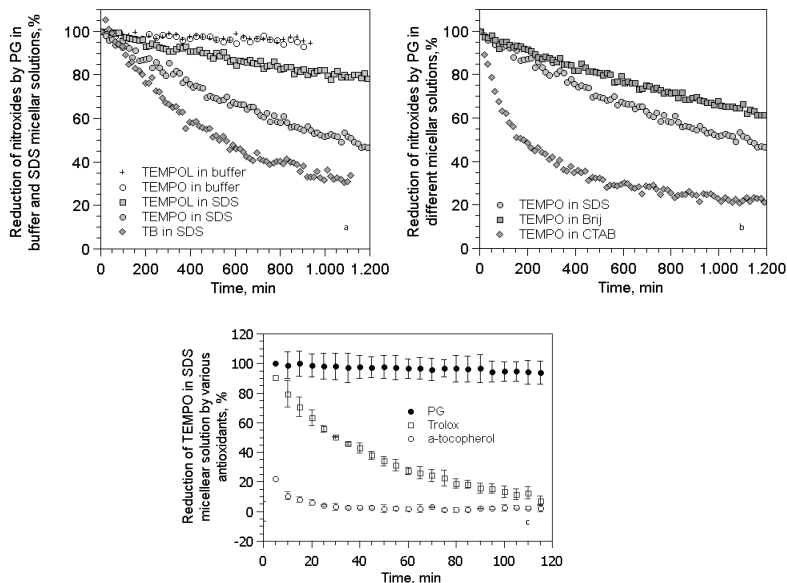


Figure 4.4: Exponential decay of different nitroxides by antioxidants in micellar solutions. Comparison of the decay of different nitroxides in buffer and SDS solution by propyl gallate (a), of TEMPO by propyl gallate in SDS, CTAB and Brij58 solution (b), and of TEMPO in SDS micellar solution by propyl gallate, Trolox and  $\alpha$ -tocopherol (c).

Although only 38 % of Trolox was solubilized in the SDS micelles (table 4.1), it showed great potential in reducing all nitroxides being fastest for TB > TEMPO > TEMPOL. The nitroxide content in SDS micelle is in accordance with the reaction kinetic, however, Trolox is also able to reduce nitroxides in the aqueous phase and benefit from the reduction opportunity also in the water phase. In addition, it was shown by Oehlke and colleagues [2011] that SDS micellar solution stabilizes Trolox by prevention of its degradation into a non antioxidative Trolox quinone. This degradation is favored in a non-polar environment; however, unlike to CTAB and Brij58 interfaces, Trolox is solubilized in the Stern layer of the SDS micelle which is much more polar than the palisade layer [Heins et al. 2007b] which in turn would support the better antioxidative activity at the SDS interface.

Although PG did not reduce any nitroxides in homogenous buffer solution, in SDS micellar solution PG was able to reduce all nitroxide radicals within 20 h but with different max-

imum reduction capacities. TEMPOL was only slightly transformed into the EPR-silent hydroxylamine, while TEMPO and TB were faster transformed due to their increasing concentration in the micellar phase (9 % > 46 % > 96 %, table 4.1) where 74 % of the PG was associated with the SDS micelle. Thus, the micelles showed catalytic effects on the reaction between the antioxidant and the radical due to their accumulation in the micellar phase of both reactants [Heins et al. 2007a]. This is in line with the study by Aliaga [2008] showing also a drastic increase of spin probe reduction in the presence of anionic and non-ionic micelles.

Regarding the reaction between PG and TEMPO in different micellar solutions, different reaction kinetics were found with the slowest reaction in Brij58 increasing to SDS and CTAB micellar solution (figure 4.4b and table 4.6). However, this is not in accordance to the partitioning of TEMPO into the three micellar phases with the same content of TEMPO being solubilized in the SDS (46 %) and in the CTAB (42 %) micelles and to a lower extent in the Brij58 micellar phase (33 %) (table 4.1). The highest concentration of the antioxidant PG was found to be in CTAB with 99 %, followed by Brij58 with 90 % and in SDS with 74 %. As TEMPO highly interacted with PG in the CTAB microenvironment as indicated by a strong increase of  $\tau_c$  (table 4.5) and a reduction of  $a_N$  (table 4.4), it may be reasonable that not only the concentration of the reactants but also their close proximity of the H-donating group of the antioxidant and the NO moiety is a crucial property that governed the reaction kinetic in micelles.

In addition the CTAB micellar environment that is particularly dehydrated by the solubilization of PG [Heins et al. 2006] which is indicated by very low  $a_N$  values for TEMPO is related to low formation of H-bonds around the NO moiety. This is due to the favored resonance structure I (figure 4.3) that in turn result in the spin density being localized on the oxygen. Beckwith and colleagues [1992] demonstrated that this scenario accelerated the reactivity of the nitroxides since it is easier for the reactants such as radical or antioxidants to react with the NO moiety when only few solvent (water) molecules has to be displaced prior to nitroxide reaction.

Within 2 h Trolox and  $\alpha$ -tocopherol reduced TEMPO much faster than PG did (figure 4.4c and table 4.6). Particularly the reduction of TEMPO by  $\alpha$ -tocopherol in a SDS micellar system is extremely fast and the reaction runs down to completion (table 4.6). Comparing the half-lives of TEMPO in the presence of Trolox and  $\alpha$ -tocopherol,  $\alpha$ -tocopherol reduced the TEMPO threefold faster than Trolox, which is in line with a threefold higher content of  $\alpha$ -tocopherol in the SDS micelle (table 4.1). Of course this is only true for antioxidants showing the same hydrogen abstraction kinetic as it was the case for Trolox ( $k_H = 0.19 \text{ mol}^{-1} \text{ s}^{-1}$ ) and  $\alpha$ -tocopherol ( $k_H = 0.21 \text{ mol}^{-1} \text{ s}^{-1}$ ) towards the TEMPO prefluorescent probe in pure buffer solution at a pH of 7.0 [Aliaga et al. 2008]. Aliaga and colleagues [2008] demonstrated a 20-fold lower hydrogen abstraction kinetic for gallic acid ( $k_H = 0.009 \text{ mol}^{-1} \text{ s}^{-1}$ ) than for Trolox and  $\alpha$ -tocopherol explaining the differences between the antioxidative capacities between the propyl gallate ester and Trolox /  $\alpha$ -tocopherol in our study.



Table 4.6: Antioxidative capacity of PG, Trolox and  $\alpha$ -Tocopherol to reduce nitroxides in different micellar solutions.

		Rotational correlation time, ns			
		no antioxidant mean $\pm$ s.d.	PG mean $\pm$ s.d.	Trolox mean $\pm$ s.d.	$\alpha$ -Tocopherol mean $\pm$ s.d.
TEMPOL	Buffer Solution	0.03 $\pm$ 0.006 <sup>a,l</sup>	0.03 $\pm$ 0.002 <sup>a,l</sup>	0.03 $\pm$ 0.001 <sup>a,l</sup>	n.d.
	CTAB	0.07 $\pm$ 0.002 <sup>b,l</sup>	0.07 $\pm$ 0.002 <sup>b,l</sup>	0.08 $\pm$ 0.018 <sup>b,l</sup>	0.06 $\pm$ 0.000 <sup>b,l</sup>
	SDS	0.09 $\pm$ 0.019 <sup>b,l</sup>	0.08 $\pm$ 0.001 <sup>b,l</sup>	0.07 $\pm$ 0.016 <sup>b,l</sup>	0.07 $\pm$ 0.019 <sup>b,l</sup>
	Brij 58	0.04 $\pm$ 0.003 <sup>a,l</sup>	0.04 $\pm$ 0.003 <sup>a,l</sup>	0.05 $\pm$ 0.017 <sup>a,l</sup>	0.04 $\pm$ 0.003 <sup>a,l</sup>
TEMPO	Buffer Solution	0.02 $\pm$ 0.001 <sup>a,l</sup>	0.02 $\pm$ 0.001 <sup>a,l</sup>	0.04 $\pm$ 0.037 <sup>a,l</sup>	n.d.
	CTAB	0.24 $\pm$ 0.095 <sup>c,l</sup>	0.59 $\pm$ 0.012 <sup>c,II</sup>	0.25 $\pm$ 0.074 <sup>c,l</sup>	0.21 $\pm$ 0.111 <sup>b,l</sup>
	SDS	0.11 $\pm$ 0.027 <sup>b,l</sup>	0.11 $\pm$ 0.027 <sup>b,l</sup>	0.12 $\pm$ 0.007 <sup>b,l</sup>	0.13 $\pm$ 0.009 <sup>b,l</sup>
	Brij 58	0.06 $\pm$ 0.021 <sup>a,l</sup>	0.06 $\pm$ 0.014 <sup>a,l</sup>	0.06 $\pm$ 0.008 <sup>a,l</sup>	0.04 $\pm$ 0.008 <sup>a,l</sup>
TEMPOL- benzoate	Buffer Solution	0.06 $\pm$ 0.003 <sup>a,l</sup>	0.06 $\pm$ 0.006 <sup>a,l</sup>	0.06 $\pm$ 0.007 <sup>a,l</sup>	n.d.
	CTAB	0.61 $\pm$ 0.029 <sup>d,l</sup>	0.58 $\pm$ 0.014 <sup>d,l</sup>	0.63 $\pm$ 0.049 <sup>c,l</sup>	0.62 $\pm$ 0.020 <sup>d,l</sup>
	SDS	0.42 $\pm$ 0.004 <sup>c,l</sup>	0.43 $\pm$ 0.004 <sup>c,l</sup>	0.41 $\pm$ 0.028 <sup>b,l</sup>	0.51 $\pm$ 0.060 <sup>c,II</sup>
	Brij 58	0.18 $\pm$ 0.038 <sup>b,l</sup>	0.21 $\pm$ 0.004 <sup>a,l</sup>	0.36 $\pm$ 0.062 <sup>b,II</sup>	0.26 $\pm$ 0.080 <sup>b,II</sup>

n.d.: Not detectable due to low solubility in water.

<sup>a-d</sup> Emulsifier effect: Values of one column with different letters indicate statistically significant differences (n=3, p<0.05, Bonferroni)

<sup>I-II</sup> Antioxidant effect: Values of one row with different roman numbers indicate statistically significant differences (n=3, p<0.05, Bonferroni)

Since this study is done at pH = 5.0 a slightly higher hydrogen abstraction kinetic is estimated. With the exception of the SDS interface, a complete reduction of nitroxide content was mostly not the case in the combination with other emulsifiers investigated. In addition, all antioxidants showed best antioxidative capacity in the SDS micellar solutions where the best reduction capacities was found with TEMPO. The better reduction of e.g. TEMPO by antioxidants in the SDS interface relative to the CTAB interface concerning equal TEMPO content and alignment of the NO moiety in both micellar phases may be due to two scenarios.

I) As we observed in our previous study using PFG-NMR for determination of self-diffusion rates (chapter 3), hydroxylamines partitioned faster into the SDS than into the CTAB micelle. This might indicate that TEMPO quickly diffuse into the SDS Stern layer being reduced to the corresponding hydroxylamine by the antioxidants present and could afterwards be exchanged with nitroxide radical solubilized in the aqueous phase. Pyter and colleagues [1982] measured also somewhat higher distribution coefficients of the nitroxide TEMPO from the aqueous phase into the interface of SDS and other anionic micelles than into the cationic CTAC micelle. This is also in line with the work of Bigati and colleagues [2002] showing that the entrance kinetic of dialkyl nitroxides into SDS micelles was very close to being controlled by diffusion and found to be faster relative to cationic micelles, which was also true for somewhat lower exit kinetics.

II) The antioxidant solubilization site in SDS micelles is the Stern layer, while in CTAB micelles antioxidants are predominately solubilized in the palisade layer [Heins et al. 2007b; Heins et al. 2006]. As Pyter and colleagues [1982] observed in addition a stabilizing effect of the anionic surface on the NO moiety, it might be in optimal proximity and alignment to react with antioxidants.

### 4.5 Conclusion

As a result of the solubilization properties, antioxidant efficiency towards stable nitroxides is accelerated in nearly all combinations with emulsifiers compared with pure buffer solution. Regardless of the nitroxide lipophilicity, the solubilization of all nitroxides within all micelles is the same, adjacent to the headgroups close to the  $\alpha$ - and  $\beta$ -CH<sub>2</sub> groups (palisade layer). Although the proton relaxation of the emulsifier protons showed a strong influence of all emulsifier protons, the strength of interactions depends on the nitroxide concentration. TEMPO was reduced the fastest by all antioxidants compared with TEMPOL and TB which may be due to a different alignment of the nitroxides. While TEMPO may align with the NO moiety to the more hydrophilic part of the interface, TB (oxycarbonyl group) and TEMPOL (hydroxyl group) have more hydrophilic groups that may be accommodated in the hydrophilic region leading to a 180° rotation with the NO moiety incorporating in the more nonpolar region of the palisade layer.

This is also supported by the observation that the reaction between the stable radicals, particularly of TEMPO, and antioxidants are best at SDS interfaces which might be a result of a quick diffusion of TEMPO into the SDS Stern layer being reduced to the corresponding hydroxylamine by the antioxidants present and could afterwards be exchanged with nitroxide radical solubilized in the aqueous phase. As in addition it was postulated that the anionic surface of SDS might stabilize the NO moiety of TEMPO it might be in optimal proximity and alignment to react with antioxidants.

For food systems the result may indicate that the interfaces are good to accumulate the radicals at one position. The relevance of the nitroxides orientation on the fast reduction kinetic by antioxidants might lead to the conclusion that free lipid radicals may be also differ in their solubilization site in food as a function of their specie and structural composition.

### Acknowledgement

We thank Dr. Bernd Steffen from the DESY, Hamburg, for his help in data analysis and Dr. Tobias Sokolowski from the Beiersdorf AG, Hamburg, for measuring the NMR data of the antioxidants.

## References

- P. Ahlin, J. Kristl, M. Sentjurc, J. Strancar, and S. Pecar. 2000. Influence of spin probe structure on its distribution in SLN dispersions. *International Journal of Pharmaceutics* 196, 2 (2000), 241–244.
- Carolina Aliaga, Juan M. Juárez-Ruiz, Scavano, J. C., and Alexis Aspée. 2008. Hydrogen-Transfer Reactions from Phenols to TEMPO Prefluorescent Probes in Micellar Systems. *Org. Lett.* 10, 11 (2008), 2147–2150.
- L. Almeida. 1998. Different Micellar Packing and Hydrophobicity of the Membrane Probes TEMPO and TEMPOL Influence Their Partition Between Aqueous and Micellar Phases Rather than Location in the Micelle Interior. *Journal of Colloid and Interface Science* 203, 2 (1998), 456–463.
- Riccardo Amorati, Gian Franco Pedulli, Derek A. Pratt, and Luca Valgimigli. 2010. TEMPO reacts with oxygen-centered radicals under acidic conditions. *Chem. Commun.* 46, 28 (2010), 5139.
- Mohamed A. Bahri, Maryse Hoebeke, Angeliki Grammenos, Lisiane Delanaye, Nicolas Vandewalle, and Alain Seret. 2006. Investigation of SDS, DTAB and CTAB micelle microviscosities by electron spin resonance. *Colloids and Surfaces A: Physicochemical and Engineering Aspects* 290, 1-3 (2006), 206–212.
- A. L.J. Beckwith, V. W. Bowry, and K. U. Ingold. 1992. Kinetics of nitroxide radical trapping. 1. Solvent effects. *Journal of the American Chemical Society* 114, 13 (1992), 4983–4992.
- Nelson Beghein, Laurence Rouxhet, Mustapha Dinguizli, M. E. Brewster, A. Ariën, Véronique Préat, J. L. Habib, and Bernard Gallez. 2007. Characterization of self-assembling copolymers in aqueous solutions using Electron Paramagnetic Resonance and Fluorescence spectroscopy. *Journal of controlled release* 117, 2 (2007), 196–203.
- M. N. Berberan-Santos, M.J.E. Prieto, and A. G. Szabo. 1992. Picosecond Electronic Energy-transfer Studies in Sodium Dodecyl Sulfate Micelles. *J. Chem. Soc. Faraday Trans.,* , 255–261 88, 2 (1992), 255–261.
- Claire C. Berton-Carabin, John N. Coupland, Cheng Qian, D. Julian McClements, and Ryan J. Elias. 2012. Reactivity of a lipophilic ingredient solubilized in anionic or cationic surfactant micelles. *Colloids and Surfaces A: Physicochemical and Engineering Aspects* 412, 0 (2012), 135–142.
- Giovanni Brigati, Paola Franchi, Marco Lucarini, GianFranco Pedulli, and Luca Valgimigli. 2002. The EPR study of dialkyl nitroxides as probes to investigate the exchange of solutes between micellar and water phases. *Research on Chemical Intermediates* 28, 2-3 (2002), 131–141.
- Alejandra N. Cimato, Lidia L. Piehl, Graciela B. Facorro, Horacio B. Torti, and Alfredo A. Hager. 2004. Antioxidant effects of water- and lipid-soluble nitroxide radicals in liposomes. *Free Radical Biology and Medicine* 37, 12 (2004), 2042–2051.
- Elisabetta Damiani, Paola Astolfi, Massimo Benaglia, Angelo Alberti, and Lucedio Greci. 2004. Hydrogen Abstraction Ability of Different Aromatic Nitroxides. *Free Radic Res* 38, 1 (2004), 67–72.
- S. I. Dikalov and R. P. Mason. 2001. Spin trapping of polyunsaturated fatty acid-derived peroxyl radicals: Reassignment to alkoxyl radical adducts. *Free Radical Bio Med* 30, 2 (2001), 187–197.
- Monika Frenzel and Anja Steffen-Heins. 2014. Whey protein coating increased bilayer rigidity and stability of liposomes in food like matrices. *Food Chemistry*, 173 (2015) 1090–1099.
- Anja Heins. 2005. Localisation and Activity of Antioxidants in Dispersed Systems Characterised by NMR and ESR Spectroscopy 29. Der Andere Verlag, Tönning. Anja Heins, Vasil Garamus, Bernd Steffen, Heiko Stöckmann, and Karin Schwarz. 2006. Impact of Phenolic Antioxidants on Structural Properties of Micellar Solutions. *Food Biophysics* 1, 4 (2006), 189–201.
- Anja Heins, Donald McPhail, Tobias Sokolowski, Heiko Stöckmann, and Karin Schwarz. 2007a. The Location of Phenolic Antioxidants and Radicals at Interfaces Determines Their Activity. *Lipids* 42, 6 (2007), 573–582.
- Anja Heins, Tobias Sokolowski, Heiko Stöckmann, and Karin Schwarz. 2007b. Investigating the Location of Propyl Gallate at Surfaces and Its Chemical Microenvironment by <sup>1</sup>H NMR. *Lipids* 42, 6 (2007), 561–572.
- T.L Hwang and A.J Shaka. 1995. Water Suppression That Works. Excitation Sculpting Using Arbitrary Wave-Forms and Pulsed-Field Gradients. *Journal of Magnetic Resonance, Series A*

- 112, 2 (1995), 275–279.
- Carmel Jolicoeur and Harold L. Friedman. 1978. ESR lineshapes and kinetic behavior of nitroxide spin probes in micellar solutions. *J Solution Chem* 7, 11 (1978), 813–835.
- Katja Jores, Wolfgang Mehnert, and Karsten Mäder. 2003. Physicochemical Investigations on Solid Lipid Nanoparticles and on Oil-Loaded Solid Lipid Nanoparticles: A Nuclear Magnetic Resonance and Electron Spin Resonance Study. *Pharmaceutical Research* 20, 8 (Aug. 2003), 1274–1283.
- Alec Keith, Grahame Bulfield, and Wallace Snipes. 1970. Spin-Labeled Neurospora Mitochondria. *Biophysical Journal* 10, 7 (1970), 618–629.
- Shin-ya Kishioka, Minoru Umeda, and Akifumi Yamada. 2002. Effect of Oxygen on the Electrochemical Reduction of Nitroxyl Radical: Interpretation of the Mechanism for a Redox Probe in Biological Systems. *Anal. Sci* 18, 12 (2002), 1379–1381.
- Nickolai Kocherginsky and Harold M. Swartz. 1995. Nitroxide spin labels: reactions in biology and chemistry. CRC Press.
- Christian Kroll. 1999. Analytik, Stabilität und Biotransformation von Spinsonden. Dissertation. Mathematisch-Naturwissenschaftliche Fakultät der Humboldt-Universität zu Berlin, Berlin.
- Marina Kveder, Greta Pifat, Slavko Pečar, Milan Schara, Pilar Ramos, and Hermann Esterbauer. 1997. Nitroxide reduction with ascorbic acid in spin labeled human plasma LDL and VLDL. *Chemistry and Physics of Lipids* 85, 1 (1997), 1–12.
- Sonia Losada-Barreiro, Marlene Costa, Carlos Bravo-DÁaz, and FÁtima Paiva-Martins. 2014. Distribution and Antioxidant Efficiency of Resveratrol in Stripped Corn Oil Emulsions. *Antioxidants* 3, 2 (2014), 212–228.
- David Julian McClements. 2010. Emulsion Design to Improve the Delivery of Functional Lipophilic Components. *Annu. Rev. Food Sci. Technol.* 1, 1 (2010), 241–269.
- J. Oakes. 1972. Magnetic resonance studies in aqueous systems. Part 1. Solubilization of spin probes by micellar solution. *J. Chem. Soc., Faraday Trans. 2* 68 (1972), 1464.
- Kathleen Oehlke, Anja Heins, Heiko Stöckmann, and Karin Schwarz. 2010. Impact of emulsifier microenvironments on acid-base equilibrium and activity of antioxidants. *Food Chemistry* 118, 1 (2010), 48–55.
- Kathleen Oehlke, Anja Heins, Heiko Stöckmann, Frank Sönnichsen, and Karin Schwarz. 2011. New insights into the antioxidant activity of Trolox in o/w emulsions. *Food Chemistry* 124, 3 (2011), 781–787.
- Constantinos M. Paleos and Photis Dais. 1977. Ready reduction of some nitroxide free radicals with ascorbic acid. *J. Chem. Soc., Chem. Commun.*, 10 (1977), 345–346.
- Richard A. Pyter, C. Ramachandran, and Pasupati Mukerjee. 1982. Micelle-water distribution coefficients of nitroxides. Correlation with dodecane-water distributions and interfacial activity. *The Journal of Physical Chemistry* 86, 16 (1982), 3206–3210.
- C. Ramachandran, Richard A. Pyter, and Pasupati Mukerjee. 1982. Microenvironmental effects on transition energies and effective polarities of nitroxides solubilized in micelles of different charge types and the effect of electrolytes on the visible spectra of nitroxides in aqueous solutions. *J. Phys. Chem.* 86, 16 (1982), 3198–3205.
- Gerald M. Rosen, Eli Finkelstein, and Elmer J. Rauckman. 1982. A method for the detection of superoxide in biological systems. *Archives of Biochemistry and Biophysics* 215, 2 (1982), 367–378.
- Andrea Rube. 2006. Development and physico-chemical characterization of nanocapsules. Mathematisch-Naturwissenschaftliche Fakultät der Martin-Luther-Universität Halle-Wittenberg, Halle-Wittenberg.
- Shirley Schreier, Carl F. Polnaszek, and Ian C.P Smith. 1978. Spin labels in membranes problems in practice. *Biochimica et Biophysica Acta (BBA) - Reviews on Biomembranes* 515, 4 (1978), 395–436.
- Karin Schwarz, Shu-Wen Huang, J. Bruce German, Brigitte Tiersch, Jurgen Hartmann, and Edwin N. Frankel. 2000. Activities of Antioxidants Are Affected by Colloidal Properties of Oil-in-Water and Water-in-Oil Emulsions and Bulk Oils. *Journal of Agricultural and Food Chemistry* 48, 10 (2000), 4874–4882.
- I. G. Shenderovich, Z. Kecki, I. Wawer, and G. S. Denisov. 1997. NMR and EPR Study of the Nitroxide

- Radical Tempo Interaction with Phenols. *Spectroscopy letters* 30, 8 (1997), 1515–1523.
- Heiko Stöckmann, Karin Schwarz, and Tuong Huynh-Ba. 2000. The influence of various emulsifiers on the partitioning and antioxidant activity of hydroxybenzoic acids and their derivatives in oil-in-water emulsions. *Journal of the American Oil Chemists' Society* 77, 5 (2000), 535–542.
- Janez Štrancar, Tilen Koklic, Zoran Arsov, Bogdan Filipic, David Stopar, and Marcus A. Hemminga. 2005. Spin label EPR-based characterization of biosystem complexity. *Journal of chemical information and modeling* 45, 2 (2005), 394–406.
- A. M. Tedeschi, E. Busi, L. Paduano, R. Basosi, and G. D'Errico. 2003. Influence of the headgroup molecular structure on the anionic surfactant. PVP interaction studied by electron paramagnetic resonance of a cationic nitroxide. *Phys. Chem. Chem. Phys* 5, 22 (2003), 5077.
- A. M. Tedeschi, G. D'Errico, E. Busi, R. Basosi, and V. Barone. 2002. Micellar aggregation of sulfonate surfactants studied by electron paramagnetic resonance of a cationic nitroxide: an experimental and computational approach. *Phys. Chem. Chem. Phys* 4, 11 (2002), 2180–2188.
- J. J. Windle. 1981. Hyperfine coupling constants for nitroxide spin probes in water and carbon tetrachloride. *Journal of Magnetic Resonance* (1969) 45, 3 (1981), 432–439.
- Hisashi Yoshioka, Hiroyuki Haga, Motoi Kubota, Yasuo Sakai, and Hiroe Yoshioka. 2006. Interaction of (+)-Catechin with a Lipid Bilayer Studied by the Spin Probe Method. *Biosci. Biotechnol. Biochem* 70, 2 (2006), 395–400.



# 5 Generation of alkyl- and alkoxy-lipid radicals in dispersed systems followed by their reaction with nitroxides

Heimke Krudopp and Anja Steffen-Heins

Institute of Human Nutrition and Food Science, Kiel University, 24118 Kiel, Germany

## 5.1 Abstract

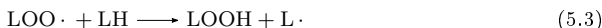
The formation of lipid radicals was studied in dispersed systems by spin probing. The reduction of stable nitroxide radicals with increasing lipophilicity by free lipid radicals was monitored by electron paramagnetic resonance spectroscopy (EPR). Free lipid radicals were formed by the thermal decay of methyl linoleate hydroperoxides (MeLOOH) and by autoxidation of purified corn oil. In dispersed systems, the carbon-centered alkyl radicals were detected due to the oxidation of the nitroxide TEMPO. However, the detection of alkoxy radicals with nitroxides is not appropriate as the reaction kinetic was too slow. The reaction of TEMPOL-benzoate (TB) with alkyl radicals is slower than with TEMPO and the hydrophilic TEMPOL was not oxidized at all, showing that not only the partitioning and solubilisation site but the orientation of the nitroxide is essential for the reaction with free lipid radicals. Therefore, TEMPO showed great potential for an EPR based spin probing technique to monitor the initiation of lipid oxidation in dispersed systems. This technique offers the opportunity for fast measurements compared to the standardized methods to monitor lipid oxidation.

## 5.2 Introduction

Lipid oxidation is one major concern in food stability. The loss of nutritional value and off-flavors caused by lipid oxidation is prevented by the addition of antioxidants. For the right selection and dosage of these food additives it is important to know what happens during the process of oxidation and where the reaction sites are. The three steps initiation, propagation and termination are well known [Roman et al. 2012; Frankel 2005]. During the initiation step primary lipid radicals in form of alkyl radicals ( $L\cdot$ ) are formed from autoxidative processes that are often accelerated due to food processing and storage time. The process starts with the homolytic fission of the lipid alkyl chain or as a consequence from the attack of reactive oxygen species, which are able to abstract hydrogen ( $H\cdot$ ) from the alkyl chain (LH).



These chemical processes require energy, which can be supplied by heat, electromagnetic radiation, redox reactions, etc. During the propagation step the unstable alkyl radicals react with oxygen producing alkyl peroxy radicals ( $LOO\cdot$ ). After hydrogen abstraction from another alkyl chain the hydroperoxides ( $LOOH$ ) are formed next to another alkyl radical.



The decomposition of hydroperoxide leads to hydroxyl ( $\cdot OH$ ) and alkoxy radicals ( $LO\cdot$ ). The formed alkoxy radicals can react with alkyl chains producing alkyl radicals and alcohol ( $LOH$ ). The decomposition of preexistent lipid hydroperoxides can also start the autoxidation process [Cimato et al. 2004].



Food matrices are often based on systems like emulsions, where the interfaces play an important role, as many reactions are located there [Mosca et al. 2013; Heins et al. 2007a, 2007b]. The emulsifiers form the micelles and surround the lipid core in oil-in-water emulsions. As the oxidation products have an increased hydrophilicity compared to the lipids they emerge towards the interface [Mosca et al. 2013]. There are different methods to monitor lipid oxidation [Serfert et al. 2009; Chan and Levett 1977; Velasco et al. 2004; Bauer et al. 2013; Yoshida et al. 2003a, 2003b; Fortier et al. 2009; Frankel et al. 1989; Tikekar et al. 2011]. The formation of hydroperoxides as an early lipid oxidation step can be monitored by their increase [Chan and Levett 1977]. The measurement of secondary



oxidation product hexanal by headspace chromatography is a well-established method to measure the lipid oxidation [Frankel et al. 1989; Serfert et al. 2009]. Fluorescent probes are often used to monitor oxidative stress [Yoshida et al. 2003b]. The emergence of hydroxyl radicals that arise from degradation of hydroperoxides [Fortier et al. 2009] as well as peroxy radicals [Tikekar and Nitin 2012] can be followed. Apart from other options the Rancimat method, the differential scanning calorimetry and the ferric thiocyanate method [Bauer et al. 2013; Velasco et al. 2004] are used.

The detection of radicals by EPR spectroscopy is considered to be the preferred method [Hawkins and Davies 2013] and provides a variety of techniques for the detection of radicals. Apart from the direct measurement the use of radical scavengers is favored for the detection of short living radicals. Spin traps are one kind of radical scavenging molecules and react with radicals and form a stable radical product [Buettner 1987]. Furthermore, the nitroxides reduced to the corresponding hydroxylamine, are used in the spin scavenging technique.

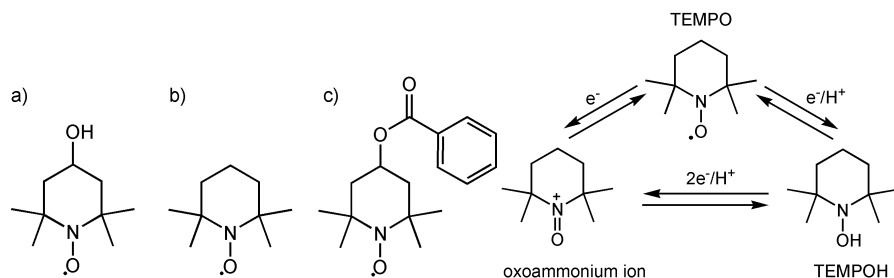


Figure 5.1: Paramagnetic nitroxides TEMPO (a), TEMPOL (b), TB (c) (left) and Interconversion of TEMPO (nitroxide), TEMPO-H (hydroxylamine) and oxoammonium ion (right).

The spin probes in form of paramagnetic nitroxides (figure 5.1) can be used to monitor lipid oxidation at the very beginning of the autoxidation process on the molecular level as they react with lipid radicals (Soule 2007, Voest 1993, Cimato 2004, Hawkins and Davies 2013). The nitroxides are reduced to hydroxylamines which are EPR silent. Therefore the signal intensity decreases caused by the reaction with generated free radicals. The localization of TEMPO and TEMPOL in the interface were studied by Almeida and colleagues [1998]. They propose that both nitroxides have an equal solubilization site, but differ in the radical orientation. TEMPO preferentially reacts with alkyl radicals and not with peroxy radicals, while TEMPOL reacts with peroxy radicals, but too slow to be relevant [Samuni et al. 2000; Amorati et al. 2010]. With the spin probe 5-doxy stearic acids it is possible to calculate rate constants for the autoxidation steps [Roman et al. 2012].

The aim of this study is to localize the free lipid radicals generated by a) autoxidation in emulsions with corn oil and b) thermal decomposition of MeLOOH in swollen micelles with

different emulsifiers. The nitroxides TEMPOL, TEMPO and TEMPOL-benzoate (TB) were used as stable radicals with increasing lipophilicity. Anionic SDS, cationic CTAB and non-ionic Brij58 as emulsifiers give a variety of interfaces showing that different reaction environments play a significant role in radical scavenging.

## 5.3 Materials and Methods

### 5.3.1 Chemicals

SDS (sodium dodecyl sulfate, >99 %), sodium acetate (>99 %, anhydrous), silica gel (0.06-0.2 mm), acetic acid, n-hexane and methanol were obtained from Carl Roth, Germany. Boron trifluoride-methanol complex was obtained from Merck, Germany. Aluminum oxide, Brij58, CTAB (cetyl trimethyl ammonium bromide, >99 %), linoleic acid, TEMPO (2,2,6,6-Tetramethyl-1-piperidinyloxy, free radical) TEMPOL (4-Hydroxy-2,2,6,6-tetramethylpiperidine 1-oxyl) and TEMPOL-benzoate (4-Hydroxy-2,2,6,6-tetramethylpiperidine 1-oxyl benzoate) were purchased from Sigma Aldrich, Germany. Chemicals were used without further purification. Medium-chain-triglycerides (MCT) oil was obtained from Gustav Hees Oleochemische Erzeugnisse GmbH, Germany. Corn oil was purchased at the local supermarket.

### 5.3.2 Preparation of MeLOOH

Linoleic acid was methylated with methanol in the presence of 10 % boron trifluoride. The mixture was kept in a 105 °C heating block for 45 min until reaction was completed [Ichihara and Fukubayashi 2010; DIN EN ISO 2011]. Methyl linoleate was washed in triplicate with hexane-water [DIN EN ISO 2000]. The collected organic phase was filtered through sodium sulfate and evaporated under reduced pressure (28 °C, 240 mbar). Residual solvent was removed under nitrogen. Fatty acid esters were oxidized at 60 °C for 48 h in the dark under atmosphere oxygen until maximum of hydroperoxides [Miyashita and Takagi 1986; Kadowaki et al. 2012]. Hydroperoxides were purified with silica column chromatography and eluted with hexane with increasing ether content [Gardner 1975]. Solvent of collected hydroperoxide fractions was evaporated under reduced pressure. The residual solvent was removed under nitrogen and the MeLOOH were kept at -20 °C in the dark under nitrogen until use. Reaction progress was controlled by thin layer chromatography according to Palgunow and coworkers [2012].

### 5.3.3 Preparation of emulsions

Commercial corn oil was chromatographically purified on an aluminum oxide column and eluted with hexane according to Lampi and Kamal-Eldin (1998). Hexane was evaporated under reduced pressure. The oil was stored under nitrogen at -20 °C until use. The absence of tocopherols was proved according to DFG-FII 4a method. MCT oil were used as a control.

The o/w emulsions consisted of 10 wt% purified corn oil in acetic acid buffer solution (0.05 M, pH 5.0) with 1 wt% emulsifier. Unless otherwise stated, nitroxide concentration was 1 mmol. For EPR measurements batches of 5 ml were prepared. 0.5 g oil was weighted into plastic sample tubes followed by 2 ml emulsifier solution (2.5 wt%). Stock solutions of nitroxides TEMPO and TEMPOL in buffer solutions were added and the pre-emulsion was formed by shaking. For TB a stock solution of nitroxide in ether was transferred to the sample tube on ice. The solvent was evaporated under nitrogen and the re-crystallized nitroxide remained in the sample tube for the emulsion preparation as described above. The pre-emulsion was sonicated for 180 s (cycle 9, 40 % power, Bandelin sonoplus HD 2200). After 30 s the remaining buffer solution was added stepwise within 30 s.

### 5.3.4 Preparation of swollen micelles

The swollen micelles consisted of 1 mmol purified MeLOOH in acetic acid buffer solution (0.005 M, pH 5.0) with 1 wt% emulsifier. The nitroxide concentration was 1 mmol. For EPR measurements batches of 5 ml were prepared. 2.2 mg MeLOOH were weighted into plastic sample tubes followed by 2 ml emulsifier solution (2.5 wt%). The pre-emulsion was sonicated for 2 s (cycle 9, 40 % power, Bandelin sonoplus HD 2200), 3 ml buffer solution were added and sonication applied for another 2 s. Stock solution of nitroxides TEMPO and TEMPOL in buffer were added and the pre-emulsion was formed by shaking. For TB stock solution of nitroxide in ether was transferred to the sample tube on ice. The solvent was evaporated under nitrogen and the re-crystallized nitroxides were covered with 1 wt% emulsifier solution and mixed in an ultrasonic bath.

### 5.3.5 Reduction of nitroxides by lipid radicals

#### 5.3.5.1 Decay products of MeLOOH

The decay of MeLOOH in swollen micelles was carried out at 100 °C a heating block. The reaction of nitroxides towards the decay products was measured by EPR. Samples of MeLOOH in micellar solution were taken after defined time points. The nitroxide stock solution was added and the mixture incubated at 60 °C for 30 minutes in a water bath. Prior to the mixing the stock solution of TB was heated up to 60 °C to ensure that TB is completely dissolved. Samples were collected and the EPR measurement started after 60 s. Experiments were carried out in triplicate.

#### 5.3.5.2 Lipid oxidation products

Lipid oxidation was indirectly measured by the decrease of nitroxide concentration due to the oxidation with lipid radicals. Due to the heat treatment during sonication oxidation time was started already with the sonication step. Afterwards the emulsions with temperature of 60 – 65 °C were immediately transferred in reaction caps and into the water bath. Samples

were collected at different time points of incubation and the measurement started after 60 s. Experiments were carried out in triplicate.

### 5.3.6 Photometric measurement of hydroperoxides

MeLOOH concentration  $c_{MeLOOH}$  [mmol/kg oil] was calculated using the extinction coefficient  $\epsilon = 0.26$  [Chan and Levett 1977]:

$$c_{MeLOOH} = \frac{E \cdot d}{\epsilon \cdot w} \quad (5.6)$$

where E is the extinction at 234 nm, d the calculated dilution factor and w is the weighted sample. The samples were diluted in isopropanol for photometrical measurements (Beckmann Coulter, Krefeld, Germany). Experiments were carried out in triplicate.

### 5.3.7 EPR measurements

EPR measurements of nitroxides were carried out on a Bruker Elexys II E500 X-band spectrometer with a microwave frequency of 9.85 GHz. EPR settings were as followed: modulation frequency: 100 kHz; modulation amplitude: 1.2 G; sweep width: 66.7 G; center field: 3510 G and microwave power: 0.2 mW. The degradation of the EPR-active form of nitroxides was calculated by the relative decrease of spin concentration. Experiments were carried out in triplicate. Double integration of the complete spectrum was calculated to give the unreacted nitroxide content. The measurements were carried out at room temperature.

## 5.4 Results and discussion

### 5.4.1 Influence of nitroxide concentration and heat stability

To exclude concentration effects the nitroxide TEMPO was used in a concentration range from 0.1 mmol to 2.0 mmol in SDS emulsions with 10 wt% corn oil. After autoxidation for 240 min there is no difference in the decrease of total TEMPO at varying concentrations (figure 5.2).

The decrease to 50 % from the initial nitroxides content was equivalent for all TEMPO concentrations used. For TEMPOL and TB the concentrations 0.25 mmol and 2 mmol were monitored revealing also a decrease of nitroxide content independently from the nitroxide concentration used. The data in figure 5.2 showed that the concentration of TEMPO had no effect on the radical scavenging. This is in agreement with a study from Voest and colleagues [1993], who investigated that even at low concentrations (0.05 mmol to 5 mmol) of TEMPO the nitroxide has an inhibitory effect on a hydroxyl radical assay. We tested the heat stability of nitroxides in emulsions at 60 °C (figure 5.3a) and micellar solutions at 100 °C (figure 5.3b) as they were used in the experiments. In micellar solution of SDS at 100 °C TEMPOL and TB remained stable while TEMPO decomposed within 120 min.

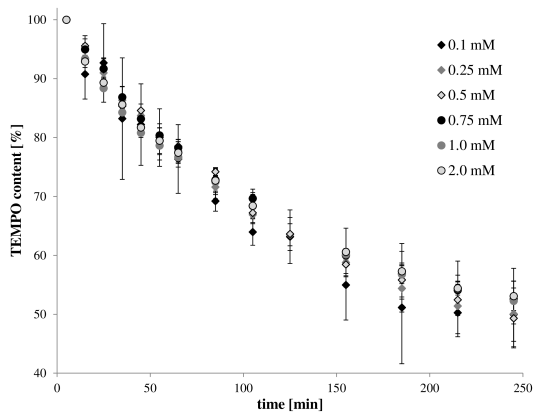


Figure 5.2: Degradation of TEMPO in emulsions with 10 wt% corn-oil in 1 wt% SDS at 60 °C for 4 h with concentrations of 0.1 mmol, 0.25 mmol, 0.5 mmol, 0.75 mmol, 1.0 mmol and 2 mmol TEMPO.

The decay of TEMPO and the other nitroxides in emulsions at 60 °C is negligible with only 3 % to 7 % depending on the emulsifier. This leads to the conclusion, that the pH value of 5.0 and temperatures of 60 °C do not interfere with the equilibrium between nitroxide and hydroxylamine (figure 5.1) and that there are no decomposition reactions of the nitroxide under this condition.

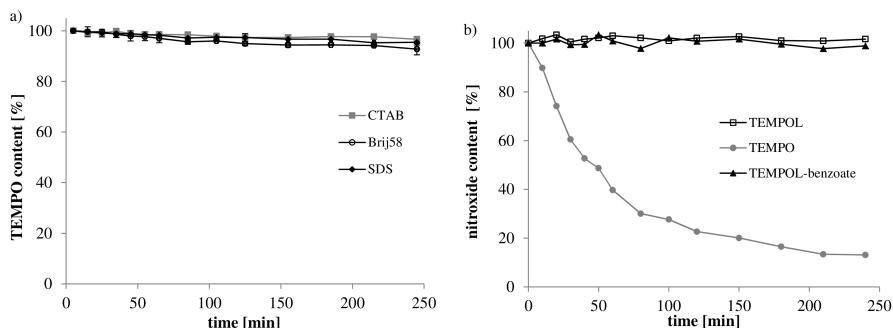


Figure 5.3: Stability of nitroxides during heat exposure: a) TEMPO in emulsions with 10 wt% corn oil and 1 wt% emulsifier (CTAB, Brij58, SDS) at 60 °C for 240 min, b) TEMPOL, TEMPO, TB in micelles of SDS (1 wt%) at 100 °C for 240 min.

TEMPOL and TB are stabilized by additional functional group in position 4. The decay of nitroxides at high temperatures in acid media was studied by few working groups [Nilsen

and Braslau 2006; Ciriano et al. 1999; Ma et al. 2011; Murayama and Yoshioka 1969]. TEMPO is known to be stable up to temperatures of more than 150 °C in solvents without H-donating capacities. In the presence of H-donators they are reduced to their corresponding hydroxylamine and amines above 107 °C. Furthermore an acid-catalyzed mechanism for TEMPO deoxygenating is proposed [Ciriano et al. 1999]. Ma and colleagues [2011] followed the disproportionation of TEMPO in sulphuric acid solution at 80 °C. They could only recover 60 % of TEMPO from the equilibrium with the hydroxylamine TEMPOH (figure 4.1) and analyzed the decomposition pathway. In acidic medium a disproportionation towards TEMPOH and oxoammonium salt occurs. They proposed that a ring-opening of oxoammonium salt at high temperatures leading to a carbocation and further reactions including dimerization products, N<sub>2</sub>O and CO<sub>2</sub> [Ma et al. 2011].

It was suggested that the carbonyl group of 4-oxo-TEMPO increases the reaction ability of the 3- and 5-hydrogen atoms, which leads to a self-reaction to the corresponding hydroxylamine and a nitroso compound at 110 °C [Murayama and Yoshioka 1969]. Nilsen and Braslau [2006] suggested the oxidation of the enol form of the hydroxylamine to a radical cation via single electron transfer with a subsequent dimerization. As these reactions depend on the keto-enol tautomerism the nitroxide TEMPO would not be concerned. Yamasaki and colleagues [2011] studied the stability with tetramethyl-substituted nitroxides such as TEMPOL, TEMPO and TB which are less stable than tetraethyl-substituted ones. They mentioned the recovery of lipid derived radical adducts with tetraethyl-substituted nitroxides after heating at 100 °C and confirmed their observation by LC/MS.

#### 5.4.2 Reactions of nitroxides with lipid radicals from decomposition of MeLOOH

The decomposition of MeLOOH was determined photometrically (figure 5.4). In SDS micelles (figure 5.4a) the decomposition to around 20 % was reached within 120 min in the absence of any nitroxides as well as in the presence of TEMPOL and TEMPO. Samples with TB showed a reduced decay to only 55 %. In Brij58 micelles (figure 5.4b) the MeLOOH decreased to 10 % in the control, while the presence of all nitroxides inhibited the decay of MeLOOH. In the control as well as in the presence of TEMPO and TEMPOL, MeLOOH in CTAB micelles (figure 5.4c) decomposed to 40 % while the presence of TB induced a decrease to 70 %. The decomposition of MeLOOH is independent of the type of emulsifier as all control samples showed a decreasing content.

The decomposition of MeLOOH in CTAB micelles is slower than in SDS and Brij58 micelles. In both ionic micellar solutions TB enhanced the decay of MeLOOH to around 30 % relative to the control and the nitroxides TEMPOL and TEMPO. The location of the nitroxides is a possible reason for the inhibition. TEMPOL is mainly solubilized in the bulk water phase (chapter 3) and therefore not in the direct environment of the MeLOOH. As shown above (figure 5.3b) TEMPO is not stable at 100 °C and the antioxidative effect is unclear. The lipophilic TB is located in the micellar structure to a high content. Hence,

it is most likely that the direct proximity of TB to MeLOOH can inhibit the decomposition.

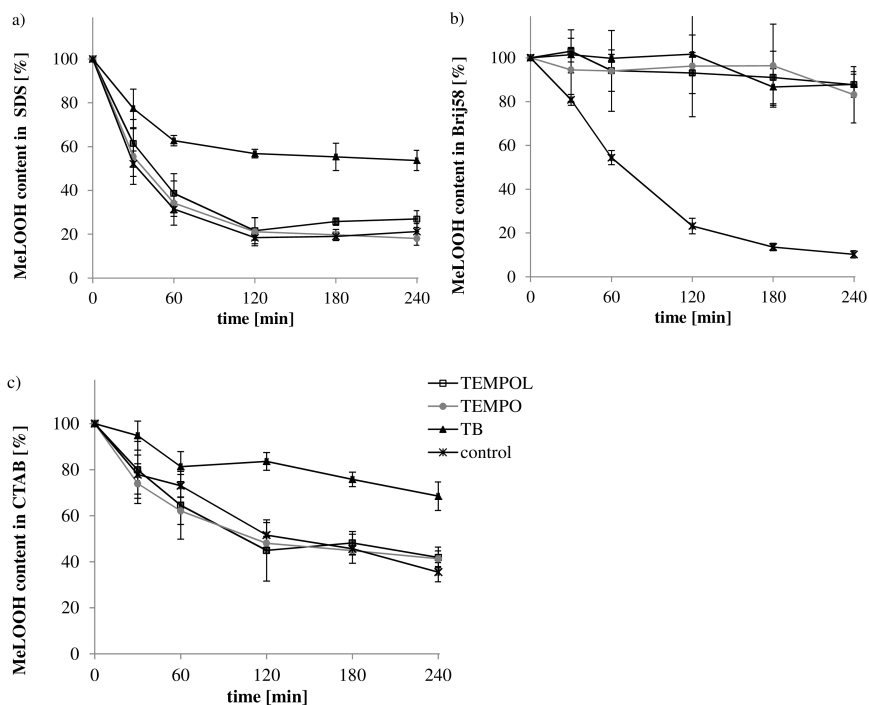


Figure 5.4: Decomposition of 1 mmol MeLOOH in swollen micelles of 1 % SDS (a), Brij58 (b) and CTAB (c) at 100 °C for 240 min in the presence of TEMPOL, TEMPO and TB and in the absence of nitroxides (control) measured by photometry.

For the decomposition of MeLOOH a temperature of 100 °C was chosen regarding to the findings of Roman and colleagues [2012]. They studied the decomposition of hydroperoxides in edible oil with 5-doxylstearic acid. A temperature around 100 °C promotes the degradation of hydroperoxides by breaking the O-O bonds (equation (5.4)). Not only the presence of nitroxides but the surface charge of the droplets influences the decomposition due to electrostatic interaction with metal ion traces. These effects were shown when emulsions stabilized with SDS oxidized more than emulsions with Tween20, Brij35 and DTAB [Mancuso et al. 1999]. The accelerated oxidation in SDS emulsions is in agreement with our findings however it contrasted to the inhibition of lipid oxidation in Brij58 emulsions. Nuchi and colleagues [2002] revealed that MeLOOH are surface active, reducing the inter-

facial tension and being protected from oxidation by large surfactants such as Brij76. This is in contrast to our results, as Brij58 did not decrease the decomposition of MeLOOH. The decreased decomposition of MeLOOH in CTAB can be due to the positively charged surface which would repel traces of metal ions that might support the heat-induced decomposition [Boon et al. 2008].

Although MeLOOH decomposed the emerging radicals could not be detected. Reaction of nitroxides with decay products of MeLOOH was measured by EPR (figure 5.5). All nitroxides showed no significant reduction due to high standard deviations. In swollen micelles of Brij58 a decrease of TEMPOL after 60 min reaction time was shown (figure 5.5a). Another trend could be deduced in SDS micelles showing slight increasing reduction from TEMPO to TB after 120 min of reaction time (figure 5.5b).

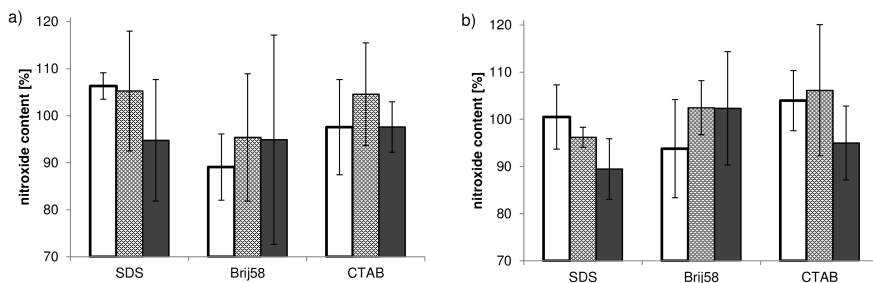


Figure 5.5: Reaction of TEMPOL (light), TEMPO (dotted) and TB (dark) with radicals from the decomposition of 1 mmol MeLOOH in swollen micelles of 1 wt% CTAB, Brij58 and SDS after 60 min (a) and 120 min (b) at 100 °C.

It has to be noticed, that the decrease of the nitroxide result from the reaction with radicals that are present at the point of time when the nitroxide was added and additional radicals that were generated during incubation time. The decomposition of MeLOOH leads to the formation of alkoxy radicals (eq.4). The detection of alkoxy radicals with the nitroxides in swollen micelles was not possible in the systems used. The reaction of nitroxides towards the alkoxy radicals, as the first decay product from MeLOOH, was carried out according to most spin trapping experiments [Sorensen et al. 2008]. Due to the inhibition of MeLOOH decomposition by TB and in the presence of Brij58 by all nitroxides (figure 5.4) as well as to the instability of TEMPO at 100 °C (figure 5.3b) a subsequent addition of nitroxides is needed. Control measurements with TEMPOL in SDS and CTAB micelles at 100 °C were carried out (data not shown) and the results confirm that there is no reduction of nitroxides.

Nitroxide radicals react readily with carbon-centered radicals and slowly with oxygen-



centered lipid radicals [Samuni et al. 1997; Samuni et al. 2000; Cimato et al. 2004; Frankel et al. 1989]. The rate constant for TEMPOL, like other nitroxides, with oxygen-centered radicals is  $10^3$  to  $10^4 \text{ mol}^{-1} \text{ s}^{-1}$  while it is  $10^8$  to  $10^9 \text{ mol}^{-1} \text{ s}^{-1}$  with carbon-centered radicals [Amorati et al. 2010; Lalevée et al. 2008; Sobek et al. 2001]. Pattison and colleagues [2012] studied the adducts of protein derived radicals with TEMPO with a subsequent mass spectroscopic analysis. They postulated that only carbon-centered species can be studied as the unstable adducts from alkoxy, peroxy and hydroxyl radicals are not readily detected.

Many authors declared that oxygen centered radicals undergo a cyclisation to carbon centered epoxyallylic radicals and other rearrangements leading to carbon centered radicals [Brandicourt et al. 2015; Koshiishi et al. 2005; Wilcox and Marnett 1993]. In contrast, Amorati and colleagues [2010] proposed that nitroxides can react with peroxy radicals under acidic conditions, because the nitroxide is in equilibrium with a protonated form where the radical is located on the nitrogen. The hydrogen atom is then transferred to the peroxy radical resulting in a hydroperoxide and an oxoammonium cation. However, in the system used no detectable amounts of radicals were trapped by nitroxides, although the MeLOOH decomposed by heat induction.

### 5.4.3 Reaction of nitroxides with lipid radicals from autoxidation of corn oil

The degradation of nitroxides by the reaction with lipid radicals arising from the autoxidation of purified corn oil is shown in figure 5.6. The first step of lipid oxidation is the formation of alkyl radicals (eq.1). The reaction of TEMPO in SDS emulsions was the highest where the alkyl radicals oxidized 43 % from the nitroxide within 240 min (figure 5.6b). The content of TB decreased to 71 % in SDS emulsions. For both nitroxides, TEMPO (figure 5.6b) and TB (figure 5.6c), the decrease in Brij58 and CTAB emulsions was significantly lower than in SDS emulsions. TEMPO content was 80 % and content for TB was between 85 % and 88 %. TEMPOL is not affected by degradation reactions in all emulsifiers used (figure 5.6a).

The hydrophilic TEMPOL and lipid radicals did not react as only a small content of TEMPOL is solubilized in the micellar phases where the radicals emerge, which is in good agreement with our previous work. We determined the partitioning of TEMPOL to be 10 % in the micellar phase (chapter 3). TB is almost entirely solubilized in the membrane whereas the reaction toward radicals is in between TEMPOL and TEMPO. We conclude that the NO moiety of TB is directed towards the inner core of the micelle and the oxycarbonyl group is orientated towards the aqueous phase.

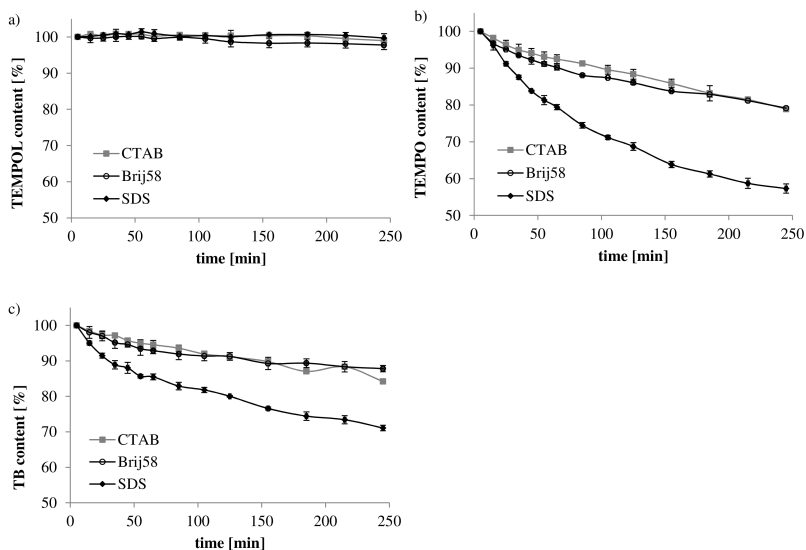


Figure 5.6: Degradation of nitroxides (1 mmol) in emulsions with 10 wt% corn oil in 1 wt% CTAB, Brij58 and SDS at 60 °C for 240 min, a) TEMPOL, b) TEMPO and c) TB.

TEMPO is partially located at the interface (60-70 %) and reacts with lipid radicals depending on the emulsifier. Almeida and colleagues [1998] showed that the binding constants for TEMPO towards pyrene in micellar solution of cationic CTAC, anionic SDS, zwitterionic N-hexadecyl-N,N-dimethyl 3-ammonio-1-propanesulfonate and non-ionic octyl phenoxy polyethoxy ethanol is higher than for TEMPOL. They also found differences between charged and uncharged micelles which is in good agreement with our results, as the reaction is accelerated in anionic SDS micelles and slower in CTAB and Brij58. They proposed that the orientation of the proportion of TEMPO located in the interface is directed with the nitroxide group towards the polar head group region while the hydroxyl group of TEMPOL reaches out to the polar head group region and the NO moiety of TEMPOL is directed toward the inner core [Almeida 1998].

In our previous work we determined the different proportions of individual populations in emulsions (chapter 3). We calculated that the TEMPO populations solubilized in the aqueous phase as well as two populations solubilized in the micellar phase are of the same magnitude in all micellar solutions. Therefore the reactivity of TEMPO towards radicals is influenced by the emulsifier and not by the proportion of nitroxide located at the interface. We conducted NMR diffusion measurements and showed that diffusion in SDS micellar

solution is faster than in Brij58 and CTAB micelles (chapter 3).

Concerning the lipid oxidation results, we measured an accelerated oxidation of the nitroxides TEMPO and TB in SDS emulsions (figure 5.6) and we concluded that there is a correlation between diffusion rate and oxidative stability apart from the influence of the emulsifier charge. The influence of emulsifiers, and therein the interface, towards the oxidative stability was also studied by Mosca and colleagues [2013]. They showed that a mixture of emulsifier with Tween80 and Span80 inhibits lipid oxidation better than other mixtures with Tween and Span of other chain length. They proposed that the physical barrier towards the entrance of pro-oxidants coming from the water phase is more resistant when the oil phase and emulsifier chain are compatible. Other findings in the literature reveal that the initiation of lipid oxidation occurs at the droplet interface [Coupland et al. 1996], which is in good agreement with our results concerning the location of TEMPO. Further they proposed that the concentration of the oxidable substrate at the interface depends on its surface activity [Coupland et al. 1996]. The importance of the close proximity of radical and antioxidant was also shown by Heins and colleagues [2007a] who investigated the depth of intercalation in the interface for galvinoxyl and fremy's radical compared to gallate esters in SDS, Brij and CTAB dispersed systems.

In our study we demonstrated, that the spin probe TEMPO is suitable to detect radicals from autoxidation of corn oil in emulsion. The lipid radicals reduced the TEMPO content to 50 % of the initial content within 4 h. This is in agreement with a study from Cimato and colleagues [2004] who monitored the peroxidation of liposomes at 37 °C by measuring conjugated dienes and TBARS. They used TEMPO and different doxylstearic acids to protect the liposomes from oxidative stress as they react with carbon-centered radicals and monitored the EPR signal intensity which was reduced to 40 % after 70 h. They also showed that there was no correlation between the lipid-water partition coefficient and the inhibition of peroxidation. During lipid oxidation the content of nitroxides was constantly reduced. However, it is most likely that the oxidized form did not interfere with the partitioning or further reactions with lipid radicals. Glandut and colleagues [2006] investigated the TEMPO/TEMPO<sup>+</sup> redox couple and showed that TEMPO<sup>+</sup> did not partition into the water/air interface. This might also be true for the water/oil interface.

Our results show, that not only the proportion of nitroxide in the interface is important to inhibit lipid oxidation, but the orientation and therefore the proximity of the nitroxide towards the radical. The partitioning increases with increasing lipophilicity. However, the reactivity towards lipid radicals does not increase in the same manner. This is in agreement with findings from Yamasaki and colleagues [2011]. They synthesized alkyl chains with increasing length on the second position of TEMPO and used the nitroxides as an antioxidant to inhibit lipid peroxidation. They found out that not only the lipophilicity, but steric factors influence their activity. Therefore, mono-alkyl substituted nitroxides are more efficient than di-alkyl-substituted nitroxides with the same partitioning coefficient and the same amount of substituted alkyl groups.

## 5.5 Conclusion

The EPR spin probe technique is a good opportunity to monitor lipid oxidation in the early stage. The nitroxide TEMPO is oxidized by alkyl radicals in micellar solution of different emulsifiers. It should be noted, that the storage temperature must be appropriate, so that the heat induced decay can be excluded. The monitoring of alkoxy radicals is not suitable for nitroxides as the reaction between alkoxy radicals and nitroxides is too slow. However, the hydrophilic TEMPOL turned out to be less appropriate in dispersed systems investigated since they were not solubilized in the same phase as the generating lipophilic alkyl radicals. Although TB shows a moderate reaction towards alkyl radicals, it might suffer from its hindered tumbling in the micellar phase that might be responsible for a lower reaction kinetic towards free radicals relative to TEMPO. We conclude that the distinct location and orientation of the nitroxide in the interface is the prerequisite for the reaction with lipid alkyl radicals.

## References

- L. Almeida. 1998. Different Micellar Packing and Hydrophobicity of the Membrane Probes TEMPO and TEMPOL Influence Their Partition Between Aqueous and Micellar Phases Rather than Location in the Micelle Interior. *Journal of Colloid and Interface Science* 203, 2 (1998), 456–463.
- Riccardo Amorati, Gian Franco Pedulli, Derek A. Pratt, and Luca Valgimigli. 2010. TEMPO reacts with oxygen-centered radicals under acidic conditions. *Chem. Commun.* 46, 28 (2010), 5139.
- Jonas Lewin Bauer, Britta Harbaum-Piayda, Heiko Stöckmann, and Karin Schwarz. 2013. Antioxidant activities of corn fiber and wheat bran and derived extracts. *LWT - Food Science and Technology* 50, 1 (2013), 132–138.
- Caitlin S. Boon, Zhimin Xu, Xiaohua Yue, D. Julian McClements, Jochen Weiss, and Eric A. Decker. 2008. Factors Affecting Lycopene Oxidation in Oil-in-Water Emulsions. *J. Agric. Food Chem.* 56, 4 (2008), 1408–1414.
- Stéphanie Brandicourt, Jacques Nicolas, Aline Boussard, and Anne-Marie Riquet. 2015. Use of ESR and HPLC to follow the anaerobic reaction catalysed by lipoxygenases. *Food Chemistry* 168, 0 (2015), 311–320.
- Garry R. Buettner. 1987. Spin Trapping: ESR parameters of spin adducts 1474 1528V. *Free Radical Biology and Medicine* 3, 4 (1987), 259–303.
- Henry W.-S Chan and Gordon Levett. 1977. Autoxidation of methyl linoleate. Separation and analysis of isomeric mixtures of methyl linoleate hydroperoxides and methyl hydroxylinoates. *Lipids* 12, 1 (1977), 99–104.
- Alejandra N. Cimato, Lidia L. Piehl, Graciela B. Facorro, Horacio B. Torti, and Alfredo A. Hager. 2004. Antioxidant effects of water- and lipid-soluble nitroxide radicals in liposomes. *Free Radical Biology and Medicine* 37, 12 (2004), 2042–2051.
- Maria Victoria Ciriano, Hans-Gert Korth, Van Scheppingen, Wibo B, and Peter Mulder. 1999. Thermal stability of 2, 2, 6, 6-tetramethylpiperidine-1-oxyl (TEMPO) and related N-alkoxyamines. *Journal of the American Chemical Society* 121, 27 (1999), 6375–6381.
- J. N. Coupland, Z. Zhu, H. Wan, D. J. McClements, W. W. Nawar, and P. Chinachoti. 1996. Droplet composition affects the rate of oxidation of emulsified ethyl linoleate. *Journal of the American Oil Chemists' Society* 73, 6 (1996), 795–801.
- Chanel A. Fortier, Bing Guan, Richard B. Cole, and Matthew A. Tarr. 2009. Covalently bound fluorescent probes as reporters for hydroxyl radical penetration into liposomal membranes. *Free Radical Biology and Medicine* 46, 10 (2009), 1376–1385.
- E. N. Frankel, M-L Hu, and A. L. Tappel. 1989. Rapid headspace gas chromatography of hexanal as a measure of lipid peroxidation in biological samples. *Lipids* 24, 11 (1989), 976–981.
- Edwin N. Frankel. 2005. Lipid oxidation. *Oily Press lipid library* (2nd. ed.). Oily Press; Lipid Technology, Bridgwater, England.
- H. W. Gardner. 1975. Isolation of a pure isomer of linoleic acid hydroperoxide. *Lipids* 10, 4 (1975), 248–252.
- Nicolas Glandut, Andrew D. Malec, Michael V. Mirkin, and Marcin Majda. 2006. Electrochemical Studies of the Lateral Diffusion of TEMPO in the Aqueous Liquid/Vapor Interfacial Region. *J. Phys. Chem. B* 110, 12 (2006), 6101–6109.
- Clare L. Hawkins and Michael J. Davies. 2013. Detection and characterisation of radicals in biological materials using EPR methodology. *Biochimica et Biophysica Acta (BBA) - General Subjects* (2013).
- Anja Heins, Donald McPhail, Tobias Sokolowski, Heiko Stöckmann, and Karin Schwarz. 2007a. The Location of Phenolic Antioxidants and Radicals at Interfaces Determines Their Activity. *Lipids* 42, 6 (2007), 573–582.
- Anja Heins, Tobias Sokolowski, Heiko Stöckmann, and Karin Schwarz. 2007b. Investigating the Location of Propyl Gallate at Surfaces and Its Chemical Microenvironment by  $^1\text{H}$  NMR. *Lipids* 42, 6 (2007), 561–572.
- Ken'ichi Ichihara and Yumeto Fukubayashi. 2010. Preparation of fatty acid methyl esters for gas-liquid chromatography. *Journal of Lipid Research* 51, 3 (2010), 635–640.

- Akio Kadowaki, Satoshi Iwamoto, and Ryo Yamauchi. 2012. Reaction products of [60] fullerene during the autoxidation of methyl linoleate in bulk phase. *Chemistry and Physics of Lipids* 165, 2 (2012), 178–185.
- I. Koshiishi, K. Tsuchida, T. Takajo, and M. Komatsu. 2005. Quantification of lipid alkyl radicals trapped with nitroxyl radical via HPLC with postcolumn thermal decomposition. *Journal of Lipid Research* 46, 11 (2005), 2506–2513.
- Jacques Lalevée, Xavier Allonas, Jean-Pierre Fouassier, and K. U. Ingold. 2008. Absolute Rate Constants for Some Intermolecular Reactions of Aminoalkylperoxy Radicals. Comparison with Alkylperoxyls. *J. Org. Chem.* 73, 17 (2008), 6489–6496.
- Anna-Maija Lampi and Afaf Kamal-Eldin. 1998. Effect of  $\alpha$ - and  $\gamma$ -tocopherols on thermal polymerization of purified high-oleic sunflower triacylglycerols. *J Amer Oil Chem Soc* 75, 12 (1998), 1699–1703.
- Yun Ma, Colin Loyns, Peter Price, and Victor Chechik. 2011. Thermal decay of TEMPO in acidic media via an N-oxoammonium salt intermediate. *Organic & Biomolecular Chemistry* 9, 15 (2011), 5573–5578.
- Jennifer R. Mancuso, D. Julian McClements, and Eric A. Decker. 1999. The Effects of Surfactant Type, pH, and Chelators on the Oxidation of Salmon Oil-in-Water Emulsions. *Journal of Agricultural and Food Chemistry* 47, 10 (1999), 4112–4116.
- Kazuo Miyashita and Toru Takagi. 1986. Study on the oxidative rate and prooxidant activity of free fatty acids. *J Am Oil Chem Soc* 63, 10 (1986), 1380–1384.
- Monica Mosca, Francesca Cuomo, Francesco Lopez, and Andrea Ceglie. 2013. Role of emulsifier layer, antioxidants and radical initiators in the oxidation of olive oil-in-water emulsions. *Food Research International* 50, 1 (2013), 377–383.
- Keisuke Murayama and Takao Yoshioka. 1969. Studies on Stable Free Radicals. IV. Decomposition of Stable Nitroxide Radicals. *Bulletin of the Chemical Society of Japan* 42, 8 (1969), 2307–2309.
- Aaron Nilsen and Rebecca Braslau. 2006. Nitroxide decomposition: Implications toward nitroxide design for applications in living free radical polymerization. *Journal of Polymer Science Part A: Polymer Chemistry* 44, 2 (2006), 697–717.
- Carla D. Nuchi, Pilar Hernandez, D. Julian McClements, and Eric A. Decker. 2002. Ability of Lipid Hydroperoxides To Partition into Surfactant Micelles and Alter Lipid Oxidation Rates in Emulsions. *J. Agric. Food Chem.* 50, 19 (2002), 5445–5449.
- Daniela Palgunow, Maja Klapper, and Frank Döring. 2012. Dietary restriction during development enlarges intestinal and hypodermal lipid droplets in *Caenorhabditis elegans*. *PLoS one* 7, 11 (2012), e46198.
- David I. Pattison, Magdalena Lam, Sujata S. Shinde, Robert F. Anderson, and Michael J. Davies. 2012. The nitroxide TEMPO is an efficient scavenger of protein radicals: Cellular and kinetic studies. *Free Radical Biology and Medicine* 53, 9 (2012), 1664–1674.
- Olesea Roman, Francis Courtis, Marie-Noëlle Maillard, and Anne-Marie Riquet. 2012. Kinetic Study of Hydroperoxide Degradation in Edible Oils Using Electron Spin Resonance Spectroscopy. *J Am Oil Chem Soc* (2012).
- Ayelet M. Samuni, Yechezkel Barenholz, Daan J. A. Crommelin, and Nicolaas J. Zuidam. 1997.  $\gamma$ -Irradiation damage to liposomes differing in composition and their protection by nitroxides. *Free Radical Biology and Medicine* 23, 7 (1997), 972–979.
- Ayelet M. Samuni, Alexander Lipman, and Yechezkel Barenholz. 2000. Damage to liposomal lipids: protection by antioxidants and cholesterol-mediated dehydration. *Chemistry and Physics of Lipids* 105, 2 (2000), 121–134.
- Y. Serfert, S. Drusch, and K. Schwarz. 2009. Chemical stabilisation of oils rich in long-chain polyunsaturated fatty acids during homogenisation, microencapsulation and storage. *Food Chemistry* 113, 4 (2009), 1106–1112.
- Jens Sobek, Rainer Martschke, and Hanns Fischer. 2001. Entropy Control of the Cross-Reaction between Carbon-Centered and Nitroxide Radicals. *J. Am. Chem. Soc.* 123, 12 (2001), 2849–2857.
- A. D.M. Sorensen, Am Haahr, E. M. Becker, L. H. Skibsted, B. Bergenstahl, L. Nilsson, and C. Jacobsen. 2008. Interactions between iron, phenolic compounds, emulsifiers, and pH in omega-3-enriched oil-in-water emulsions. *J Agr Food Chem* 56, 5 (2008), 1740–1750.

- Rohan V. Tikekar, Andrew Johnson, and N. Nitin. 2011. Fluorescence imaging and spectroscopy for real-time, in-situ characterization of interactions of free radicals with oil-in-water emulsions. *Food Research International* 44, 1 (2011), 139–145.
- Rohan V. Tikekar and N. Nitin. 2012. Distribution of Encapsulated Materials in Colloidal Particles and Its Impact on Oxidative Stability of Encapsulated Materials. *Langmuir* 28, 25 (2012), 9233–9243.
- Joaquín Velasco, Mogens L. Andersen, and Leif H. Skibsted. 2004. Evaluation of oxidative stability of vegetable oils by monitoring the tendency to radical formation. A comparison of electron spin resonance spectroscopy with the Rancimat method and differential scanning calorimetry. *Food Chemistry* 85, 4 (2004), 623–632.
- Emile E. Voest, Ernst van Faassen, and Joannes J. M. Marx. 1993. An electron paramagnetic resonance study of the antioxidant properties of the nitroxide free radical TEMPO. *Free Radical Biology and Medicine* 15, 6 (1993), 589–595.
- Allan L. Wilcox and Lawrence J. Marnett. 1993. Polyunsaturated fatty acid alkoxyl radicals exist as carbon-centered epoxyallylic radicals: A key step in hydroperoxide-amplified lipid peroxidation. *Chem. Res. Toxicol.* 6, 4 (1993), 413–416.
- Toshihide Yamasaki, Yuko Ito, Fumiya Mito, Kana Kitagawa, Yuta Matsuoka, Mayumi Yamato, and Ken-ichi Yamada. 2011. Structural concept of nitroxide as a lipid peroxidation inhibitor. *The Journal of Organic Chemistry* 76, 10 (2011), 4144–4148.
- Yasukazu Yoshida, Etsuo Niki, and Noriko Noguchi. 2003a. Comparative study on the action of tocopherols and tocotrienols as antioxidant: chemical and physical effects. *Chemistry and Physics of Lipids* 123, 1 (2003), 63–75.
- Yasukazu Yoshida, Shuichi Shimakawa, Nanako Itoh, and Etsuo Niki. 2003b. Action of DCFH and BODIPY as a Probe for Radical Oxidation in Hydrophilic and Lipophilic Domain. *Free Radical Res.* 37, 8 (2003), 861–872.





## 6 General discussion

To accomplish the aim of this study, the behavior of free lipid radicals in the presence of interfacial structures was investigated by various EPR and NMR experiments. As food matrices are complex systems, model emulsions and micellar solutions of SDS, CTAB, Brij58 and Tween20 were used. The short half-lives of free lipid radicals required spin scavenger for detection of these radicals [Hawkins and Davies 2013]. Therefore, studies on radical behavior at interfaces were carried out with spin traps and spin probes. A systematical characterization of the spin probe properties in dispersed systems was required for deduction of the reaction behavior of free lipid radicals in dispersed food model systems.

### 6.1 Spin Scavenging

Spin traps are one kind of radical scavenging molecules which react with radicals by formation of a stable radical adduct [Buettner 1987]. The nitroxide hydroxylamine redox couples are also used in the spin scavenging technique where the radicals oxidize the EPR active nitroxide to EPR silent hydroxylamines [Hawkins and Davies 2013]. In dispersed systems different combinations of hydrophilic and lipophilic radical generators and spin traps were used in the presence and absence of linoleic acid (LA) to localize the origin of the generated radicals. The addition reaction of a free radical to a spin trap leads to a stable radical adduct that can be identified by its fingerprint hyperfine splitting [Bosnjakovic and Schlick 2006]. Therefore, a distinction between oxygen-centered and carbon-centered radicals is possible [Guo et al. 2003].

Regardless of the radical initiator and emulsifier used, the spin trapping experiments with DMPO showed a predominant generation of hydroxyl radicals (figure 2.3). The oxidation of the aqueous continuous phase led to the exceeding formation of hydroxyl radical adducts which superimposed the EPR spectra of other radical specie adducts (see 6.2). The same was true for the lipophilic DMPO derivates OMPO and DBPMPO (figure 2.4) synthesized by Stolze and colleagues [2000; 2002]. The lipophilic derivates were supposed to be localized in the hydrophobic core of the micelles and therefore in direct proximity to lipid radicals which should accelerate the reaction. However, the detection of hydroxyl radical adducts was predominant due to the preferred formation of DMPO-hydroxyl radical adducts [Dikalov and Mason 2001], the longer half-lives of oxygen-centered DMPO adducts [Guo et al. 2003; Marriott et al. 1980] and enhanced rate constants for the hydroxyl addition [Janzen et al. 1992]. Further distinction between the oxygen-centered radical adducts is only possible by means of simulation [Qian et al. 2000] or other downstream analytical

methods to identify the adduct structures. As the spin trapping of alkyl radicals, generated from oxidation of LA, was possible in Tween20 micellar solutions, it was assumed that the non-ionic headgroup promoted the distinct proximity of alkyl radical and spin trap (figure 2.3 and 2.4).

Owing to the incapability of the spin traps to trap the oxidized LA radicals in micellar solution a DMPO derivate attached to a stearic acid (C17-DMPO) was synthesized (figure 2.1). Due to the structure it was supposed that stearic acid moiety aligned with the membrane-like structure of the emulsifiers and therefore the NO moiety would be in proximity of lipid radicals. However, in dispersed systems it was not possible to detect any stable adducts (figure 2.5). This might be due to a restricted motion of the spin trap and the instability of the adducts as the C17-DMPO was without stabilizing methyl substituents in  $\alpha$ -position [Soule et al. 2007]. In chloroform as a solvent it was possible to detect DMSO derived radicals; however it had a short half-life which made it impossible to determine the partitioning behavior of free radicals in dispersed systems. For this reason further work was focused on spin probes.

Spin probes are EPR active and due to the inter-conversion between nitroxide, hydroxylamine and oxoammonium ion (figure 1.6) [Ma et al. 2011; Soule et al. 2007; Kishioka et al. 2002] the reaction of nitroxides with lipid radicals and antioxidants leads to EPR silent products. Lipid radicals oxidize the paramagnetic nitroxides to diamagnetic hydroxylamines. Therefore, lipid oxidation can be monitored on molecular level [Soule 2007, Voest 1993, Cimato 2004]. The advantage of spin probes is their sensitivity to the microenvironment as the motion of nitroxides is strongly influenced by the dynamics and local structure of its surrounding such as fluidity, viscosity and polarity as well as the molecular structure next to the unpaired electron. Thus it is possible to determine the exact location of the nitroxide and molecules in close proximity [Hawkins and Davies 2013; Weil and Bolton 2007; Hubbell et al. 2000; Kocherginsky and Swartz 1995]. The behavior of three nitroxides with increasing lipophilicity TEMPOL, TEMPO and TEMPOL-benzoate (TB) was further investigated in this study (6.3 and 6.4).

## 6.2 Generation of free lipid radicals

Lipid radicals were generated using different approaches. The Fenton reaction was used to generate the small and highly reactive hydroxyl radicals. Azo-radical generators are available in different lipophilicities and decompose into two radicals at elevated temperatures. To imitate lipid radicals generated during the autoxidation process the heat-induced decomposition of methyl linoleate hydroperoxides (MeLOOH) led to the formation of lipid alkoxy radicals while alkyl radicals were formed in the autoxidation process of oil-in-water emulsions. Hydroxyl radicals from Fenton reaction oxidized LA in Tween20 micellar solutions, but in other micellar solutions the oxidized LA radicals were not detectable. This led to the conclusion that the hydroxyl radicals can penetrate into the interface of Tween20 micelles.

However, in the presence of highly reactive free radicals such as hydroxyl radicals the spin trapping results should be interpreted with caution [Janzen 2012](see 2.5.3). Janzen pointed out, that Piette and colleagues predominantly trapped oxidation products from water and organic Tris buffer compounds (unpublished data). The same was true using methanol as a solvent [Bosnjakovic and Schlick 2006]. Stolze and colleagues [2000] revealed that the iron ions from the Fenton reaction mix might attack the spin adducts which necessitates the presence of chelators for prevention of the spin adducts.

A targeted generation of radicals was performed using the hydrophilic AAPH and the lipophilic AIBN (see 2.4.1 and 2.4.2). It was assumed that they partition either in the aqueous phase (AAPH) or in the micellar phase (AIBN) which would result in radical generation either in the continuous phase or in the interface. However, this concept did not succeed as only hydroxyl radicals were trapped. This implies that the azo-compounds immediately oxidized the water of the continuous phase after their decomposition by which neither the LA was oxidized and trapped nor the decomposition products of the azo-compounds could be trapped (see 2.5.4).

Findings in the literature were contrary about the radical species generated with azo-initiators [Kraiev and Bigelow 1996; Mojumdar et al. 2004]. Mojumdar and colleagues [2004] reported the generation of peroxy radicals using azo-initiators such as AIBN, AMVN and AAPH. Kraiev and Bigelow [1996] investigated the differences of AAPH and AMVN, where AAPH were found to produce alkoxy radicals in aqueous media and AMVN decomposed to give peroxy radicals.

In addition, the positively charged AAPH and the negatively charged SDS precipitated, which was indirectly mentioned by Dai and colleagues [2009], but not noticed in other literature findings [Mojumdar et al. 2004; Freyaldenhoven et al. 1998]. Fenton like reactions as well as azo-compounds are widely used to initiate lipid oxidation. However, in dispersed systems the LA was not entirely oxidized as assumed and the highly reactive hydroxyl radicals dominated.

During the autoxidation steps hydroperoxides play an important role as they are formed in the autoxidation process but also act as secondary initiators [Roman et al. 2012; Cimato et al. 2004]. The heat induced decomposition of MeLOOH at 100 °C result in the formation of alkoxy and hydroxyl radicals by breaking the O-O bonds [Roman et al. 2012]. The decomposition of the MeLOOH was monitored photometrically (figure 5.4). In dispersed systems the MeLOOH decomposed within 120 min to 20 % of their initial content in SDS and Brij58 and to 40 % in CTAB. The surface charge of the droplets influenced the decomposition due to electrostatic interaction with metal ion traces. This is partially in agreement with Mancuso and colleagues [1999] who determined an accelerated oxidation in SDS emulsions compared with Tween20, Brij35 and DTAB. The positively charged surface of CTAB repelled traces of metal ions that might support the heat-induced decomposition [Boon et al. 2008]. Nuchi and colleagues [2002] showed that MeLOOH are surface active as they reduced the interfacial tension. They also revealed that large surfactants such as Brij76 protected the MeLOOH from oxidation, which is in contrast to our results, as Brij58

did not decrease the decomposition of MeLOOH (figure 5.4).

Alkyl radicals are formed during the initiation step of lipid autoxidation [Roman et al. 2012; Frankel 2005]. The production of alkyl radicals in the autoxidation process of 10 wt% purified corn oil emulsions at elevated temperatures was monitored by EPR. As the alkyl radicals are not directly detectable spin probes were used. In this study, it was demonstrated that the spin probe TEMPO is suitable to detect radicals from autoxidation of corn oil in emulsion (see 5.4.3) which is in agreement with Cimato and colleagues [2004] who monitored the peroxidation of liposomes at 37 °C using, amongst others, TEMPO as an antioxidant.

### 6.3 Solubilisation properties of nitroxide spin probes

The dynamics of the dispersed systems were determined by self-diffusion coefficients using PFG-NMR. The corresponding hydroxylamines were used as this technique requires slowly relaxing proton signals [Furtado et al. 2011]. The results indicated that the micellar solutions were a highly dynamic system as shown by high diffusion rate constants in magnitude of  $10^{-10} \text{ m}^2 \text{ s}^{-1}$ . Diffusion rates in buffer decreased to TEMPO > TEMPOL > TB with a further decrease in micellar solutions to TEMPOL > TEMPO > / < TB (table 3.1). Self-diffusion coefficients of nitroxides in SDS micellar solutions were considerably low; even lower than SDS micelles indicating a great affinity of nitroxides toward the micelles. SDS concentration used, was the 4-fold cmc so that a high amount of monomers is present. Other authors determined the dynamics in SDS solution with high concentrations up to 8 wt% [Vinogradova et al. 1998; Söderman et al. 2004; Aizawa et al. 1979]. However, Södermann and colleagues [2004] obtained decreasing self-diffusion coefficients for SDS micelles in D<sub>2</sub>O at concentrations above 0.2 % and therefore they calculated a much higher cmc than in acetic buffer. The self-diffusion coefficients for Brij58 and CTAB are in agreement with literature [Dupont-Leclercq et al. 2007; Hanzhen et al. 1999].

To the best of our knowledge, literature about self-diffusion coefficients of nitroxides determined by PFG-NMR was missing due to relaxation times of  $\mu\text{s}$  for paramagnetic substances. Therefore other methods were chosen to compare the obtained results. Aizawa and colleagues [1979] used EPR spin exchange interactions to determine self-diffusion coefficients of  $2 \cdot 10^{-11} \text{ m}^2 \text{ s}^{-1}$  for TB in SDS 4-7 wt% which disagreed with our results. Furtado and colleagues [2011] determined the self-diffusion coefficient for TEMPO in homogenous aqueous solution with  $6.7 \cdot 10^{-10} \text{ m}^2 \text{ s}^{-1}$  by paramagnetic relaxation enhancement (PRE) NMR which is in same magnitude with  $7.2 \cdot 10^{-10} \text{ m}^2 \text{ s}^{-1}$  for TEMPO-H obtained in this study by PFG-NMR. However, in dispersed systems the determination of self-diffusion coefficients from small molecules by PFG-NMR is often used to study the incorporation of substances and the dynamic of solubilizing environment [Dupont-Leclercq et al. 2007; Fischer et al. 2009; Kreilgaard et al. 2000].

The determination of the partitioning behavior of spin probes is essential to interpret their reaction kinetics towards lipid radicals and antioxidants [Berton-Carabin et al. 2013a, 2013b]. The nitroxides TEMPOL, TEMPO and TEMPOL-benzoate (TB) were studied

by UF, PFG-NMR and EPR deconvolution (EPRSIM-C)(see chapter 3). With increasing lipophilicity the proportion of interfacial solubilized nitroxides increased in micellar solution to TEMPOL > TEMPO > TB. TEMPOL is solubilized in the interface up to 15 % and TB to 90-100 %. For TEMPO the variation is highest between 20-65 % depending on the emulsifier and the method used (table 3.4). A further increase of the proportion solubilized in the interface of emulsions was obtained due to an extended interfacial area, which was the favored environment in dispersed systems [Heins et al. 2007a]. This was considerably shown by EPRSIM-C for TEMPO with an increase from approximately 40 % to 80 % (table 3.5).

The partitioning results obtained for UF and EPR deconvolution were comparable (table 3.4 and 3.5), whereas high self-diffusion coefficients resulted in low nitroxide proportions solubilized in the interfaces. It has to be considered, that the UF technique is an invasive method while PFG-NMR and EPR represent non-invasive methods. The non-invasive spectroscopic methods differ in the time scale of milliseconds to seconds for NMR and nanoseconds for EPR [Borbat 2001], which allows EPR to study the fast dynamics of paramagnetic molecules. With UF and PFG-NMR equilibrium between two populations is preconditioned which can be influenced by additional populations that cannot be further characterized. Nevertheless, the UF method is a quick and easy method to determine the partition behavior between aqueous and micellar phase for most applications [Oehlke et al. 2008] and the obtained data for nitroxides were in agreement with the EPR results. The corresponding hydroxylamines (reduced nitroxides) were used for PFG-NMR as this technique is unsuitable for paramagnetic substances [Furtado et al. 2011]. However, the obtained data were only comparable with the other methods to a limited extent and it was not possible to determine the partitioning behavior in SDS micellar solutions.

EPR line shape deconvolution [Štrancar et al. 2005] is the preferred method to determine the partitioning of paramagnetic molecules in dispersed systems as different individual populations can be distinguished and further characterized. The nitroxide EPR spectra consist of several superimposed spectral components which were divided by deconvolution of the experimental spectra (figure 3.2). In lipid based structures such as solid lipid nanoparticles [Jores et al. 2003] and liposomes [Frenzel and Steffen-Heins 2014] the division into three different domains revealed best fits. In the dispersed systems different biophysical models were adopted [Štrancar et al. 2005; Berliner 1976].

The first population was indicated by a low  $\tau_c < 0.03$  ns and the hyperfine splitting constants in range of  $a_N = 17.2 - 16.8$  G (table 3.1). The range of  $a_N$  depended on the substituents of the nitroxide, which lowered  $a_N$  of TB and TEMPOL compared with TEMPO [Windle 1981]. The rotational correlation time  $\tau_c$  describes the rate of motion of the nitroxide as a function of its micro environment [Dejanovic et al. 2008], which was very low for population 1 as it was solubilized in the bulk water phase. This is in agreement with Ahlin and colleagues [2003] who found  $\tau_c = 0.04$  ns for TEMPOL in the bulk water phase of solid lipid nanoparticles. Concerning population 3,  $\tau_c > 0.1$  ns and  $a_N < 16.5$  G were determined. Population 2 was set as concentrated nitroxide spin probes in an isotropic

environment for  $a_N > 16.5$  which led to  $a_N$  in the range of 16.5-16.8 G associated with a reduced molecular motion indicated by  $\tau_c > 0.1$  ns. The micro environmental polarity gave two rough ranges of  $a_N$ : between 15 G  $< a_N < 16.5$  G for the interface resembling a variety of solvents with low to medium dielectric constants [Knauer and Napier 1976] and below  $a_N = 15$  G for the oil phase as also found by Mäder [2006] for TB in MCT oil. The obtained data were in line with the observations of Jores and colleagues [2003] who determined values for TB of  $a_N = 17.2$  G for the aqueous phase,  $a_N = 16.5 - 16.8$  G for high concentrated nitroxides at the surface and  $a_N = 15.1 - 15.8$  G for the lipophilic environment in solid lipid nanoparticles and emulsions. The third population revealed a much lower  $a_N < 15$  G and  $\tau_c > 0.3$  ns in emulsions compared to the micellar solutions indicating a solubilization in the oil phase for all nitroxide-emulsifier combinations (table 3.3) [Jores et al. 2003].

The influence of antioxidants towards the microenvironment of the nitroxides was investigated by means of  $\tau_c$  and  $a_N$  values (table 4.4 and 4.5). In CTAB micellar solution  $\tau_c$  obtained for TEMPO and TB were twice as high compared with SDS micellar solution although their partitioning is equivalent. Concerning the presence of antioxidants  $\tau_c$  of nitroxides in Brij58 micellar solution were the lowest which may be due to the bigger particle size of Brij58 relative to the ionic emulsifiers [Heins et al. 2006]. Although PG is nearly complete solubilized in the CTAB micellar phase, it showed no influence on the  $\tau_c$  of TEMPO and TB, but significantly increased the  $\tau_c$  of TEMPO accompanied by a strong reduction of  $a_N$  (Tab. 4.4). This indicated a same solubilization site for PG and TEMPO with might result in a displacement of TEMPO from the palisade layer deeper into the micellar core leading to an increased sterically hindrance.

Apart from EPR, NMR  $T_1$  relaxation times were used to determine the location of nitroxides in dispersed systems according to Heins and colleagues [2007a]. The nitroxides caused strong reduction of the  $T_1$  relaxation times for all emulsifier protons, which may be a result of strong hydrogen-bonding interactions of the NO moiety [Pyter et al. 1982]. However,  $T_1$  relaxation times showed slightly stronger reduction at the  $\alpha$ - and  $\beta$ -CH<sub>2</sub> groups of the alkyl chains of all emulsifiers in the presence of nitroxides (figure 4.2), relatively to the nitroxide proportion solubilized in the interface (table 4.3). Therefore, the estimated solubilization site for the nitroxides is the palisade layer, which is in agreement with literature findings [Almeida 1998; Oakes 1972]. With EPR deconvolution technique and NMR  $T_1$  relaxation the location of nitroxides in dispersed systems can be determined.

## 6.4 Reactivity of spin probes towards antioxidants and free lipid radicals

In dispersed systems the reaction kinetics are known to be accelerated if the reaction participants are in close proximity to one another [Heins et al. 2007a]. As the nitroxides can react with antioxidants and lipid radicals (figure 1.6) an accelerated reaction kinetic indicated an equal solubilization site of lipid radicals or antioxidants and the nitroxides.

### 6.4.1 Alkyl radicals but not alkoxy radicals are able to reduce nitroxides

While the localization of the antioxidants were investigated by  $T_1$  relaxation times and chemical shifts (table 4.1 and 4.2) [Heins et al. 2007a], the localization of lipid radicals were indirectly obtained by their reaction towards nitroxides. To determine the reaction kinetics between nitroxides and free lipid radicals, alkoxy (figure 5.4) and alkyl (figure 5.6) were produced.

As the generation of the free lipid radicals required elevated temperatures the stability of the nitroxides was tested prior to radical detection. The nitroxides were stable at 60 °C, but at temperatures of 100 °C, required for the decomposition of the MeLOOH, TEMPO decomposed (figure 5.3). While TEMPOL and TB are stabilized due to their additional functional group in position 4, the decay of TEMPO occurs at high temperatures in acidic media with H-donating solvents [Ma et al. 2011; Ciriano et al. 1999]. In addition, the nitroxides inhibited the decomposition of MeLOOH shown for TB in SDS and CTAB and for all nitroxides in Brij58 (figure 5.4). Therefore, the nitroxides were added after heat-treatment to detect alkoxy radicals. However, no significant reduction of the nitroxide content was obtained due to high standard deviations; only trends were shown for TEMPOL in Brij58 and TEMPO and TB in SDS (figure 5.5). This might be due to the instability of the adducts of the oxygen-centered radicals [Pattison et al. 2012] which preferentially undergo further rearrangements [Brandicourt et al. 2015].

Several authors showed that the reaction of nitroxides with carbon-centered radicals, like alkyl radicals, is accelerated towards the oxygen-centered radicals, such as alkoxy radicals [Kocherginsky and Swartz 1995; Amorati et al. 2010; Cimato et al. 2004]. Indeed, the alkyl radicals oxidized the nitroxides and the reduced nitroxide content was followed over the time. In all emulsions the nitroxides were oxidized by alkyl radicals increasing to  $\text{TEMPOL} < \text{TB} < \text{TEMPO}$  (figure 5.6). The nitroxide concentration had no effect on the spin scavenging ability (figure 5.2) which is in agreement with [Voest et al. 1993]. However, the reaction of TEMPO with alkyl radicals was accelerated (see 6.4.2) and the emulsifier influenced the reaction kinetic (see 6.4.3).

### 6.4.2 The alignment of the nitroxides NO moiety

Both, the reaction with antioxidants and lipid radicals showed an accelerated reaction of TEMPO which is solubilized in the interface to a higher content than TEMPOL, but a lower content than TB (figure 5.6 and table 4.6). This might be due to the different alignment of the NO moiety of TEMPO that has no substituent compared with TB and TEMPOL possessing polar substituents (see 4.4.1). The highest reaction rate of alkyl radicals was determined with TEMPO in SDS emulsions where they oxidized 43 % of the TEMPO content within 240 min (figure 5.6). The accelerated oxidation of TEMPO would therefore be in agreement with Coupland and colleagues [1996] who revealed that the initiation of

lipid oxidation occurs at the droplet interface. The strong reduction of TEMPO by the antioxidant propyl gallate in CTAB was accompanied by a strong increase of  $\tau_c$  (table 4.5) and a reduction of  $a_N$  (table 4.4) indicating a close proximity of the reactants.

Therefore, not only the concentration of the reactants in the interface but the close proximity of the H-donating group of the antioxidant and the NO moiety governed the reaction kinetics. The enhanced reaction of lipophilic TB towards radicals and antioxidants became particularly conspicuous with  $\alpha$ -tocopherol, which is entirely solubilized in Brij58 and CTAB micelles. Apart from the proximity of the NO moiety towards antioxidants or radicals, steric factors of the nitroxide influence their reaction towards radicals [Yamasaki et al. 2011], which might be true for TB where the benzene structure could be a hindrance. Nevertheless, the orientation of TB might be most likely with the NO moiety into the more nonpolar region whereas its oxycarbonyl group might align to the more hydrophilic interface. Brigati and colleagues [2002] studied dialkyl nitroxides with increasing chain length and showed that  $a_N$  values in the micellar phases of SDS, HTAB and  $C_{10}E_6$  remained approximately constant, while the  $a_{2H\beta}$  decreased significantly, indicating that the NO moiety is deeply inside the micelle irrespective of the alkyl chain length. Furthermore, they suggested that nitroxides with a polar hydroxyl group might not pass the micellar interface and solubilize in the micellar phase due to possible reactions with head groups, counterions, and hydration water at the surface. An alignment of the NO moiety of TEMPO to the more hydrophilic part of the micelle may result in formation of H-bondings [Pyter et al. 1982; Shenderovich et al. 1997] Studies of Ramachandran and colleagues [1982] even assumed a predominant solubilization of TEMPO in the interface region with the NO moiety in contact with water, which is in line with Almeida and colleagues [1998].

These findings imply, that not only the distinct location, but the orientation of the molecules is the prerequisite for a high reaction kinetic.

### 6.4.3 The SDS interface accelerated the nitroxides reactions

Comparing the reaction kinetic of TEMPO in SDS and CTAB micellar solutions, TEMPO was faster oxidized by alkyl radicals (chapter 5) or reduced by antioxidants (chapter 4) in the SDS micellar interface, although the content and the alignment of its NO moiety were equivalent. It could be reasonable that TEMPO partitioned faster into SDS micelles than into CTAB micelle as the self-diffusion coefficients showed higher diffusion for TEMPO in SDS (table 3.1), which is in agreement with literature [Brigati et al. 2002; Pyter et al. 1982]. The highest reaction rate of alkyl radicals towards nitroxides was determined in SDS emulsions (figure 5.6).

Furthermore, the surface charge of the droplets influenced the decomposition of MeLOOH (figure 5.3) most likely due to electrostatic interaction with metal ion traces [Boon et al. 2008; Mancuso et al. 1999]. Almeida and colleagues [1998] found differences between charged and uncharged micelles concerning binding constants for TEMPO and TEMPOL towards pyrene in different micellar solutions.



Another effect of SDS is the solubilisation site of the antioxidants that were solubilized in the SDS Stern layer, while in CTAB micelles antioxidants are predominately solubilized in the palisade layer [Heins et al. 2006, 2007b]. Trolox was solubilized in the SDS micelles to only 38 % (table 4.1), but showed great potential in reducing all nitroxides being fastest for TB > TEMPO > TEMPOL. Oehlke and colleagues [2011] showed that SDS micellar solutions stabilized Trolox by preventing its degradation. A stabilizing effect of the anionic surface on the NO moiety was observed by Pyter and colleagues [1982] indicating an optimal proximity and alignment of TEMPO to react with antioxidants.

## 6.5 Concluding remarks and Outlook

The results of this thesis show that the detection of free lipid radicals is possible by means of EPR spin probing technique. Prior to the detection of the free lipid radicals it was necessary to determine the partitioning of the spin scavengers in dispersed systems. It was shown that not only the partitioning but the distinct location determines the reaction kinetics towards the free lipid radicals. Nevertheless, further investigations would obtain information to open questions.

The use of spin traps was not suitable to detect lipid radicals. However, the lipid autoxidation experiments with spin probes showed that alkyl radicals were produced (figure 5.6). As the radical initiators led to a preferred oxidation of the continuous water phase this problem could be solved by renouncement of initiators. Furthermore, the line shape analysis (chapter 3) revealed good results by deconvolution experimental spectra of the nitroxides. This might also be true for the identification of oxygen-centered spin trap adducts, if this model is suitable to identify radical species as a function of their solubilization site.

It would be beneficial to use EPRSIM-C deconvolution to determine the influence of antioxidants towards the  $a_N$  and  $\tau_c$  of nitroxides solubilized in the interface of dispersed systems (chapter 4). The different populations of nitroxides showed individual spectral characteristics depending on their microenvironment (see 3.4.2). The calculation of the superimposed  $a_N$  and  $\tau_c$  showed that the presence of antioxidants influenced the spectral characteristic of the nitroxides (table 4.4 and 4.5). With deconvolution technique the displacement and restricted molecular tumbling of each individual proportion due to the same solubilisation site of the antioxidants can be characterized.

An accelerated reaction kinetic was shown in dispersed systems with the emulsifier SDS. However, this might be due to the anionic character, the high diffusion in SDS micellar solutions or the specifics for SDS. Investigation with further anionic emulsifiers would prove this question.

In this thesis a method to monitor free lipid radicals generated by autoxidation was investigated in model emulsions. The knowledge of the behavior of the nitroxide spin probes in dispersed systems led to the conclusion that TEMPO can be used to detect lipid alkyl radicals. The stability at elevated temperatures up to 60 °C indicates that TEMPO can be added prior to storage time. Comparing the spin probes with the spin

trap technique, the nitroxides benefit from their property being EPR active from the very beginning which facilitates to follow their continuous reaction towards free radicals. Further investigations in more complex matrices need to be experimented as matrix components such as antioxidants may influence the reduction of the nitroxide content. To conclude, EPR spin probing method is an alternative and promising method to monitor free lipid radicals in dispersed systems.

## References

- P. Ahlin, J. Kristl, S. Pečar, J. Štrancar, and M. Sentjerc. 2003. The effect of lipophilicity of spin-labeled compounds on their distribution in solid lipid nanoparticle dispersions studied by electron paramagnetic resonance. *Journal of Pharmaceutical Sciences* 92, 1 (2003), 58–66.
- Masayuki Aizawa, Tsuyoshi Komatsu, and Tsurutaro Nakagawa. 1979. Electron Spin-Spin Interaction and Translational Diffusion of Nitroxide Radicals in Sodium Dodecyl Sulfate Micelles. *Bulletin of the Chemical Society of Japan* 52, 4 (1979), 980–983.
- L. Almeida. 1998. Different Micellar Packing and Hydrophobicity of the Membrane Probes TEMPO and TEMPOL Influence Their Partition Between Aqueous and Micellar Phases Rather than Location in the Micelle Interior. *Journal of Colloid and Interface Science* 203, 2 (1998), 456–463.
- Riccardo Amorati, Gian Franco Pedulli, Derek A. Pratt, and Luca Valgimigli. 2010. TEMPO reacts with oxygen-centered radicals under acidic conditions. *Chem. Commun.* 46, 28 (2010), 5139.
- L. J. Berliner. 1976. *Spin Labeling: Theory and Applications*. 1976. Academic Press, New York.
- Claire C. Berton-Carabin, John N. Coupland, and Ryan J. Elias. 2013a. Effect of the lipophilicity of model ingredients on their location and reactivity in emulsions and solid lipid nanoparticles. *Colloids and Surfaces A: Physicochemical and Engineering Aspects* 431 (2013), 9–17.
- Claire C. Berton-Carabin, Ryan J. Elias, and John N. Coupland. 2013b. Reactivity of a model lipophilic ingredient in surfactant-stabilized emulsions: Effect of droplet surface charge and ingredient location. *Colloids and Surfaces A: Physicochemical and Engineering Aspects* 418, 0 (2013), 68–75.
- Caitlin S. Boon, Zhimin Xu, Xiaohua Yue, D. Julian McClements, Jochen Weiss, and Eric A. Decker. 2008. Factors Affecting Lycopene Oxidation in Oil-in-Water Emulsions. *J. Agric. Food Chem.* 56, 4 (2008), 1408–1414.
- P. P. Borbat. 2001. Electron Spin Resonance in Studies of Membranes and Proteins. *Science* 291, 5502 (2001), 266–269.
- A. Bosnjakovic and S. Schlick. 2006. Spin trapping by 5,5-dimethylpyrroline-N-oxide in Fenton media in the presence of Nafion perfluorinated membranes: Limitations and potential. *Journal of Physical Chemistry B* 110, 22 (2006), 10720–10728.
- Stéphanie Brandicourt, Jacques Nicolas, Aline Boussard, and Anne-Marie Riquet. 2015. Use of ESR and HPLC to follow the anaerobic reaction catalysed by lipoxygenases. *Food Chemistry* 168, 0 (2015), 311–320.
- Giovanni Brigati, Paola Franchi, Marco Lucarini, GianFranco Pedulli, and Luca Valgimigli. 2002. The EPR study of dialkyl nitroxides as probes to investigate the exchange of solutes between micellar and water phases. *Research on Chemical Intermediates* 28, 2-3 (2002), 131-141.
- Garry R. Buettner. 1987. Spin Trapping: ESR parameters of spin adducts 1474 1528V. *Free Radical Biology and Medicine* 3, 4 (1987), 259–303.
- Alejandra N. Cimato, Lidia L. Piehl, Graciela B. Facorro, Horacio B. Torti, and Alfredo A. Hager. 2004. Antioxidant effects of water- and lipid-soluble nitroxide radicals in liposomes. *Free Radical Biology and Medicine* 37, 12 (2004), 2042–2051.
- Maria Victoria Ciriano, Hans-Gert Korth, Van Scheppingen, Wibo B, and Peter Mulder. 1999. Thermal stability of 2, 2, 6, 6-tetramethylpiperidine-1-oxyl (TEMPO) and related N-alkoxyamines. *Journal of the American Chemical Society* 121, 27 (1999), 6375–6381.
- J. N. Coupland, Z. Zhu, H. Wan, D. J. McClements, W. W. Nawar, and P. Chinachoti. 1996. Droplet composition affects the rate of oxidation of emulsified ethyl linoleate. *Journal of the American Oil Chemists' Society* 73, 6 (1996), 795–801.
- F. Dai, W. F. Chen, B. Zhou, L. Yang, and Z. L. Liu. 2009. Antioxidative Effects of Curcumin and its Analogues against the Free-radical-induced Peroxidation of Linoleic Acid in Micelles. *Phytotherapy Research* 23, 9 (2009), 1220–1228.
- Branka Dejanovic, Krunoslav Miroslavljevic, Vesna Noethig-Laslo, Slavko Pecar, Marjeta Sentjerc, and Peter Walde. 2008. An ESR characterization of micelles and vesicles formed in aqueous decanoic acid/sodium decanoate systems using different spin labels. *Chemistry and Physics of Lipids* 156, 1-2 (2008), 17–25.

- S. I. Dikalov and R. P. Mason. 2001. Spin trapping of polyunsaturated fatty acid-derived peroxy radicals: Reassignment to alkoxyl radical adducts. *Free Radical Biology and Medicine* 30, 2 (2001), 187–197.
- Laurence Dupont-Leclercq, Sébastien Giroux, Bernard Henry, and Patrice Rubini. 2007. Solubilization of amphiphilic carboxylic acids in nonionic micelles: determination of partition coefficients from pK<sub>a</sub> measurements and NMR experiments. *Langmuir* 23, 21 (2007), 10463–10470.
- Elmar Fischer, Wolfgang Fieber, Charles Navarro, Horst Sommer, Daniel Benczedi, Maria Inés Velazco, and Monika Schönhoff. 2009. Partitioning and localization of fragrances in surfactant mixed micelles. *Journal of surfactants and detergents* 12, 1 (2009), 73–84.
- Edwin N. Frankel. 2005. Lipid oxidation. *Oily Press lipid library* (2nd. ed.); Lipid Technology, Bridgwater, England.
- Monika Frenzel and Anja Steffen-Heins. 2014. Whey protein coating increased bilayer rigidity and stability of liposomes in food like matrices. *Food Chemistry*, 173 (2015) 1090–1099.
- M. A. Freyaldenhoven, P. A. Lehman, T. J. Franz, R. V. Lloyd, and V. M. Samokyszyn. 1998. Retinoic acid-dependent stimulation of 2,2'-azobis(2-amidinopropane)-initiated autoxidation of linoleic acid in sodium dodecyl sulfate micelles: A novel prooxidant effect of retinoic acid. *chem res toxicol* 11, 2 (1998), 102–110.
- Filipe Furtado, Petrik Galvosas, Frank Stallmach, Ulf Roland, Jörg Kärger, and Frank-Dieter Kopinke. 2011. Paramagnetic Relaxation Enhancement (PRE) as a Tool for Probing Diffusion in Environmentally Relevant Porous Media. *Environ. Sci. Technol.* 45, 20 (2011), 8866–8872.
- Qiong Guo, Steven Y. Qian, and Ronald P. Mason. 2003. Separation and identification of DMPO adducts of oxygen-centered radicals formed from organic hydroperoxides by HPLC-ESR, ESI-MS and MS/MS. *Journal of the American Society for Mass Spectrometry* 14, 8 (2003), 862–871.
- Yuan Hanzhen, Du Youru, Zhao Sui, and Yu Jiayong. 1999. Self-aggregation of surfactants in water solution by NMR. *Sci. China Ser. A-Math.* 42, 3 (1999), 319–324.
- Clare L. Hawkins and Michael J. Davies. 2013. Detection and characterisation of radicals in biological materials using EPR methodology. *Biochimica et Biophysica Acta (BBA) - General Subjects* (2013).
- Anja Heins, Vasil Garamus, Bernd Steffen, Heiko Stöckmann, and Karin Schwarz. 2006. Impact of Phenolic Antioxidants on Structural Properties of Micellar Solutions. *Food Biophysics* 1, 4 (2006), 189–201.
- Anja Heins, Donald McPhail, Tobias Sokolowski, Heiko Stöckmann, and Karin Schwarz. 2007a. The Location of Phenolic Antioxidants and Radicals at Interfaces Determines Their Activity. *Lipids* 42, 6 (2007), 573–582.
- Anja Heins, Tobias Sokolowski, Heiko Stöckmann, and Karin Schwarz. 2007b. Investigating the Location of Propyl Gallate at Surfaces and Its Chemical Microenvironment by <sup>1</sup>H NMR. *Lipids* 42, 6 (2007), 561–572.
- Wayne L. Hubbell, David S. Cafiso, and Christian Altenbach. 2000. Identifying conformational changes with site-directed spin labeling. *Nature Structural & Molecular Biology* 7, 9 (2000), 735–739.
- Edward G. Janzen. 2012. A critical review of spin trapping in biological systems. *Free radicals in biology* 4 (2012), 115.
- Edward G. Janzen, Yashige Kotake, and RANDALL D. HINTON. 1992. Stabilities of hydroxyl radical spin adducts of PBN-type spin traps. *Free Radical Biology and Medicine* 12, 2 (1992), 169–173.
- Katja Jores, Wolfgang Mehnert, and Karsten Mäder. 2003. Physicochemical Investigations on Solid Lipid Nanoparticles and on Oil-Loaded Solid Lipid Nanoparticles: A Nuclear Magnetic Resonance and Electron Spin Resonance Study. *Pharmaceutical Research* 20, 8 (Aug. 2003), 1274–1283.
- Shin-ya Kishioka, Minoru Umeda, and Akifumi Yamada. 2002. Effect of Oxygen on the Electrochemical Reduction of Nitroxyl Radical: Interpretation of the Mechanism for a Redox Probe in Biological Systems. *Anal. Sci* 18, 12 (2002), 1379–1381.
- Bruce R. Knauer and James J. Napier. 1976. The nitrogen hyperfine splitting constant of the nitroxide functional group as a solvent polarity parameter. The relative importance for a solvent polarity parameter of its being a cybotactic probe vs. its being a model process. *J. Am. Chem. Soc.* 98, 15 (1976), 4395–4400.

- Nickolai Kocherginsky and Harold M. Swartz. 1995. Nitroxide spin labels: reactions in biology and chemistry. CRC Press.
- Arkadi G. Krainev and Diana J. Bigelow. 1996. Comparison of 2,2'-azobis(2-amidinopropane) hydrochloride (AAPH) and 2,2'-azobis(2,4-dimethylvaleronitrile)(AMVN) as free radical initiators: a spin-trapping study. *J. Chem. Soc., Perkin Trans. 2*, 4 (1996), 747-754.
- Mads Kreilgaard, Erik J. Pedersen, and Jerzy W. Jaroszewski. 2000. NMR characterisation and transdermal drug delivery potential of microemulsion systems. *Journal of controlled release* 69, 3 (2000), 421-433.
- Yun Ma, Colin Loyns, Peter Price, and Victor Chechik. 2011. Thermal decay of TEMPO in acidic media via an N-oxoammonium salt intermediate. *Organic & Biomolecular Chemistry* 9, 15 (2011), 5573-5578.
- Karsten Mäder (Ed.). 2006. *Nanotechnologies for the Life Sciences. Characterization of nanoscaled drug delivery systems by Electron Spin Resonance (ESR). Nanosystem Characterization Tools in the Life Sciences.* chapter 7 241-258. Wiley-VCH Verlag.
- Jennifer R. Mancuso, D. Julian McClements, and Eric A. Decker. 1999. The Effects of Surfactant Type, pH, and Chelators on the Oxidation of Salmon Oil-in-Water Emulsions. *Journal of Agricultural and Food Chemistry* 47, 10 (1999), 4112-4116.
- Paul R. Marriott, Perkins, M. John, and David Griller. 1980. Spin trapping for hydroxyl in water: a kinetic evaluation of two popular traps. *Can. J. Chem.* 58, 8 (1980), 803-807.
- Subhash C. Mojumdar, David A. Becker, Gino A. DiLabio, James J. Ley, L. Ross C. Barclay, and K. U. Ingold. 2004. Kinetic Studies on Stilbazulenyl-bis-nitron (STAZN), a Nonphenolic Chain-Breaking Antioxidant in Solution, Micelles, and Lipid Membranes. *The Journal of Organic Chemistry* 69, 9 (2004), 2929-2936.
- Carla D. Nuchi, Pilar Hernandez, D. Julian McClements, and Eric A. Decker. 2002. Ability of Lipid Hydroperoxides To Partition into Surfactant Micelles and Alter Lipid Oxidation Rates in Emulsions. *J. Agric. Food Chem.* 50, 19 (2002), 5445-5449.
- J. Oakes. 1972. Magnetic resonance studies in aqueous systems. Part 1.- Solubilization of spin probes by micellar solution. *J. Chem. Soc., Faraday Trans. 2* 68 (1972), 1464.
- Kathleen Oehlke, Vasil M. Garamus, Anja Heins, Heiko Stöckmann, and Karin Schwarz. 2008. The partitioning of emulsifiers in o/w emulsions: A comparative study of SANS, ultrafiltration and dialysis. *Journal of Colloid and Interface Science* 322, 1 (2008), 294-303.
- Kathleen Oehlke, Anja Heins, Heiko Stöckmann, Frank Sönnichsen, and Karin Schwarz. 2011. New insights into the antioxidant activity of Trolox in o/w emulsions. *Food Chemistry* 124, 3 (2011), 781-787.
- David I. Pattison, Magdalena Lam, Sujata S. Shinde, Robert F. Anderson, and Michael J. Davies. 2012. The nitroxide TEMPO is an efficient scavenger of protein radicals: Cellular and kinetic studies. *Free Radical Biology and Medicine* 53, 9 (2012), 1664-1674.
- Richard A. Pyter, C. Ramachandran, and Pasupati Mukerjee. 1982. Micelle-water distribution coefficients of nitroxides. Correlation with dodecane-water distributions and interfacial activity. *The Journal of Physical Chemistry* 86, 16 (1982), 3206-3210.
- S. Y. Qian, H. P. Wang, F. Q. Schafer, and G. R. Buettner. 2000. EPR detection of lipid-derived free radicals from PUFA, LDL, and cell oxidations. *free radical bio med* 29, 6 (2000), 568-579.
- C. Ramachandran, Richard A. Pyter, and Pasupati Mukerjee. 1982. Microenvironmental effects on transition energies and effective polarities of nitroxides solubilized in micelles of different charge types and the effect of electrolytes on the visible spectra of nitroxides in aqueous solutions. *J. Phys. Chem.* 86, 16 (1982), 3198-3205.
- Olesea Roman, Francis Courtois, Marie-Noëlle Maillard, and Anne-Marie Riquet. 2012. Kinetic Study of Hydroperoxide Degradation in Edible Oils Using Electron Spin Resonance Spectroscopy. *J Am Oil Chem Soc* (2012).
- I. G. Shenderovich, Z. Kecki, I. Wawer, and G. S. Denisov. 1997. NMR and EPR Study of the Nitroxide Radical Tempo Interaction with Phenols. *Spectroscopy letters* 30, 8 (1997), 1515-1523.
- Olle Söderman, Peter Stilbs, and William S. Price. 2004. NMR studies of surfactants. *Concepts Magn. Reson.* 23A, 2 (2004), 121-135.
- Benjamin P. Soule, Fuminori Hyodo, Ken-ichiro Matsumoto, Nicole L. Simone, John A. Cook, Murali C. Krishna, and James B. Mitchell. 2007. The chemistry and biology of nitroxide compounds.

- Free Radical Biology and Medicine 42, 11 (2007), 1632–1650.
- K. Stolze, N. Udilova, and H. Nohl. 2000. Spin trapping of lipid radicals with DEPMPO-derived spin traps: Detection of superoxide, alkyl and alkoxy radicals in aqueous and lipid phase. *Free Radical Bio Med* 29, 10 (2000), 1005–1014.
- K. Stolze, N. Udilova, and H. Nohl. 2002. Spin adducts of superoxide, alkoxy, and lipid-derived radicals with EMPO and its derivatives. *Biol Chem* 383, 5 (2002), 813–820.
- Janez Štrancar, Tilen Koklic, Zoran Arsov, Bogdan Filipic, David Stopar, and Marcus A. Hemminga. 2005. Spin label EPR-based characterization of biosystem complexity. *Journal of chemical information and modeling* 45, 2 (2005), 394–406.
- Olga Vinogradova, Frank Sönnichsen, and Sanders II, Charles R. 1998. On choosing a detergent for solution NMR studies of membrane proteins. *Journal of biomolecular NMR* 11, 4 (1998), 381–386.
- Emile E. Voest, Ernst van Faassen, and Joannes J. M. Marx. 1993. An electron paramagnetic resonance study of the antioxidant properties of the nitroxide free radical TEMPO. *Free Radical Biology and Medicine* 15, 6 (1993), 589–595.
- John A. Weil and James R. Bolton. 2007. *Electron paramagnetic resonance: elementary theory and practical applications*. John Wiley & Sons.
- J. J. Windle. 1981. Hyperfine coupling constants for nitroxide spin probes in water and carbon tetrachloride. *Journal of Magnetic Resonance (1969)* 45, 3 (1981), 432–439.
- Toshihide Yamasaki, Yuko Ito, Fumiya Mito, Kana Kitagawa, Yuta Matsuoka, Mayumi Yamato, and Ken-ichi Yamada. 2011. Structural concept of nitroxide as a lipid peroxidation inhibitor. *The Journal of Organic Chemistry* 76, 10 (2011), 4144–4148.

# Curriculum Vitae

## Personal Data

Name Heimke Krudopp  
Date of Birth April 9<sup>th</sup>, 1984  
Place of Birth Neumünster, Germany

## Professional Experience

02/2010 – 03/2014 Research associate at the Division of Food Technology,  
Micro- and Nanostructures in Foods,  
Institute of Human Nutrition and Food Science,  
Kiel University, Germany  
06/2014– 11/2014 Scholarship from the Central Office for Gender Equality,  
Diversity and Family,  
Kiel University, Germany

## Education

02/2010 – 12/2014 Ph.D student at the Division of Food Technology  
and the Chemistry Section, Kiel University, Germany  
04/2005 – 09/2009 Student at the Hamburg School of Food Science,  
University of Hamburg, Germany  
*State examination and Diploma in Food Chemistry*  
08/2001 – 06/2004 Student at the Integrierte Gesamtschule Brachenfeld,  
Neumünster, Germany  
*Abitur (Certificate of maturity)*

### **Eidesstattliche Erklärung**

Die vorliegende Dissertation wurde selbstständig und ohne unerlaubte Hilfe von mir angefertigt. Die Arbeit wurde weder vollständig noch in Teilen in einem Prüfungsverfahren angemeldet. Die Manuskripte der Dissertation wurden für das Einreichen in Journalen mit peer review Verfahren vorbereitet. Die Inhalte der Arbeit sind unter Einhaltung der Regeln guter wissenschaftlicher Praxis der Deutschen Forschungsgemeinschaft angefertigt worden.

Kiel, den 14.12.2015    Heimke Krudopp